COMPLIANT SHAPE ADAPTIVE CHICORY GRIPPING

for robotic sorting processes

Author: Thomas Hester
Chair: Prof. dr. ir. P. Breedveld
Supervisor: Dr. ir. G. Smit

Date: 27 August 2020

TU Delft

Executive summary

This thesis contains the design process of a compliant shape adaptive chicory gripper for robotic sorting processes. The robotic sorting line consists of an input and output conveyor-belt. The input line contains unsorted chicories which are scanned by a robotic vision system. Overhead FlexPicker robots, equipped with chicory grippers, sort the chicories size by size onto the output line. The output line can contain a transportation crate or flowpack in which the chicories will be packed and shipped after sorting. Chicories are vulnerable for internal and external damages when touching the outer skin which makes robotic sorting difficult. The acceleration forces performed by the robot requires a strong but gentle grip on the chicory without any damaging marks. By designing a specific compliant shape adaptive gripper, sorting can be done faster, cheaper and more accurate than manual sorting. Current patents, academic literature or business applications had no solution for this chicory gripping problem. The design process for a suitable gripper started with an analysis of current patents and literature within compliant gripping in general. This provided insights in the the possibilities of compliant gripping. Based on the design requirements for the robot sorting setup, several concepts are obtained and selected. The concepts have been translated into four working gripper prototype layouts which are evaluated on force and damage requirements. Based on the results of these experiments, a first iteration prototype was made. Three additional optimizing iterations were needed to result in a prototype which reached the damage and force requirements. Further evaluation of this prototype proved a sufficient performance on robustness, endurance, operational speed and food grade requirements. The iteration 4 prototype reached therefore 17 of the total 19 gripper design requirements. To be able to accomplish the two remaining requirements, several recommendations are provided for a final gripper end product which is ready for industrial application.

Contents

1 Introduction

1.1 Background

Adaptive shape gripping is a principle of object grasping without essential presents of friction forces. The gripper adaptively encloses the outer contours of the object to create a normal force which supports the object. Demands for adaptive shape grippers in agricultural industries are growing according to appendix A were different mechanisms within adaptive gripping literature have been analysed. Among these mechanisms, elastic-compliant linkage-based grippers are promising in terms of shape adaptation with increasing demands over time (appendix A). Agricultural application shows a dominant appearance of these linkage-based adaptive shape grippers (appendix A). Therefore, development of a compliant agricultural gripper is relevant at this moment.

Agricultural grippers are used for robotic sorting and harvesting processes of fruits and vegetables. The sorting process is based on estimated weight and dimensions by visual data interpretation. Scanned products receive a digital size label at the input conveyor belt. The unsorted input crates with fruits or vegetables are moved through the machine and are picked by overhead picking robots, know as FlexPicker robots. These robots grasp each individual object and sort them size by size into output crates or belts as shown in figure 1.1.

Within gripping, three principles are known: grasping, suction and adhesion based gripping. Suction based gripping of vegetables with leaves (chicory, corn, cabbage or lettuce for example) is hard because the outside leaves attach to the suction actuator but can not hold the load of the entire object taking acceleration forces applied by the sorting robot into account. Adhesion based grippers in general complicate food handling regulations because of adhesion additives or micro structures in which product residues remain. Therefore, grasping principle solutions remain promising in agricultural sorting processes as described in appendix A.

Chicory is one of the vegetables with leaves on the outside which are not graspable by conventional vacuum techniques. In addition, chicory is extremely vulnerable for internal and external damage and creates therefore a mechanical gripper design challenge for robotic gripping. Until now, no academic or industrial solution for this chicory gripping problem has been invented. Looking at existing grippers for agricultural industries showed an extensive amount of soft grippers. In general, soft grippers refer to balloon-based grippers which are inflated by compressed air causing a hollow chambers to expand. This expansion results in the actuation (bending) of the soft finger. Due to the elastic materials used in these soft grippers, actuation pressures are low and gripper output forces are limited. This results in relatively low operational actuation speeds and holding forces. To put this in perspective, the sorting robots are able to accelerate the objects with an acceleration up to 9 G. Dependent on the object weight, high reaction forces, of the accelerating object onto the gripper, are created. Conventional soft grippers are not (yet) able withstand the forces created by these accelerations.

Controversially, linkage-based compliant mechanisms can be as elastic as balloon-based grippers but are not covered by the soft grippers terminology. However, because compliant mechanisms can be designed with stronger material types combined with infinite form freedom, they are able to outperform the shortcomings of soft grippers. Nowadays, several industrial compliant grippers are on the market. Inspecting these closely showed a majority of compliant grippers which are shape adaptive due to normal contact forces. This causes the gripper to deform according to the outer shape of the object. However, a minority of the grippers is able to deform prior to the contacting phase by a prescribed form

Figure 1.1: Beef tomatoes sorting line as illustration for a similar chicory sorting line. The input conveyor belt on the right contain unsorted products and the output conveyor belts on the left side contain sorted products based on estimated weight. The weight estimation and object localisation is computed by automated visual data interpretation at the beginning of the input line. Overhead FlexPicker robots grasp the objects piece by piece and places them in the correct output crates. Figure reference: [78]

deformation to mimic the shape of the object. This is the type of conditions where compliant mechanism are able to excel with the right design.

1.2 Problem statement and goal

Sorting chicory with a fast sorting robot requires a fast actuating, food safe and strong but gentle gripper which is able to withstand acceleration forces without damaging the chicory. The goal of this graduation project is to design and test a working compliant shape adaptive gripper for robotic sorting processes of chicories. The fundamental gripper elements of the final prototype resulting from this design driven theses, need to be implementable in industry.

1.3 Contents of this report

After this introduction, a state of the art of current compliant grippers is presented in chapter 2. This analysis takes current literature and patents into account. Based on the results from this state of the art, several conclusions are formulated. To start the design process, a list of design requirements is set in chapter 3. This contains all requirement for the gripper to be implementable in industry. With the requirements taken into account, a concept design phase was created and documented in chapter 4. This chapter contains idea generation with drawings and basic FEM analysis. The concept design ends with an improved concept design. Elaborating on the concept design, a prototyping phase is described in chapter 5: prototyping. A first proof of concept has been build followed by four working prototypes which are evaluated on force and damage requirements. Based on the performance of these working prototypes, a prototype optimization is done in four iterative steps in chapter 6. The results obtained during the evaluation of the gripper prototypes is presented in chapter 7: results. A discussion is formulated based on the results as described in chapter 8.

2 State of the art

2.1 Literature

To investigate compliant grippers within available literature, scopus search engine was used. By searching for "compliant gripper" within title, abstract and key-words, 653 articles were found. These articles have been accessed and visually scanned quickly to collect interesting compliant adaptive grippers for the shape adaptive chicory gripper. The inclusion criteria for the literature refers to the ability to be shape adaptive and applicable on macro scale (chicory size). Within the results of the search query, a large number of micro compliant grippers were found. Although the mechanisms used are very interesting, the majority of the micro scale grippers were not relevant for a potential chicory gripper due to the lag of adaptability. The remaining adaptive compliant grippers consisted of significant redundant publications of the same grippers. Therefore, I was able to collect and compose a relatively small group of relevant articles consisting of 30 adaptive compliant gripper designs (figure 2.1). Five grippers within the selected literature make use of a so called classical fin gripper structure: A-I, B-I, A-II, C-II and E-II in figure 2.1 ([3, 7, 14, 18, 20], respectively). These fins generate shape adaptation due to contact forces. In [14] (A-II in figure 2.1), this fin is used to create a deformation of the fin by specific input forces. Contact force with the object is not essential for this deformation but supplementary. The lag of contact force adaptation in this gripper could be an opportunity for avoiding damage on the chicory. A different aspect of the fin grippers is the shape and orientation of the cross bars inside the fin contours. In [7] (B-I in figure 2.1), the effect of the angle and curvature of these crossbars is studied. The ability to reach underneath the object increases with the tilt of the cross bars. In [20] (E-II in figure 2.1) the effect of flexible 3D printable material variations applied on the fins are studied and can be a source of inspiration in the prototyping phase of the design process. To be able to withstand thousands of gripping repetition, a tough but flexible material is probably essential.

Looking at mechanisms to create a specific tip movement of the gripper, articles [8, 12, 19, 31, 33, 49, 79] (C-I, E-I, D-II, D-III, E-III, E-IV and D-VI in figure 2.1) are very interesting. The finger tips of these grippers are able to reach underneath the object to create a supporting normal force on the object instead of a friction force. Therefore, they are potentially able to grip the object with less contact pressure which reduces the potential damage on the object. Flexible hinges within these mechanisms have to last for thousands of gripping repetitions. Depending on the materials used, the majority of these plastic hinges is probably not able to last duty sufficiently. Therefore, mechanisms in [33, 49] (E-III and E-IV in figure 2.1) are specifically interesting. The hinges in these grippers look solid enough for industrial application. The materials used in these grippers in combination with the design layout could potentially contribute to the chicory gripper design. Unfortunately, the endurance performance of both of these grippers is not specified. Looking at the hinge mechanisms, a flexible or rigid hinge can be used. Rigid hinges are not real compliant mechanism (appendix A), but are used in combination with compliant parts. Flexible hinges are created by reducing the amount of material at the point where the mechanism needs to flex or by bending the entire beam structure of the gripper as an elastic structure (appendix A). A different method is to implement a more compliant material at the hinge point, resulting in similar effects. Using flexible hinges consisting of the same material as the rigid body parts has the advantage of part integration. Therefore, assembly is less costly and production is easier.

A different aspect of compliant grippers is the implementation of topology optimized structures as shown in [33, 34, 49, 50] (E-II, A-IV, E-IV and A-V in figure 2.1). These optimization algorithms are used as first design suggestion and are manually detailed afterwards, or vice versa. So, manual design processing is still present and essential with the use of topology optimization. Therefore, using an optimisation algorithm to optimize the structure of the gripper can be useful for isolated parts of the gripper, thinking of hinges or tip designs. Simulation and testing the gripper designs is done using ANSYS finite element software within the majority of the studied literature. This software program will therefore be used from the concept design phase until the result phase of this project to simulate and evolve the concepts towards working gripper prototypes.

The majority of the grippers within the found literature consists of 2D sketches which are extruded into a 3D structure. Only [86] (D-VI in figure 2.1) makes use of a 3D varying internal structure of the gripper finger. Looking at the chicory damage resistance problem, the objects withstands a varying contact pressure over the length of the chicory. Therefore a 3D varying internal gripper structure along the length of the chicory gripper provides an opportunity. In addition, extending the contact surface along the length of the chicory will decrease or even remove the effect of damaging the chicory surface theoretically.

Looking at the input types within the found literature, rotation or displacement values are applied on the compliant mechanisms to actuate the gripper. in [45] (C-IV in figure 2.1) rotation and displacement input are combined with vacuum techniques. The vacuum causes the compliant mechanism to adapt to the shape of the object. Due to the volume of the balloon which covers the compliant mechanism, actuation takes several seconds. Improving the actuation time with a larger vacuum flow or higher under pressurization will result in material failure of the balloon or the internal compliant mechanism, as described in [45]. Although this combination of inputs looked very promising on damage resistant performance, endurance becomes an issue (as described in [45]).

Looking further into actuation types of the compliant grippers, apart from simple displacement and rotation inputs, showed shape morphing compliant systems activated by heat ([58] shown in B-V of figure 2.1). Although this is an interesting mechanism, implementation in agricultural industry requires future research beyond the scope of this graduation project. Current research shows an actuation time of these morphing compliant systems in terms of seconds to minutes. These mechanisms are therefore simply to slow for the application of this project.

2.2 Patents

To make an analysis of the compliant grippers within patents, European patent office's (EPO) espacenet database has been accessed. The patents are organized by a classification structure. Grippers in general are located at: B25J15/00: gripping heads. Within the B25J15/00 classification, a subclassification for flexible finger members is present (table 2). The compliant mechanism grippers which are interesting for this project are located in this subclassification. This flexible finger member class consisted of 560 gripper patents. 55 of them have been selected based on the same selection criteria as the previously discussed academic literature. The compliant grippers within patent literature are depicted in figure 2.2.

An important annotation prior to the analysis of the patents is the lag of information about the performance of the patented designs. A gripper does not have to function at all for a patent request. Therefore, a critical view on the selected patents is essential to evaluate whether the design contributes as a useful inspiration source.

In contrast with the grippers found in literature, the patented grippers consist of several spring steel gripper designs (grippers A-1, A-6, A-8, C-1, C-7, D-4, D-5 and E-7 in figure 2.2). Although these are very interesting gripper mechanisms, problems in terms of shape adaptation and object damage avoidance are foreseen. The majority of these spring metal grippers are used in industrial applications where object damage is less critical. The advantage of these grippers is however the operation speed. Due to the use of metal hinges and rigid body parts, higher operation forces can be used, resulting in faster closing and opening cycles. Working principles among these spring metal grippers which can potentially be converted in softer materials are taken into consideration in the design phase.

In terms of shape adaptation, grippers A-4, A-6, A-7, A-8, B-5 , B-6, C-2, C-3, C-6, C-11, D-1, D-7, D-9, D-10, D-11, E-2, E-3, E-5, E-8, E-9 and E-11 in figure 2.2 are very interesting. The majority of these shape adaptive grippers consist of a fin gripper structure (A-7, A-8, B-5, C-2, C-3, C-11, D-7, E-2, E-3, E-5, E-9 and E-11). The working principle of these fins have been explained within the academic literature analysis paragraph. All these patented adaptive fin grippers consist of contact force shape adaptation. Compared to literature, non of the patents consists of fins with force or displacement input to pre-curve the fin structure and therefore reach underneath the object.

A different contact force shape adaptive mechanism is shown at C-6. The special internal cross links created a shape adaptive structure which forces the tips of the gripper to reach underneath the object. To this extent, several uniform membrane shape adaptation mechanisms can be noticed: B-6, D-9 and D-10. The membrane uniformly deforms around the outer contours due to the normal contact forces of the object onto the membrane. This could be useful for a potential chicory gripper design for which large contact areas reduce surface pressure on the object, resulting in non-damaged chicories.

Looking at actuation mechanisms, A-5, A-10 A-11, B-2, B-3, B-7, B-8, B-9, B-11, C-9, D-1 and D-6 are interesting. These mechanisms translate input rotation or translation into grasping motion. The same limitation for these mechanisms holds as for the grippers found in literature: sufficient life time of the hinges is essential. To this extent, the hinges in grippers A-11, B-11 and D-1 look sufficient robust. Patent descriptions do not elaborate on the performance of the gripper unfortunately. During the detailing and prototyping phase, robustness will be evaluated on the gripper designs.

Gripping based on friction forces only is not preferred. To this extent, gripper mechanisms D-1 and D-3 are promising due to the movement of the finger tips. In both designs, the tips of the grippers follow a trajectory which first touches the object from underneath. This would be beneficial to avoid normal forces on the chicory.

Because the grippers in this paragraph are patented, limitations of implementing certain mechanisms in a chicory gripper mechanism are present. Sales related actions with these specific gripper components are not allowed. Using them as inspiration to boost creativity in a design process is permitted though.

Table 2.1: EPO compliant gripper classification structure. The first column represents the classification symbol and number (provided by EPO) for easy access and search within the compliant gripper database. The second column presents the description of the corresponding classification symbol.

Classification symbol:	Title and description:
B	Performing operations; transporting,
B25	Hand tools; portable power-driven tools; manipulators
B25J	Manipulators; chambers provided with manipulation devices
B25J15/00	Gripping heads
B25J15/12	With flexible finger members

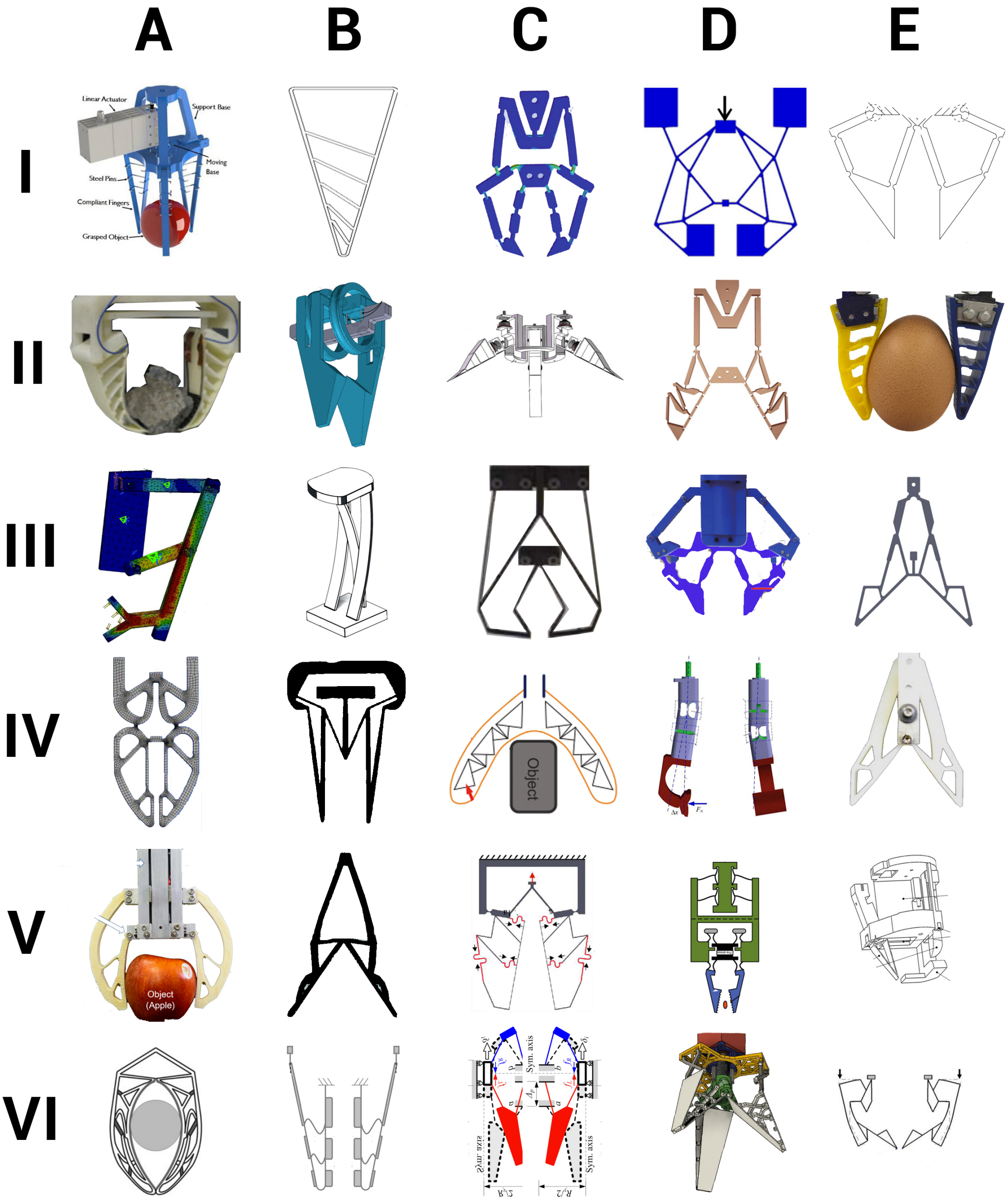

Figure 2.1: Literature overview of interesting compliant grippers, form left to right, top to bottom [3, 7, 8, 10, 12, 14, 17–20, 24, 26, 30, 31, 33, 34, 41, 45, 46, 49, 50, 58, 62–65, 76, 79, 86, 87]. The roman numerals represent the y axis of this figure grid and the letters represent the x axis of the figure grid. A combination of x and y coordinates refers to a single gripper picture within the figure (for example: A-I refers to the left top gripper picture of [3]). The coordinate system is used to refer to a specific gripper picture within this chapter. This figure represents academic literature only and is indicated by roman numerals on the y axis.

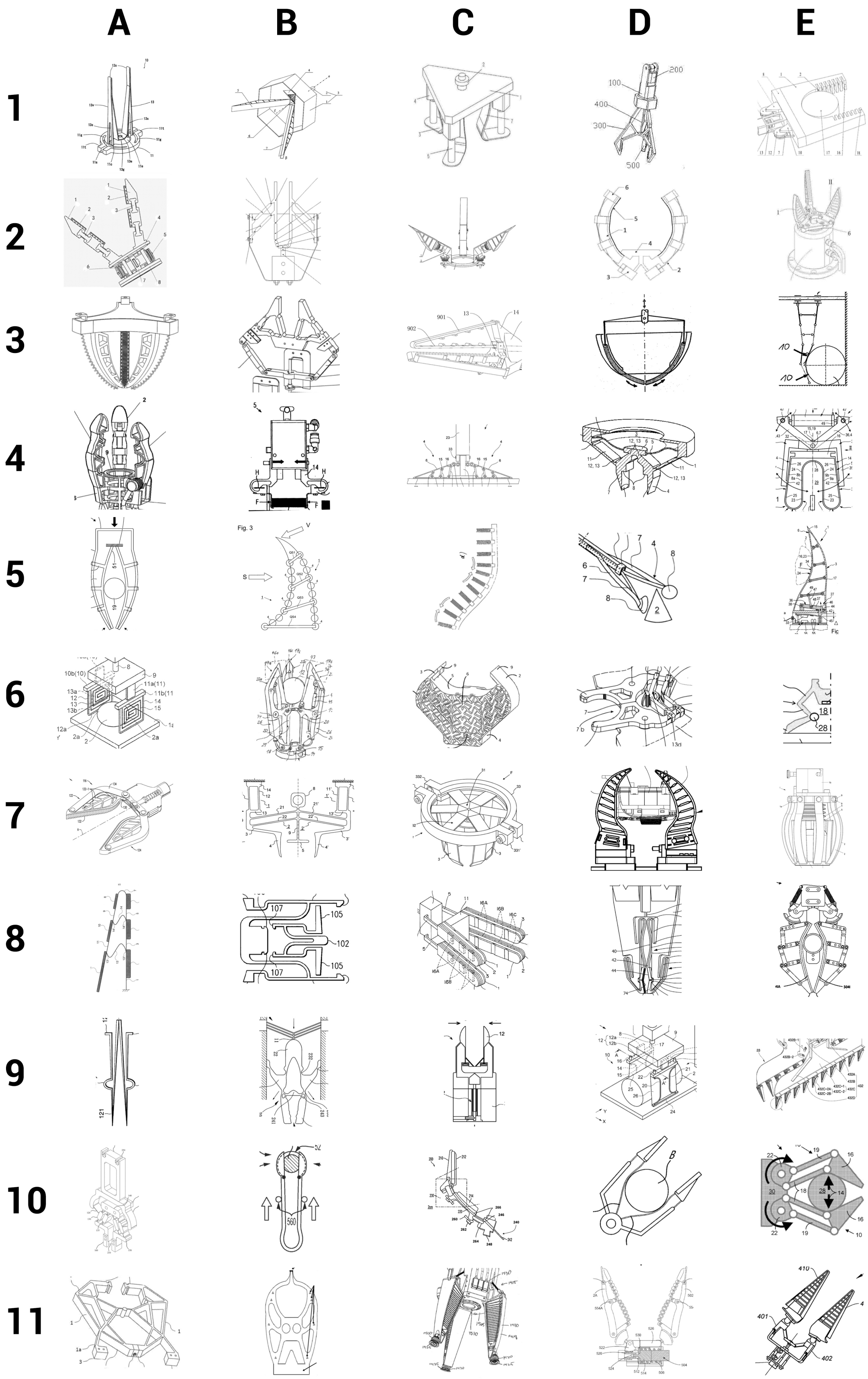

Figure 2.2: Patents overview of interesting compliant grippers from left to right, top to bottom: [59], [77], [80], [84], [83], [52], [47], [25], [15], [51], [6], [32], [85], [82], [67], [68], [37], [38], [61], [48], [23], [27], [28], [39], [57], [73], [5], [36], [53], [21], [81], [55], [56], [29], [22], [40], [2], [4], [75], [54], [60], [75], [16], [74], [13], [43], [72], [1], [11], [42], [69], [70], [44], [35] and [71] within B25J15/12/ patent classification. The numbers represent the y axis of this figure grid and the letters represent the x axis of the figure grid. A combination of x and y coordinates refers to a single gripper picture within the figure (for example: A-1 refers to the left top gripper picture of [59]). The coordinate system is used to refer to a specific gripper picture within this chapter. This figure represents patent literature only and is indicated by regular numbers on the y axis to deviate form the academic literature of figure 2.1

2.3 Conclusions

Among the grippers extracted from current academic literature and patents, several core working principles are noticed. Compliant grippers deform due to rotation input, displacement input and/or contact forces of the object onto the finger mechanism (disregarding exotic mechanisms as magnetism and shape memory alloy grippers). Rotation and displacement inputs are also combined with contact force deformation as visualised in figure 2.3. Looking at rotation and displacement inputs, movement conversion form rotation into translation or vice versa is caused by the compliant mechanism.

The contact deformation can be subdivided in uniform shape adaptation and hinged shape adaptation. Uniform bending structures can be seen as one part without specific hinging locations which bend entirely. Hinged structures do have clear hinges, usually indicated by material thickness reduction or classical rigid hinges (figure 2.3). Uniform shape adaptation can be separated in membrane shape adaptive grippers and fin adaptive gripper. The difference between these is the presents of crossbars in the fin structure. Membrane structures are only supported at the begin and end of the membrane.

Investigating the stain energy (U) stored in a hinge or uniformly bending beam shows a clear difference.

$$U = \frac{M^2 L}{2EI} = \frac{6M^2 L}{Ebh^3} \tag{2.1}$$

with $I = \frac{bh^3}{12}$ for rectangular cross-sectional beams. Hinges are typically thinner (h) and smaller (L) compared to the surrounding rigid bodies. Therefore, strain energy (U) stored in a hinge is generally less compared to a uniformly bended beam due to the larger length (L) and larger cross-sectional height (h). Therefore, uniform beam bending is probably more suitable to withstand relatively high acceleration forces of the object onto the gripper.

Important considerations are the robustness of hinges within the design. The hinges are typical weak spots for compliant mechanisms. Using tough and ductile materials within the entire design and especially within the hinges is essential for decent lifetime expectations. Speaking about materials, [20] uses extremely flexible and tough material for the fin structure. This material is called Ninjaflex and can be 3D printed. Due to the use of a 3D printer, significant form freedom is created. In addition, stiffness variations of this material are available. This material needs to be taken in serious consideration for the design process.

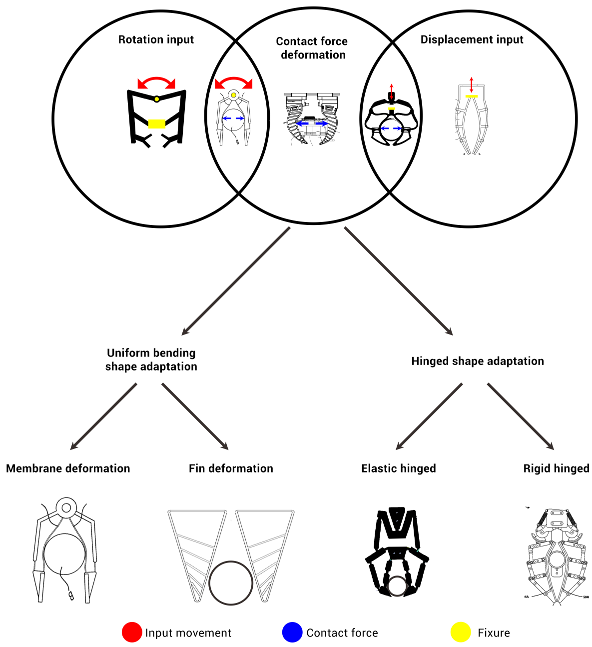

Figure 2.3: Adaptive compliant gripper deformation mechanisms principles scheme as a systematic categorisation of compliant grippers. Grippers can consist of rotation input or displacement input. Both can be combined with contact force deformation. The contact deformed grippers can be subdivided in uniform bending shape adaptation grippers or hinged shape adaptation grippers. These two sub groups can be subdivided in membrane deformation or fin deformation and elastic hinged or rigid hinged respectively. The arrows in red indicate the motion of the input, blue indicates the contact forces and yellow indicates the fixation point. Image references: [24],[11],[29],[33],[27],[7],[8] and [74]

3

Design requirements

3.1 Object

The length of the chicory is varying from 90 mm – 200 mm. According to the length variation, a diameter variation of 30 mm – 60 mm is present. The gripper needs to be able to grip and hold the chicory of all size variation combinations. The weight depends on the size obviously. Therefore, the gripper needs to be able to grip and hold chicory of 40 gram – 300 gram, excluding the acceleration forces. The orientation of the chicory refers to figure 3.1.

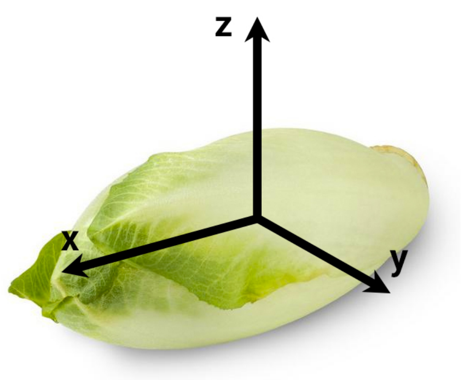

Figure 3.1: Coordinate system of the chicory. X axis corresponds to length or depth, y axis corresponds to width and z axis corresponds to height of the chicory.

3.2 Robot handling

The FlexPicker robot (ABB IRB 360-6/1600) is generally used in industry to perform pick and place actions of a variety of objects. This robot type is the industrial standard for fruit and vegetable sorting as well. This specific robot variant can be loaded up to 6 kg, but is preferably loaded as light as possible to increase the translation speed of the robot head. The linear acceleration of the robot reaches up to 9 times gravitational acceleration. This acceleration depends on the loading due to the weight of the object and the gripper. A heavy robot head moves slower than a light weight robot head due to inertia. The working range of the robot is defined in figure 3.2.

A fast sorting process is needed to make the sorting machine profitable. This affects the pick and place cycle time. A maximum cycle time of 1.3 seconds on average, including: picking, placing and returning to the home position is required depending on the pick and place location. Longer travel distances require longer cycle times obviously. The cycle times are achieved by loading the robot up to a maximum of 2 kg containing gripper and object. These requirements result in an estimated gripping and release time of 0.3 seconds each.

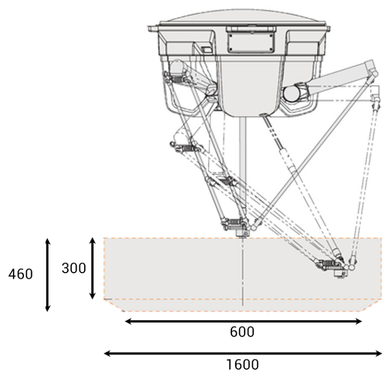

Figure 3.2: FlexPicker Robot work space according to [9]. The robot head can move max. 1600 mm in horizontal direction with a corresponding max. vertical movement of 300 mm. The max. gripper height is therefore 300 mm to reach within the full horizontal work space of the robot.

The working space defines the maximum height of the gripper. To ensure that the gripper is able to reach within the full working space of the robot, a maximum height of 300 mm, including an attached chicory, is required. Not only the working space requires a gripper height limitation, also the transporting crates in which the chicories are placed are involved in this height restriction. Due to the working space limits, the robot head, including the gripper, needs to be able pass over the edge of the transporting crate without collision. With a maximum gripper height of 300 mm, collision can be avoided.

To be able to mount the gripper onto the robot, two M6 bolts separated 40 mm (centre to centre) need to be present. The bolts are screwed into the robot mounting head. Speaking of actuation facilities at the robot head, compressed air, vacuum and electricity are present.

3.3 Design space

The first phase of the gripping cycle requires picking the widely separated chicory from the flat-belt conveyor (figure 3.3). The second phase of holding the object during translation provides no additional requirements for the design space. The third phase of placing the object requires the gripper-robot combination to be able to place the chicory side by side without damage, with a maximum spacing of 10 mm (figure 3.4). A small drop of the chicory during placement on the supporting drop surface is preferably avoided. An additional task contains releasing the chicory into a transportation crate, side by side and on top of each other with the same side by side spacing of 10 mm (figure 3.5). No further explicit dimensional restrictions are present, disregarding the previously discussed gripper height.

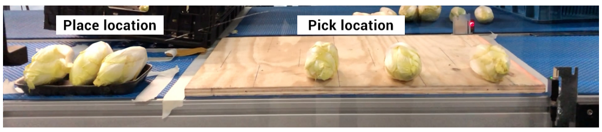

Figure 3.3: Flat surface pick and place locations. On the right: pick up configuration were chicory is separated over 10 cm from each other. The place location is on the left were the chicory is placed side by side on a flowpack containing three chicories separated 10 mm max.

Figure 3.4: Side by side placing of chicories in close up with a max. separation distance of 10 mm after placement.

Figure 3.5: Side by side positioned and stacked chicory in a transportation crate. This crate is carried by the output conveyor belt of figure 1.1.

3.4 Food grade

Because the gripper is in direct contact with the chicory during handling, food grade product regulations are obtained. Therefore, non-food additives for lubrication or friction are prohibited. To avoid poisoning chicory consumers with gripper material transferred onto the chicory surface, a migration limit of 60 mg/kg food or 10 mg/dm^2 food is required (according to [66]). This requirement includes a food grade contact material of the gripper. In addition, the gripper design needs to be thoroughly cleanable and maintainable to avoid cross contact contamination of different product batches.

3.5 Performance metrics

To account for acceleration forces of the chicory onto the gripper, several force performance experiments can be done. The acceleration acts in three directions x,y and z, or a combination. Z-directional acceleration corresponds with the vertical direction, x-direction along the length of the chicory, and y- direction corresponds to the width direction (figure 3.1). The 9G acceleration applied onto the chicory results in a maximum of $F_{res} = 0.3kg * 9 * G = 26.5N$. To check for this requirement, an easy experiment with a 2.7 kg gravitational payload in x,y and z direction on the object can be performed. Loading in z direction is essential to be able to hold the chicory during lift off. To translocate the chicory, the gripper needs to be able to withstand the 2.7 kg load in ether x or y direction. Because the robot is able to rotate the gripper around the z axis, x directional displacements can be converted in y direction and vice versa. So, ether x or y directional loading in combination with z directional loading is sufficient for the force requirement of the gripper. Ideally, the gripper can hold the load in x,y and z direction. In addition, the gripper needs to hold the loading conditions for a cycle time of 1.3 seconds minimal.

To test for robustness of gripping variable orientated objects of varying weights and dimensions, a series of picking and release actions needs to be performed. Because the gripper is not always positioned ideally, small position perturbations of the chicory need to be compensated by the gripper as well. These position perturbations can be in terms of object rotations (around z axis) and translations in xy plane, or in gripper positioning height in z direction. An allowable gripping failure rate is therefore set to 1:1000.

To be able to make the gripper implementable for industrial purposes, an endurance test needs to be done. The endurance is a tradeoff between retail price and life time of the gripper. Expensive industrial grippers (thousands of euros) are admissible but have to survive duty for years. In contrast to cheap suction cup replacements of several euros which are allowed to withstand duty in terms of days. A metric for the endurance is therefore expressed in cost per sorting action. Manual sorting can be done with 30 chicories every minute maximum, resulting in 1800 chicories per hour, divided by a €30/hour employee salary cost, results in approximately €0.016 cost per manual sorting action. The harvesting period of chicory reaches from the beginning of October to the end of November. These two months contains 320 working hours. Within these 320 working hours, almost 1 million sorting actions can be performed by the robot based on a 1.2 second cycle time. In terms of salary costs, sorting 1 million chicories manually would cost around €16.660. To be able to return investment costs of the entire robotic sorting machine by the farmer, an estimated gripper purchase price is set to 10% of the employee costs. Therefore, an allowable price for a gripper which is able to perform 1 million gripping actions is estimated on 1666 euro. Because acceptable gripper price depends on the life time, every gripping action (pick up and drop off) requires a maximum depreciation of 0.001666 euro on the gripper purchase price. So for example, by successfully performing an endurance test of 500,000 gripping repetitions, a gripper retail price of 833 euro is viable.

3.6 Checklist

Table 3.1 provides an overview of all requirements discussed in this chapter. The requirements are grouped to be able to evaluate the requirements systematically. A potential gripper is not ready for industrial application if one of the requirements is not reached. A prototype version of the gripper leaves margin for improvement on the requirements if the limitations of the prototype are certainly resolved by the final gripper end product. In this case, additional argumentation will be required.

Table 3.1: Measurable gripper requirements numbered and subdivided in categories.

Requirement:	No.	Description
Object	1	Gripper is able to grip chicories with length variation 90 mm - 200 mm.
	2	Gripper is able to grip chicories with diameter variation 30 mm - 60 mm.
Forces	3	Gripper is able to grip chicory weight variations 40 gram - 300 gram.
	4	Gripper withstands 26.5N of acceleration force in x or y and z direction for 1.3 seconds.
Damage	5	Gripper is able to grip the chicory without contact surface pressure damage.
	6	Gripper is able to grip the chicory without cutting edges.
Robustness	7	Gripper as a pick up or release failure less than or equal to 0.1%.
	8	Gripper withstand a maximum depreciation of 0.001666 euro per gripping cycle on the gripper retail price.
Speed	9	Gripper has a pick up and release time less or equal to 0.3 seconds each.
Pick up and drop off	10	Gripper is able to pick up chicories on flat surfaces.
	11	Gripper is able to place chicory side by side on a flat surface.
	12	Gripper is able to place chicory side by side in crates.
Design space	13	Gripper is mountable on the robot head.
	14	Gripper has a weight equal to or less than 1.7 kg.
	15	Gripper has a height equal to or less than 300 mm.
Food grade	16	Gripper is able to perform without non-food additives
	17	Gripper has a migration limit less than 60 mg/kg or 10 mg/dm^2
	18	Gripper is thoroughly cleanable
	19	Gripper is thoroughly maintainable

4
Concept design

4.1 Idea generation

4.1.1 Morphological chart

The ideation phase started with generating ideas. During this phase wrong or bad ideas do not exist. A useful tool to generate principal solutions for the gripping problem is the morphological chart. With this chart, an analytical and systematic overall function sub deviation is provided. This function sub deviation serves as starting point for the concept drawings. Figure 4.1 shows the morphological chart which is used to gather ideas. On the vertical direction, all relevant sub-functions for the gripper problem are specified. Horizontal direction shows all possible solutions for that specific sub problem suggested by (patent) literature. The first important function is to be able to reach underneath the object to avoid unnecessary normal forces on the side of the object. This can be done by regular fin curvatures, tilted crossbar fin curvature, flexible hinging tips, rigid tips or sliding tips according to existing literature. The next important aspect of the gripper problem is the force and shape adaptation behaviour. According to current literature, this can be solved by six possible solutions: contact deforming fins, 3D varying contact deformation structures, prescribed form deformation, complex energy absorption, normal force membranes and guided membranes. The actuation mechanism for a compliant gripper consists of uniform beam bending, hinge bending or a combination of both. To this extent, the actuation input can be varied among these actuation mechanisms. Therefore, actuation input can be specified as linear displacement input, rotational input, pressure input, magnetism input or heat input. By connecting principle solutions for the essential sub problems, a general solution for the gripping problem can be formed.

General remarks according to this morphological chart: the heat actuation input is not suitable for a compliant mechanism in this application. Operational speed of the heat actuation is to slow currently. Therefore, the heat actuation symbol has been crossed. A different remark refers to the striped circles which indicate three additional features which can be included in all concepts to improve the gripping behaviour. The 3D varying contact structure for example can be extended along the length (x direction) of the chicory to adapt the griping force to the specific local damage resistance requirements of the chicory. To this extent, the energy absorbing structure can also be used in all potential concepts to influence contact forces or gripper stiffness. Slightly different, but probable still applicable to some of the concepts, pressure input into an internal hollow structure can be used to create a certain motion. This pressure input type can for example be substituted with the conventional linear displacement input.

The blue principal solution (figure 4.1) contains a regular fin curvature with fin contact deformation, uniform bending and linear input displacement. This combination is not very innovative and is already widely used in industry by companies as Festo for example. Creating concepts based on a regular fin gripping working principle creates better understanding of current gripping solutions. Gripper concept 1 will be based on this blue principal solution.

The bright green principal solution consists of a fin with tilted crossbars to reach underneath the product, combined with a prescribed form deformation, uniform beam bending and linear displacement. Gripper concepts 2 and 3 will make use of these principle solutions combinations.

The Dark green combination is similar to the bright green principal solution but deviates in principle to position the tip underneath the object. This dark green principle solution uses flexible hinging tips instead of tilted crossbar fins. Gripper concepts 4,5 and 6 are based on this combination of sub solutions.

The orange idea cluster combines flexible hinging tips with a prescribed form deformation via hinge bending actuated by linear displacement. Gripper concept 7 is based on this combination.

The red concept creation consists of rigid tips combined with a guided membrane and uniform beam bending mechanism, actuated by linear displacement. Gripper concept 8 is based on this combination.

Finally, the pink solution combination consists of flexible hinging tips with a prescribed motion and a hing bending structure which is activated by magnetism. This is similar to the orange idea combination except for the magnetism part. Concept 9 is based on this pink idea combination.

The next step was to design a gripper mechanism on paper and evaluate the performance of the concepts by a FEM analysis using the ANSYS APDL 19.2 software. With this software a combination of points in space can be linked together with an element. These elements form the gripper mechanism. By fixing specific nodes and applying forces on others, a gripping motion can by simulated. The elements of the gripper bend according to the specified material properties. To be able to compare gripper concepts, material properties are equal. The E-modules for all concepts has been set to 3 Gpa, as average plastic. Similarly, poisson's ratio has been set to 0.3 for all concepts. Actuating the gripper concepts in the simulation is done by a force or moment input up until the gripper was closed entirely if this was possible. The first task was to create a decent motion of the tip to reach underneath the object. This objective can be measured by evaluating the angle between the the inside of the gripper tips and the horizontal x-axis (for example, element 6-9 of concept 1 in the left top image of figure 4.2 after actuation as shown in the top right image of figure 4.2). The second task was to handle the object gentle without damage. This part will be addressed as soon as the tip movement mechanism is selected. This order of design priority within the compliant gripper was deliberately chosen. Simply because damage and form adaptation are useless when the gripper is unable to pick the object properly. Nevertheless, handling and picking mechanisms are equally important for the final gripper design.

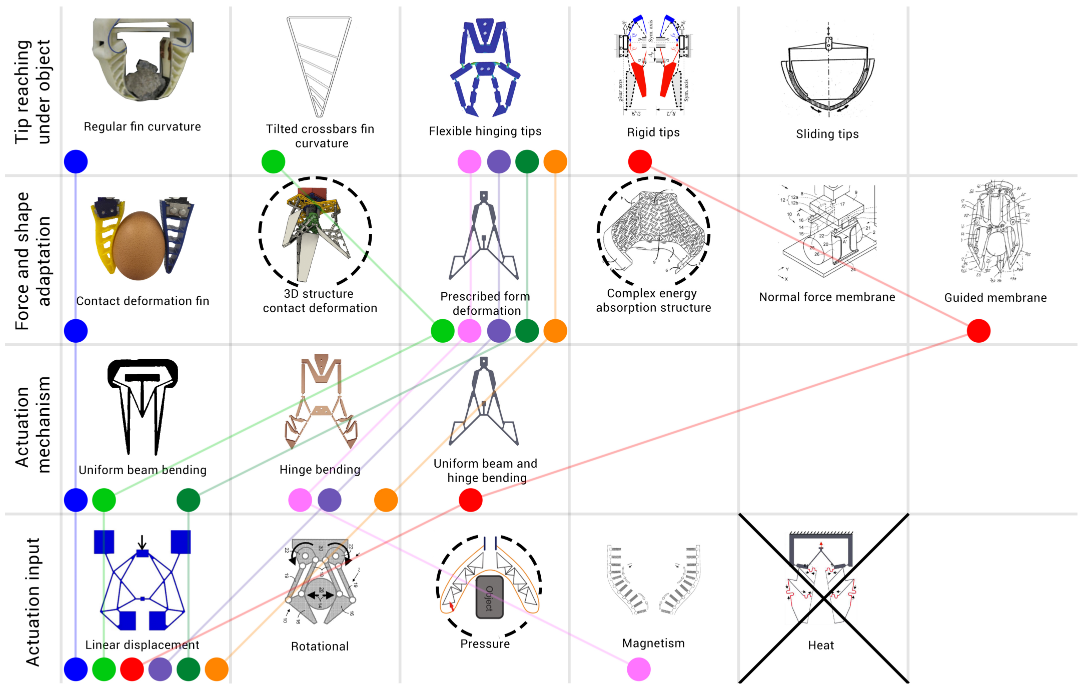

Figure 4.1: Morphological chart for compliant gripper idea generation based on current (patent) literature. The first column represents the sub functions of the gripper problem. The other columns represent possible solutions for the sub functions. The colored dots and lines represent a combination of sub solutions to potentially solve the entire gripping problem. Blue represents concepts 1, bright green represents concepts 2 and 3, dark green represents concepts 4,5 and 6, orange represents concept 7, red represents concept 8 and pink represents concept 9 of the concept drawings. The sub solution of heat input is crossed because the actuation speed is to slow. The circled solutions of pressure, complex energy absorption and 3D contact deformation can be applied to all individual concept afterwards to improve gripping performance.

4.1.2 Concept drawings

The first concept drawing consist of a diamond shaped compliant actuation mechanism (node 1 to 4 in figure 4.2). The node 4 of the diamond is fixed and node 1 is displaced by an input force in negative z direction (corresponding to figure 3.1), as indicated in figure 4.2. The fingers of the gripper are regular fin grippers with slightly precurved edges. The cross bars within the fins are only for contact force shape adaptation and do not contribute to the movement of the tips. Therefore, the simulation is performed without the crossbars. This reduced the programming and computation effort. Due to the bending of the diamond shape, the two fingers rotate inward. The precurved inside of the fingers generate an empty space to hold the object. In terms of tip movement (nodes 5 and 6) of the fingers, this concept design is probably not reaching under the object sufficiently according to the animated FEM simulation. The tips of the fingers are thicker than preferred and will cause a local contact pressure peak on the object sides which results in damage. This concept uses uniform beam bending to complete the gripping motion. Compared to hinge bending, uniform beam bending requires more input energy to deform. However, the advantage of uniform beam bending refers to the holding strength of the gripper. When the object is locked in the gripper, and an acceleration force on the object is applied, a uniform beam bended gripper is able to withstand higher forces due to the higher strain energy stored. Thin hinges require less force to oppose the obtained gripper closing direction. Therefore, it is assumable that uniform beam bending is more suitable for this specific gripper problem due to the presents of high acceleration forces generated by the sorting robot.

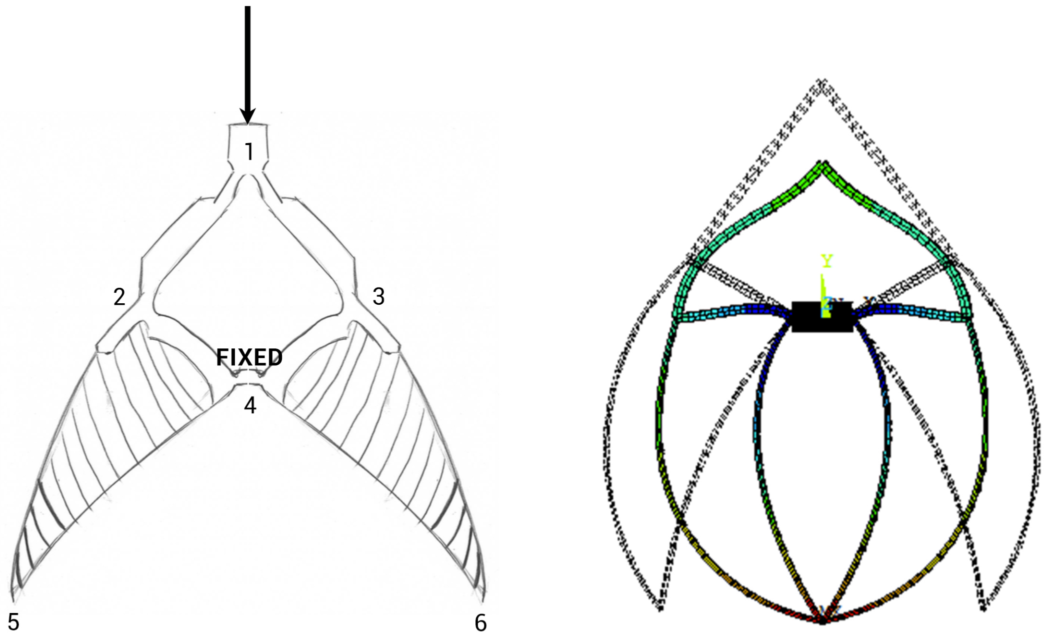

Figure 4.2: Gripper concept 1, design drawing (left) and FEM displacement estimation (right). The numbers in the drawing represent nodes on which elements between the nodes are connected. Node 4 is fixed and node 1 is vertical displaced as indicated by the arrow. The color gradient in the FEM model represents the relative displacements of the finite elements reaching from blue to red were blue indicates small relative displacement and red large relative displacement.

The second design drawing (figure 4.3) consists of a fin structure as well. In this case, the crossbars in the fins are tilted and precurved. As expected in the first design drawing, crossbars do not influence the tip movement without the presents of object contact force. The shape of the actuation mechanism (nodes 1 to 8) is different as well. The relative thicker and "undeformable" bridge (nodes 1 to 5) on which the force is applied consists of five elements. The two outermost elements (element 2-4 and 3-5) of the bridge contain a bump which presses into the fin structure on the top side. This force should improve the precurved behaviour of the fins. The bump in the design drawing has been modeled as a link which presses on top of the fins, as shown in the top right image of figure 4.3.

To validate the impact of this bump/extra link, the exact same gripper without this extra link has been simulated (left bottom of figure 4.3). When we overlay the deformed results of the gripper with and without extra link/bump (bottom right of figure 4.3), the effect of reaching under the object is unexpectedly worse for the gripper with the extra link. This insight indicates that the obtained principle of pressing on top of the fin structure is not contributing to the aimed motion of the gripper tips to reach underneath the object.

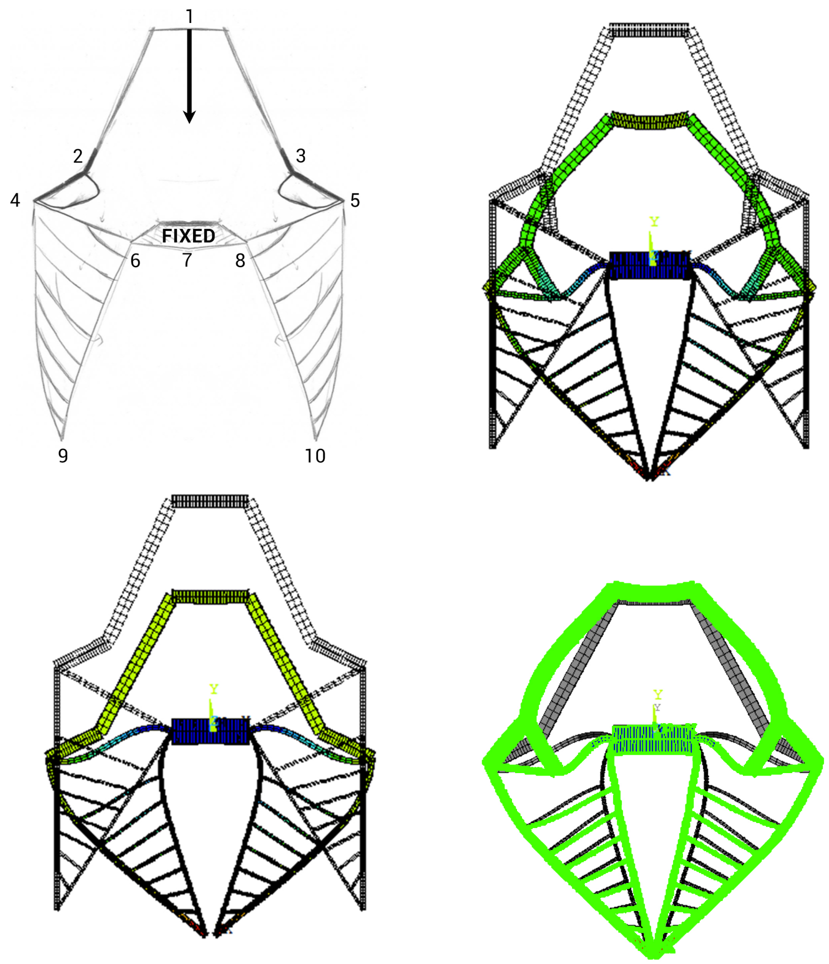

Figure 4.3: Gripper concept 2 drawing (left top) with vertical input displacement indicated by the arrow and fixation at node 7. The to right image shows a FEM analysis of concept 2 with additional links to replace the thickenings between node 2 and 4 and nodes 3 and 5 to be able to push on the middle of the element between nodes 4 and 6 and nodes 5 and 8 to enforce an extra curvature movement of the tip. The image bottom left shows the same FEM analysis of the gripper without these additional links. The image bottom right shows an overlay of the FEM models with and without extra link. The green FEM model represents the concept with additional link and the gray FEM analysis represents the concept without additional link. The model without additional link reaches more underneath the object than the model with additional link. The additional link is therefore not beneficial for the gripper performance. Again, colors of the elements indicate relative displacement reaching from blue (small displacement) to red (large displacement).

The third gripper concept differs fundamentally from the first two concepts. The "undeformable" bridge consists of three elements (node 1 to 4 in figure 4.4). In this case, the input force is applied on top of the bridge in between node 1 and 2, and the compliant mechanism is fixed at the center of the gripper (node 5). This fixation and force application location can be interchanged if this is preferable. The relative displacement between node 6 and nodes 1 and 2 matters for the actuation. Looking beyond the actuation mechanism, each finger consists of two sections: a compliant section (node 5 to 11) and a stiff tip section (node 8 to 13). The complex linkage system of this compliant section generates the best performance so far in terms of reaching underneath the object (right image of figure 4.4). This compliant section uses two bar elements (node 6 to 9 and 6 to 10) which connect the fixation point (node 6) and the rigid tip structure on the inside of the gripper mouth (node 9 and 10). These two elements cause the rigid tips to rotate inwards during actuation. This increases the performance of reaching under the object. The elements between node 3-8 and 4-11 push the outside of the rigid tip downwards under the object. To be able to hold the object without damage, both fingers enclose an empty space in actuated state. Similar to concept 2, this concept uses uniform beam bending for the actuation mechanism. Therefore the holding force is expected to be higher compared to hinge bending as previously explained.

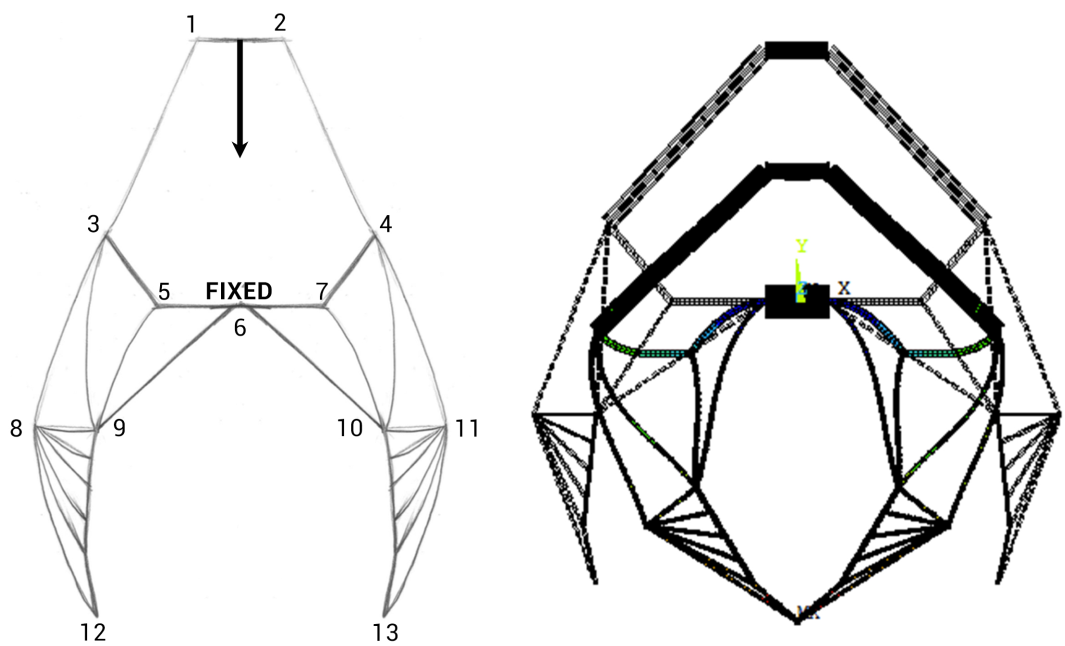

Figure 4.4: Gripper concept 3 with the design drawing on the left with vertical input indicated by the arrow and fixation at node 6. The FEM analysis on the right required a refined mesh to be able to compute the displacement of this concept. Colors of relative displacement are therefore hardly visible. This concept reaches more under the object compared to concept 1 and 2. This is beneficial to the potential gripper performance.

Gripper concept 4, 5 and 6 have similar principles. Concept 4 consists of an three element bridge (Nodes 1 to 3 in figure 4.5). The bridge is pushed down in node 1 and the mechanism is fixed in node 7. The compliant mechanism consisting of elements 2-6, 4-9,7-10, 6-9-10 on the left side, and 3-8, 5-12, 7-11, 8-12-11 on the right side, deform according to this force. Although the design drawing is not only consisting of uniform beam bending, the corresponding FEM analysis is. The tips of this gripper are based on tilted crossbar fins as previously described. The internal fin structure does not contribute to the movement of the tip significantly. In theory, this mechanism should push the tips underneath the object due to negative y directional force on nodes 6, 8, 9, 12 and positive y directional pulling forces on nodes 10 an 11. However, the FEM analysis shows just small deformations. Even with relative large forces, the mechanism is not rotating the tips inwards. Due to the shape of the mechanism, closing the gripper entirely was not possible. Therefore, the performance of this gripper is not expected to be good enough for a prototype. Changing the design parameters of the thicknesses of the beams did not improve the performance of this design. Improvements were made by adding a link between node 4-7 and 5-7. This improved the performance slightly (right image of figure 4.5).

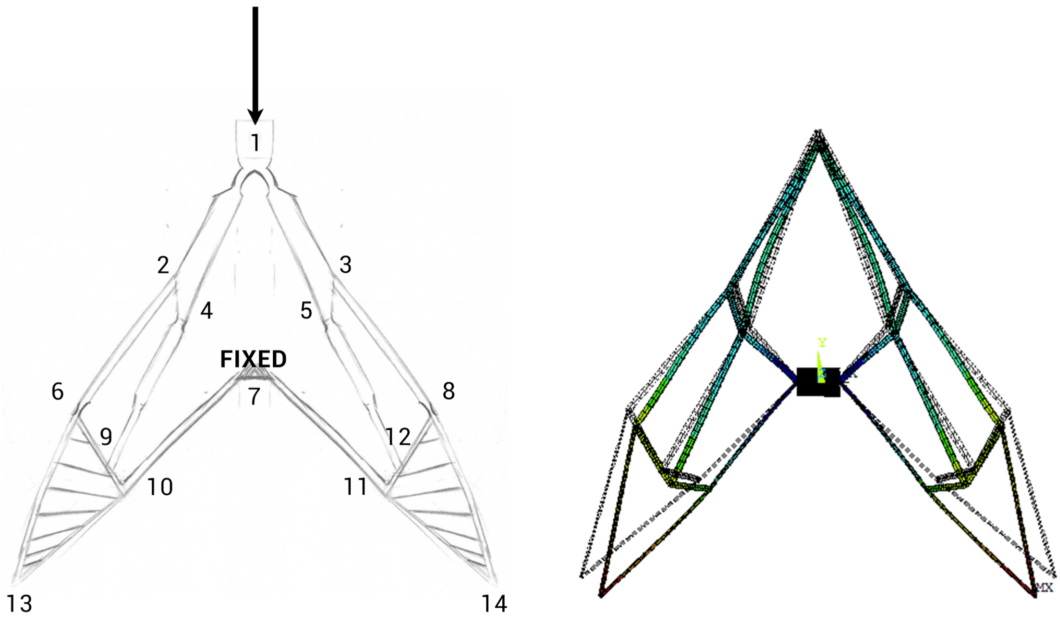

Figure 4.5: Gripper concept 4 with the design drawing on the left were the arrow indicates vertical input displacement. The model is fixed at node 7. The links between nodes 5 and 12 and nodes 4 and 9 should pull the tips of the gripper inwards. The FEM model on the right shows the max. displacement possible without running into element degree of freedom (DOF) runaway errors. Potential gripper performance is estimated to be limit for this model. Therefore, no further modeling effort is devoted to this model. Colors in the FEM model represent relative displacement reaching from blue (small displacement) to red (large displacement).

Concept 5 (figure 4.6) is similar to concept 4 but elements 4-9 and 5-12 of concept 4 have been changed to elements 2-4 and 3-4 of concept 5 respectively. The force location and fixation nodes are similar to concept 4. After applying force on the mechanism, the gripper closed entirely. The deformation of linkages 2-4 and 3-4 contributed mainly to the tip movement of concept 5 (right image of figure 4.6). Comparing this to the performance of gripper concept 3, gripper 5 does not reach under the object sufficiently.

By modifying the orientation of linkages 5-7 and 6-8 in gripper 5 to linkages 7-8 and 9-10 in concept 6, using thinner beams for elements 2-5 and 3-6 and adding new elements 4-5 and 4-6, concept 6 was created. Due to the changes, concept 6 has a larger empty space to hold the object compared to concept 5. Even the ability to reach under the object improved slightly as determined by comparing the angels between element 7-9 in concept 5 and element 8-11 in concept 6 with corresponding x-axis at closed state. To this extent, horizontal orientation (in passive state) of elements 7-8 and 9-10 in gripper 6 and elements 8-9 and 10-11 in gripper 3 contributes positively to the performance of reaching under the object. In this concept phase, a qualitative evaluation of this performance insight is not relevant yet. The effect of individual elements will be focused on in the improved concept design section.

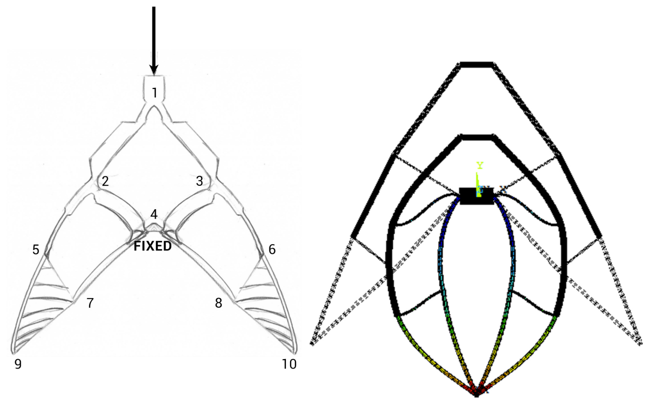

Figure 4.6: Gripper concept 5 with design drawing on the left with a fixation at node 4 and a vertical input at node 1. The FEM model on the right shows the displacement of the elements with the relative displacement of the elements indicated by the color scale reaching from blue (small displacement) to red (large displacement)

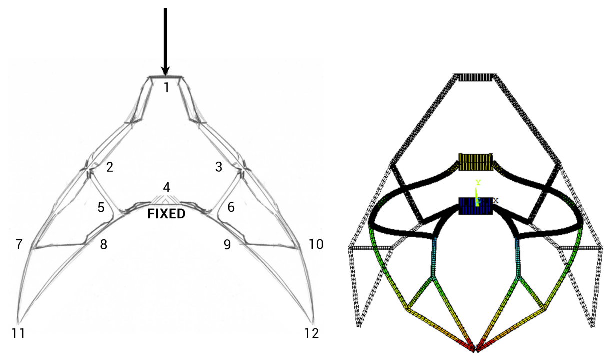

Figure 4.7: Gripper concept 6 which is similar to concept 5 with a different input compliant mechanism. Concept 5 contains a diamond shaped input mechanism and this model of concept 6 shows a variation on the mechanism. Node 4 is fixed and node 1 is vertically displaced as indicated by the arrow. The FEM model on the right shows the gripper deformation and the color scale indicates the relative displacement of the elements reaching from blue (small displacement) to red (large displacement).

Concept 7 uses the same diamond shaped actuation mechanism as gripper 6, but is elaborated with several additional elements in the top section of the compliant finger mechanism. The fingers consist of two parts, a top part (nodes 2-6-9-12 and 3-7-10-13 of figure 4.8) and a bottom part (nodes 8-9-12-14 and 10-11-13-16). The bottom part acts as a regular fin and the top part extents the working principle of the compliant diamond shaped actuation mechanism (nodes 1 to 3 and 6 to 7). The main focus of this concept is gaining insight in the influence of the crossing elements 4-12, 6-9, 5-13 and 7-10. These crossed elements are not linked together on the intersection. In practice, this should be designed as two linkages behind each other. In fist instance, the FEM model was identical to the concept drawing. After the first simulation run, the essential presents of linkages 2-8 and 3-11 was discovered. These have been added to the FEM analysis gripper design of concept 7 (right image of figure 4.8).

In theory, elements 4-12 and 5-13 should rotate the tips of the fingers inward by pulling the inside of the tips upwards. In combination with the force of elements 7-10 and 6-9 applied on the outside of the tips should result in a rotation of the tips underneath the object. In practice, this appears to be partially true according to the right image of figure 4.8. Comparing the performance of gripper 7 to gripper 6 and/or gripper 3 shows an insufficient tip rotation of concept 7. In addition, the impracticality of the overlapping linkages resulted in low performance expectation of this concept.

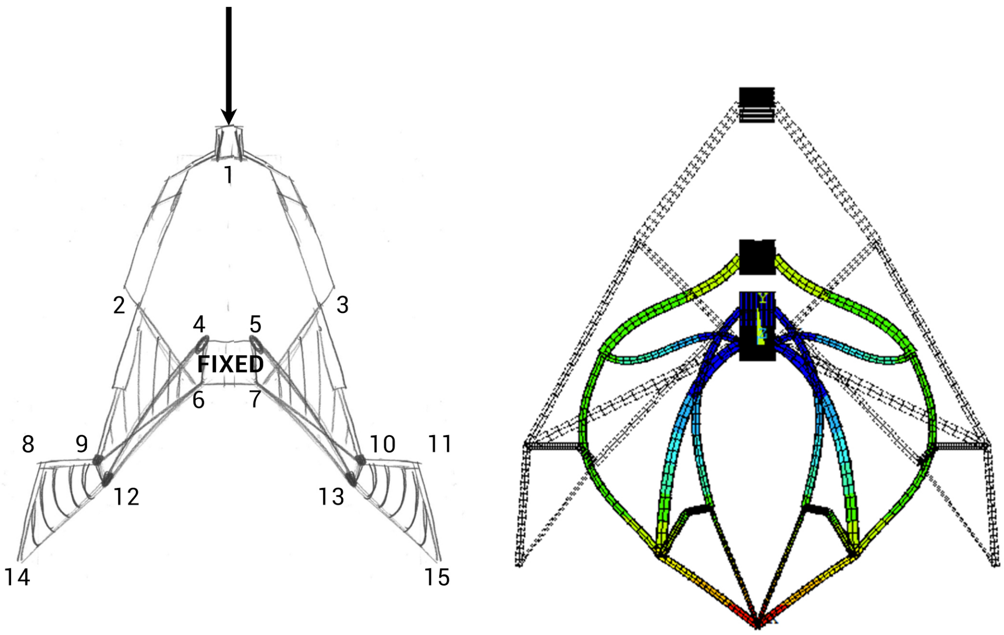

Figure 4.8: Gripper concept 7 with concept drawing on the left were nodes 4,5,6 and 7 are fixed on displacement but not on rotation. Node 1 is vertically displaced as indicated by the arrow. The links between nodes 5 and 13, nodes 7 and 10, nodes 4 and 12 and nodes 6 and 9 are designed to turn the tips of the gripper inward during actuation. The FEM analysis shows the displacement of the gripper with a colorized relative displacement indication scale from blue (small displacement) to red (large displacement).

Gripper concept 8 (figure 4.9) made use of the membrane concept. By enclosing the object with a relative "undeformable" structure (elements 5-10 and 9-11) and the deformation of the membranes (elements 7-10 and 8-11) according to the shape of the object, a shape adaptive normal force grip is formed. This concept used flexible hinges (elements 3-7, 3-8, 4-6 and 5-9) to establish the rotation of the fingers. These hinges need to be tuned to be able to hold the object in all required conditions. Thicker hinges require more input force, but are able to withstand higher acceleration forces.

Looking at the movement of the finger tips is less relevant for this gripper concept because the grip is based on a normal force grip on the sides of the object instead of load carrying normal forces from underneath the object. By applying force on node 3 and fixing element 1-2, the fingers start to rotate inwards. The fixation and force input location can be interchanged. Due to the normal contact forces on the sides of the object, the membranes start to deform. This deformation is adaptive to the outer contours of the object. By tuning the thickness and the pretension of the membranes, a contact force threshold can be set. In addition, a thickness variation over the length of the membrane can be created to suit damage criteria for all sizes of objects.

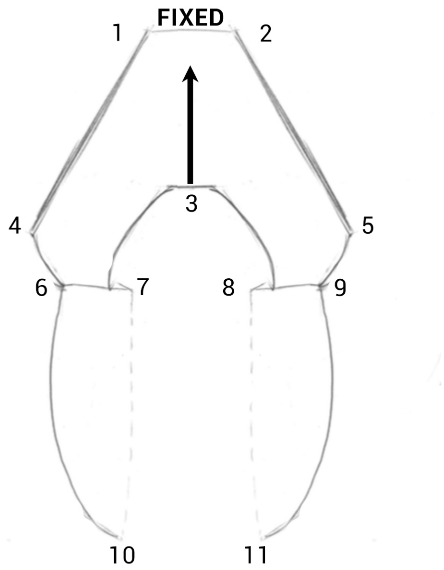

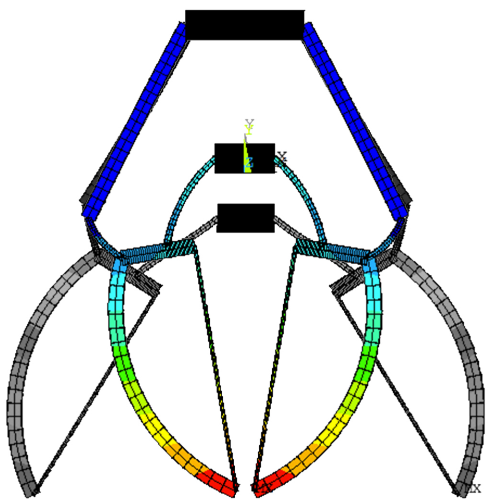

Figure 4.9: Gripper concept 8 with a contact deforming membrane to maximize contact surface to reduce object damage. The arrow indicates the vertical displacement input of node 3. Nodes 1 and 2 are fixed. The right image shows the FEM model of the gripper deformation. The color scale indicates the relative displacement of the elements reaching from blue (small displacement) to red (large displacement).

In gripper concept 9 (figure 4.10), tip rotation differs fundamentally form the other concepts. This concepts uses magnetic forces to rotate the tips. The fixation and force input locations are similar to the previous concepts. Therefore, the actuation mechanism reduces the relative distance between the fixation and force input location. This input force resulted in a pinching motion of the finger tips. The next step was to rotate the finger tips inwards by exerting a magnetic repulsive force from the top section of the fingers (element 3-6-8-9 and 5-7-10-11) onto the lower tip section (elements 8-9-12 and 10-11-13). In the FEM simulation of figure 4.10, this is modeled as a moment input at nodes 9 and 10. The moments enforced the tips to rotate inwards. The magnetic force is illustrated with dashed lines around nodes 8, 9, 19 and 11. The timing between the displacement and magnetic input actuations is essential to ovoid collision of the fingers. Integration of the magnetic mechanism involves complex electrical wire guidance to the tips to power the electric magnets. Due to recent innovations among conductive 3D printable filaments, the power supply to the magnets can be facilitated by the structure itself. In addition, introducing magnetism into the gripper contributes to the complexity of assembling the gripper. To this extent, tuning the magnetic repulsive force will be a challenge.

4.1.3 Concept selection

Concepts 3 and 8 are most promising in terms of tip movement and shape adaptation respectively. Therefore, these two concepts will be analysed in detail on stiffness and shape adaptation. Concept 3 provides sufficient tip movement and concept 8 provides decent membrane shape adaptation. The force requirement of 26.5N in x,y and z direction is challenging for concept 8 due to the thin hinges which cause the tip motion. Combining the movement of the tip of concept 3 with the membranes of concept 8, creates a combination which potentially holds the force requirements and reduces normal forces on the object due to reaching under the object in the pick up phase and distributing the surface pressure during the holding phase.

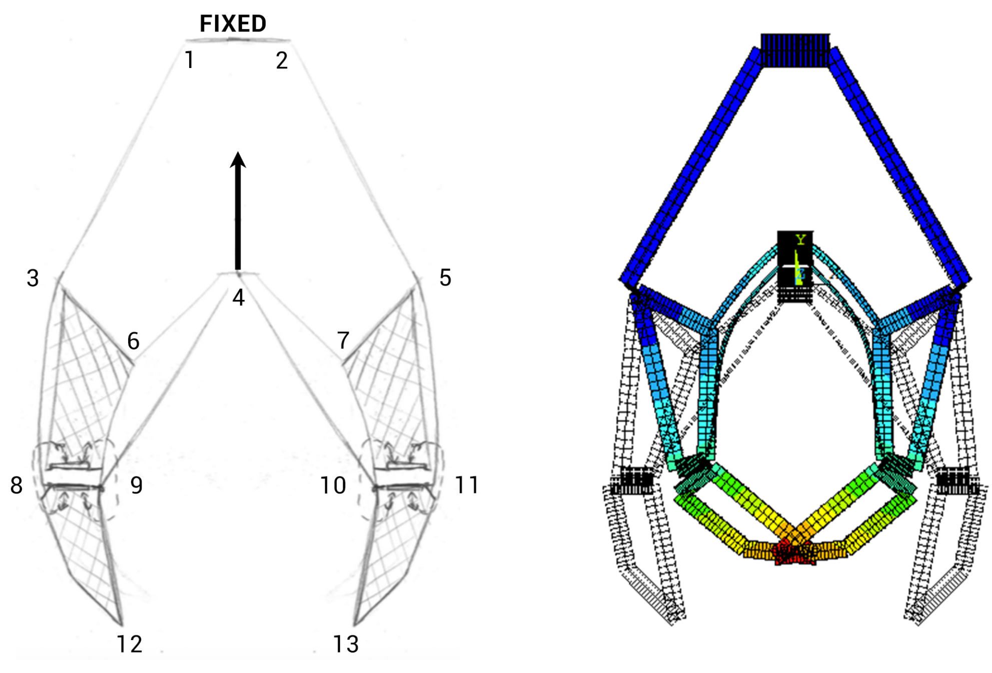

Figure 4.10: Gripper concept 9 with the concept drawing on the left and the FEM model on the right. The model is fixed in nodes 1 and 2 and displaced in node 4 as indicated by the arrow. To rotate the finger tips inward, repelling magnets are placed in nodes 8, 9, 10 and 11. The color scale of the FEM model illustrates relative displacements of the elements indicated by a gradient from blue (small displacement) to red (large displacement).

4.2 Improved concept design

4.2.1 Stiffness analysis

To create a better understanding of the working principle of gripper concept 3, a first prototype has been 3D-printed (figure 4.12). The material used for this first print is called semi-flex TPU, which is elastic and ductile. The specific brand name of the material used is "NinjaTek Cheetah". The material properties of this TPU are presented in table 4.2.1.

Table 4.1: TPU material properties

Material property:	Value:
Yield strength	9 Mpa
Yield strain	0.55
E modules	16.4 Mpa

A similar 3d printable material was used in [20]. By applying forces on the prototype (right picture of figure 4.12), linkages 10-19, 19-24, 4-12 and 12-17 (see figure 4.11) had to be made stronger to increase the chance of holding the required loading of 26,5 N. This force requirement holds for a roughly estimated linkages thickness of 3 mm for linkages 10-19, 19-24, 4-12 and 12-17 with a total gripper depth of 110 mm (figure 4.14). The acceleration force of the object is modeled on the tips distributed along the depth of the gripper as visualised in figure 4.14. With the roughly estimated stiffness adjustments, the smallest object (30 mm in diameter) and larges object (60 mm in diameter) will be capt inside the gripper (figure 4.13 and 4.13). In this case, the smallest object is loaded with the highest acceleration forces required for the gripper, even though these maximum forces correspond to the largest objects with larger mass. This principle of maximum loading in combination with the smallest object diameter represents the most extreme theoretical loading situation possible (figure 4.13). Current gripper design which holds the force requirement is set as initial reference for the performance of this gripper concept on which optimizations need to be done.

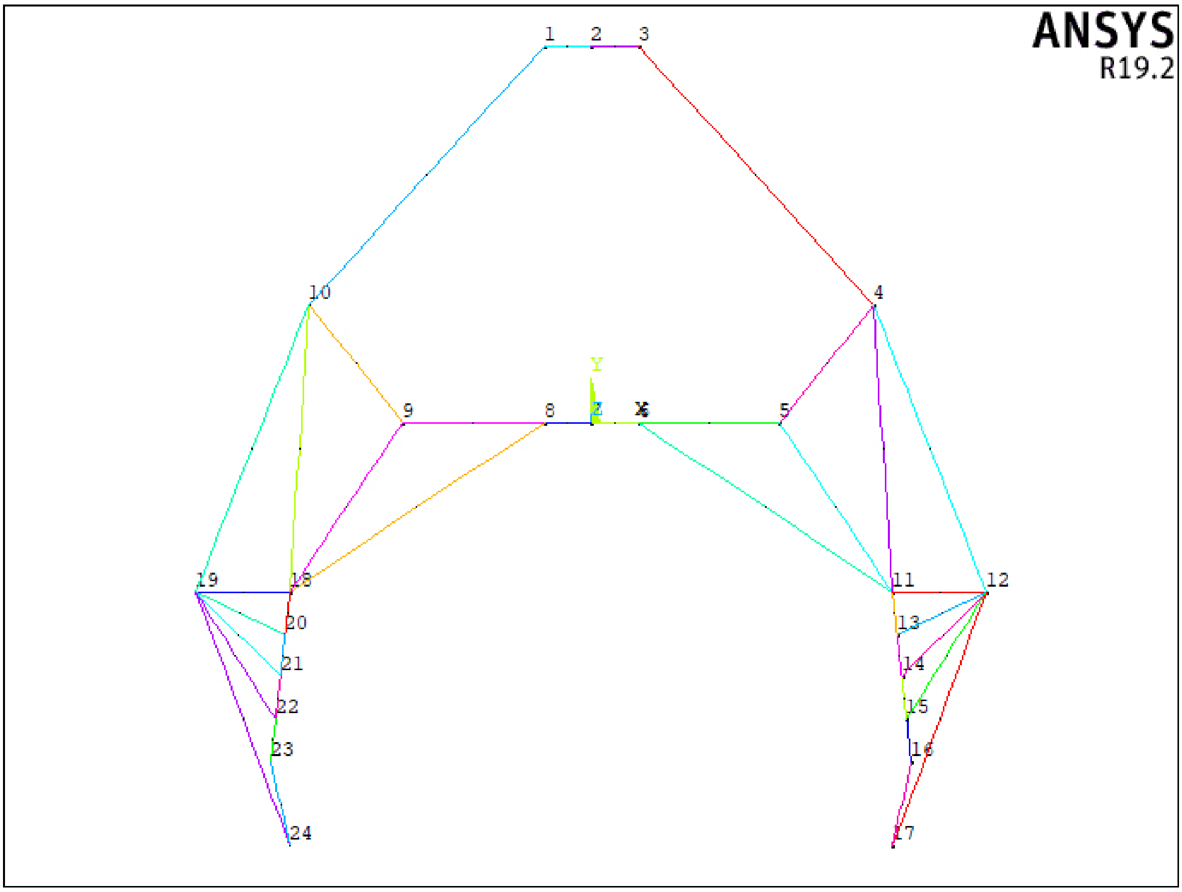

Figure 4.11: Nodes of gripper concept 3 with corresponding connecting links used to model the gripper in ANSYS.

The next step was to investigate the contribution of each link within the gripper. To this extend, linkages 1-2-3-4-10, 10-19 and 4-12 (figure 4.11) will be kept constant because these links are the main load carrying elements. Adjusting these essential links will inevitably result in failure on the force requirements. Meanwhile, the linkages presented in table 4.2 can potentially be removed, made stiffer or more compliant. These effects will be compared to the current gripper performance by a visual overlay in actuated state with and without object acceleration forces. The stiffening effect will be gained by increasing the element height to 5 mm. The compliance effect will be modeled by reducing the element height to 1 mm to be able to see the effect on the displacement of the gripper (figure 4.15).

The stiffness adjustment variations investigated in figure 4.15 have been visually evaluated by comparing the adjusted configuration with the reference (background blend in). The contribution of the adjustments of the actuation state (first column of figure 4.15) is evaluated on tip movement only. Positive effects on the ability to reach under the object have been indicated by a + sign, negative effects by a - sign and neutral effects by a 0 sign. The vertical and horizontal loading is evaluated based on finger displacement by comparing the adjusted configuration with the reference. A less deformed or bended finger is evaluated as positive contribution and a larger deformation as negative. Again, 0 indicates a neutral effect on the displacement. An overall positive effect of the proposed adjustment is reached when no negative counter effects are present. For example, the removal of element 9-18 and 5-11 results in a positive contribution only. Also stiffening element 9-10 and 4-5 serves a positive contribution on the gripper performance only. In contrast to the compliance of line 8-9 and 5-6, which result in positive effects in vertical loading but a negative counter effect on the horizontal loading. Therefore, this adjustment is not preferable. The proposed positive contributing adjustments have been updated to the design model and the overall configuration have been stiffened until horizontal en vertical loading requirements were reached. This overview of the effect of each link can be used in the iterative design process as well.

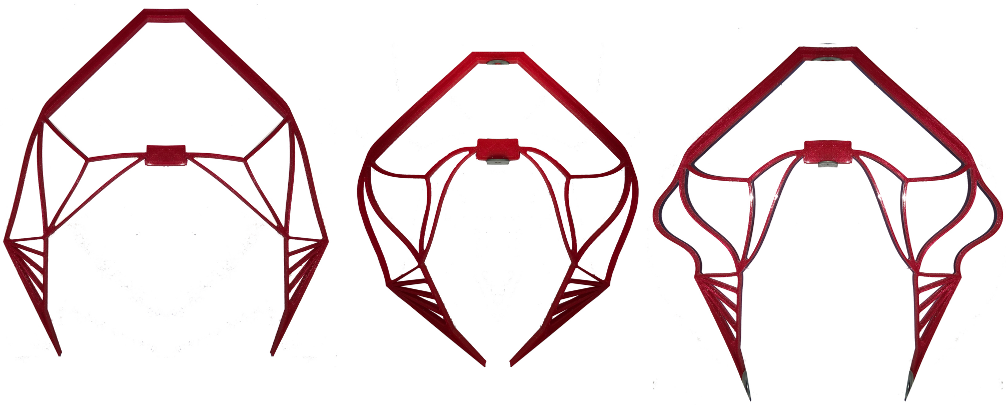

Figure 4.12: 3D printed 5 mm thick slice concept 3, in rest state (left), actuated state (middle) and deformed state by horizontal and vertical acceleration forces (right).

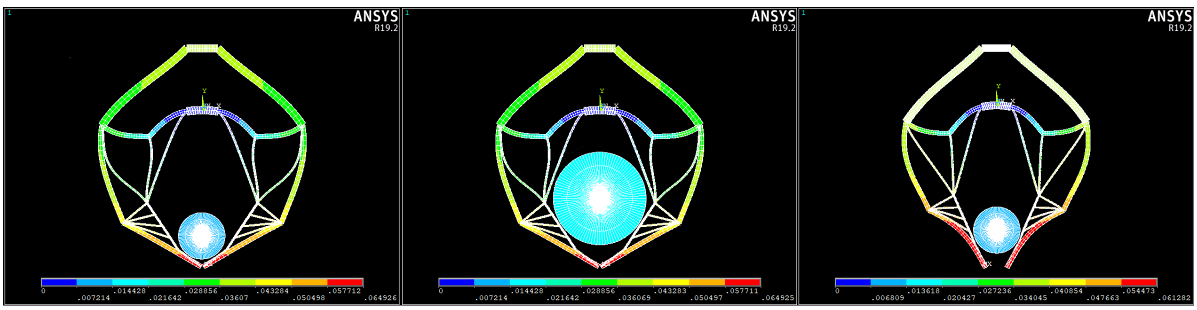

Figure 4.13: Gripper concept 3 holding large object in static conditions (left), holding small object in static conditions (middle), holding small object with max. acceleration forces in vertical direction (right). The color range indicates the displacement of the elements in meters.

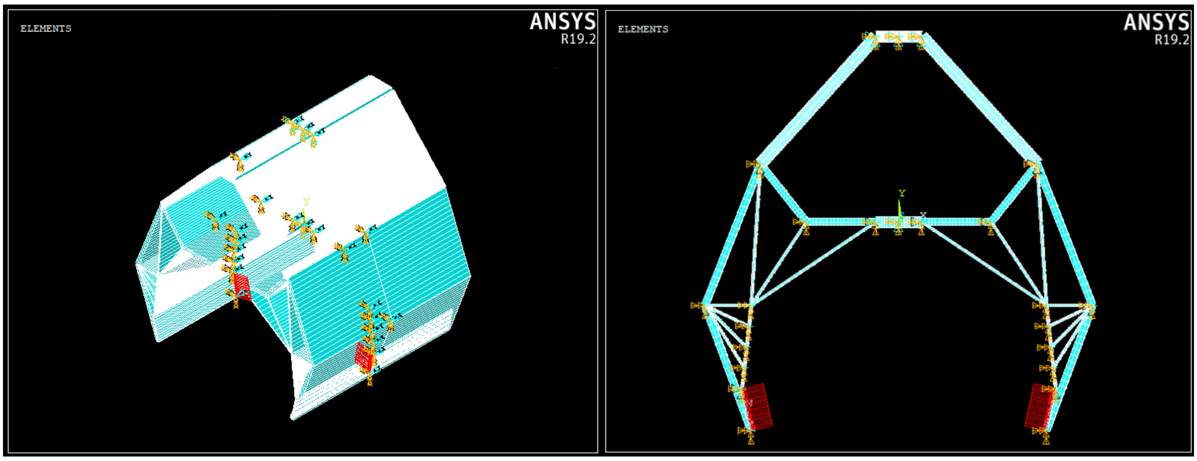

Figure 4.14: 3D view of gripper modeling in ANSYS with 110 mm gripper depth (left) and acceleration force of the object onto the gripper tips (red arrows) at the right image. After actuation of the gripper, the acceleration forces will be applied to simulate the acceleration of the robot head and translation of the chicory.

Table 4.2: Overview of linkage to be analyses on affecting the gripper performance by removing, stiffening or making the individual link more compliant.

Linkage removal:	Linkage stiffness:	Linkage compliance:
10-18 & 4-11	8-9 & 5-6	8-9 & 5-6
9-18 & 5-11	9-10 & 5-4	9-10 & 5-4
8-18 & 6-11		
19-18 & 11-12		
19-20 & 12-13		
19-21 & 12-14		
19-22 & 12-15		

4.2.2 Shape adaptation

By investigating the shape adaptation of concept 3, a lag of performance for small objects is visible (figure 4.13). When the robot translates a small chicory, with current gripper design, the chicory is able to move freely within the gripper claw. This is an unwanted effect regarding damage avoidance. However, the gripper does perform shape adaptation on larger objects, figure 4.13. To extend this shape adaptation effect towards the smaller objects several membrane layouts have been investigated. Starting with gripper concept 3.2 (figure 4.16) which has a membrane (elements 7-36-35-34-33-32-31-24 and elements 7-56-55-54-53-52-51-17 in figure B.1) with supporting cross-bars. After 3d printing this concept as 5 mm thick slice, a manual actuation have been performed by fixing elements 6-7-8 and displacing elements 1-2-3 towards element 7. This resulted in a gripper motion as predicted by previous similar gripper simulations. However, both membranes touched each other and resulted in asymmetry of the gripper displacement. This is unwanted for pinpointed place action of the chicory by the robot. In addition, the cross-bar connecting nodes of the membranes (nodes 31 to 36 and 51 to 56 of figure B.1) result in high local contact pressures on the object. This will result in damaging the chicory. Therefore, this membrane configuration is not further developed.

The next shape adaptive membrane variation is visualised in figure 4.17. This concept is called gripper concept 3.3 and features two curved membranes. The gripper configuration has been evaluated similarly to to gripper 3.2. Actually, the same limitations occur in this design: membrane interference and high local pressure on the object at nodes 16 and 23 of gripper 3.3 (see figure 4.11 respectively). This membrane is therefore also not suitable for the chicory gripper.

The next setup is called gripper 3.4 (figure 4.18). The straight membranes are similar to the membranes of gripper concept 8 (figure 4.9). The overall performance of this gripper configuration looks promising. A 5 mm thick slice of this configuration has been 3d printed as well and is evaluated similar to the other membrane setups. This membrane configuration does not interfere and does not have any high local pressure points. However, the membrane is not completely tensioned in actuated state. This could result in free movement of small objects within the gripper. To tension the membranes in actuated state, linkage 19-24 and 12-17 have been made more compliant. Therefore, the membranes will be tensioned due to the contact force of the tips, touching each other. The contact force results in a bending movement of elements 19-24 and 12-17. The bending direction increases the relative distance between node 7 and both finger tips, nodes 17 and 24 (figure 4.19). With this new working membrane configuration, a first prove of concept can be build.

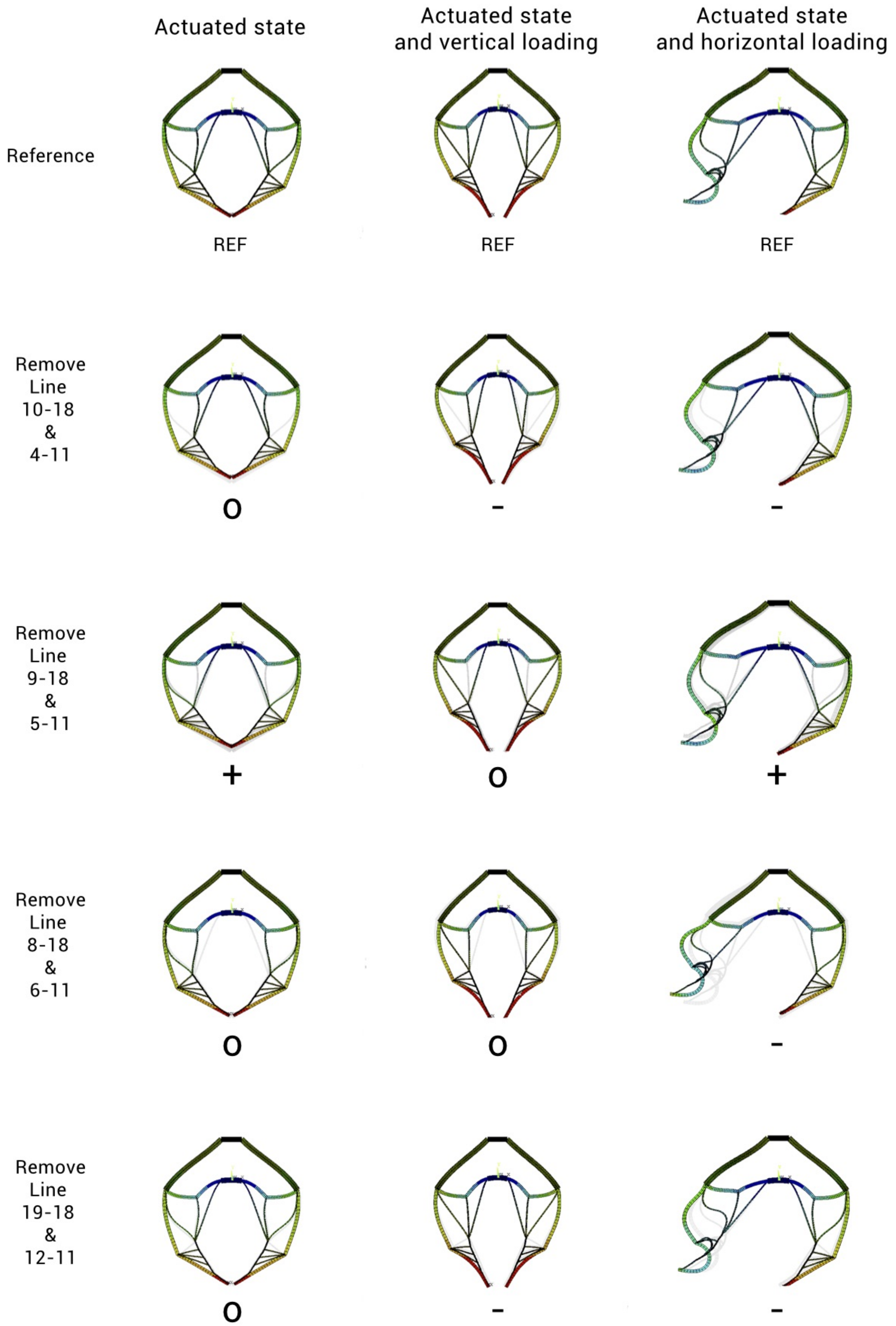

Figure 4.15: Contribution of each individual linkages of gripper concept 3. The first column contains the obtained analysis, the second column shows the actuated state of this obtained analysis action. Column three and four show the actuated state with vertical loading the gripper tips and the actuated state with horizontal loading conditions respectively. The first row of simulations is the reference. No changes are applied to the model in this reference. By a visual overlay over the reference model, the clear deformation effect of each change in the design can be seen. Changes with positive contribution to the gripper design are indicated by a + sign. Negative contributions are indicated by - sign and neutral contributions by a 0 sign.

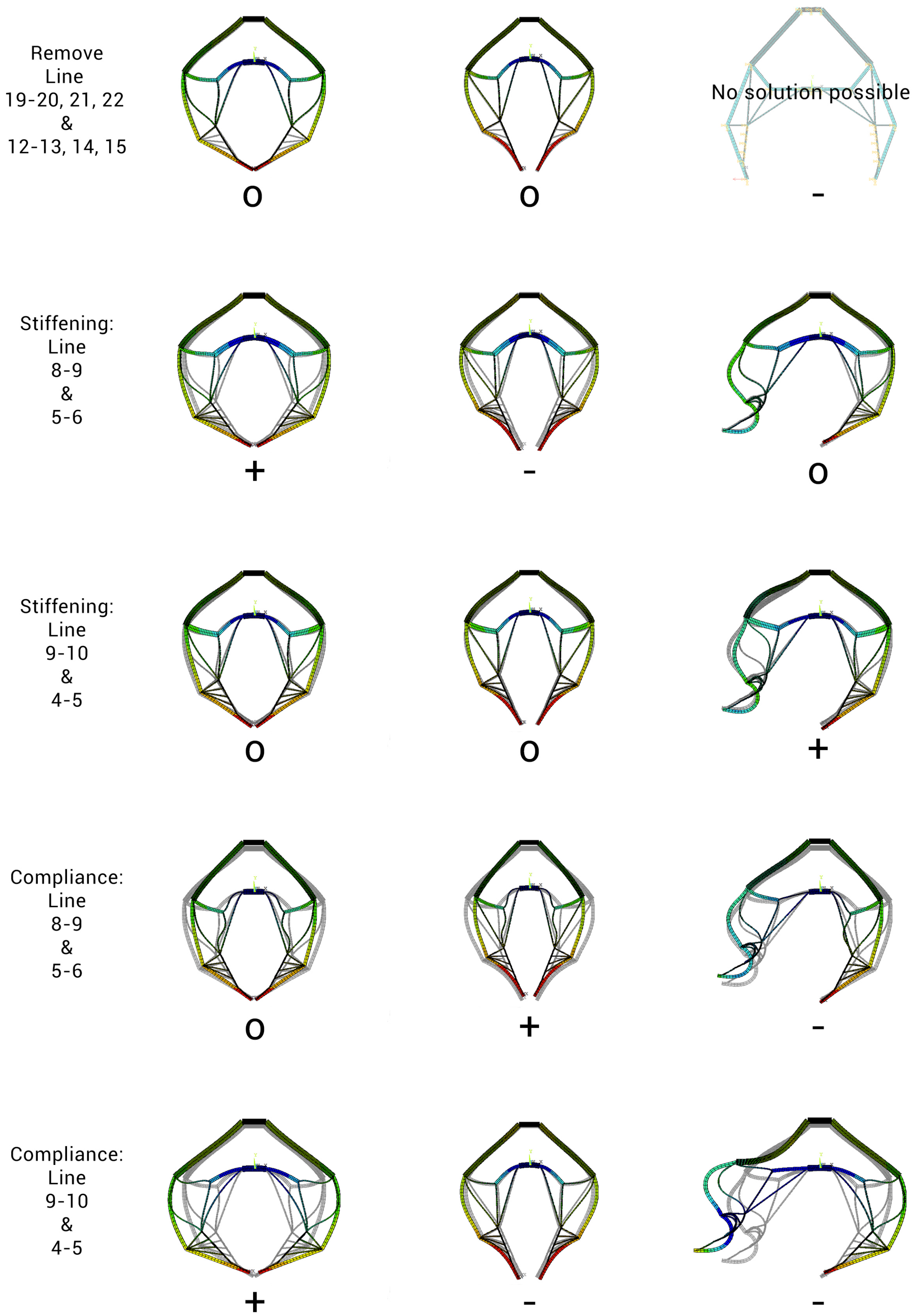
Remove
Line
19-20, 21, 22
&
12-13, 14, 15
o
o
No solution possible
-
Stiffening:
Line
8-9
&
5-6
+
-
o
Stiffening:
Line
9-10
&
4-5
o
o
+
Compliance:
Line
8-9
&
5-6
o
+
-
Compliance:
Line
9-10
&
4-5
+
-
-

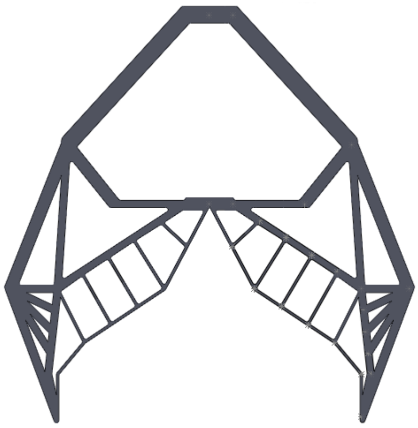

Figure 4.16: Gripper concept 3.2 with shape adaptation membranes containing interconnecting links which resulted in local pressure peaks at the object contact surface.

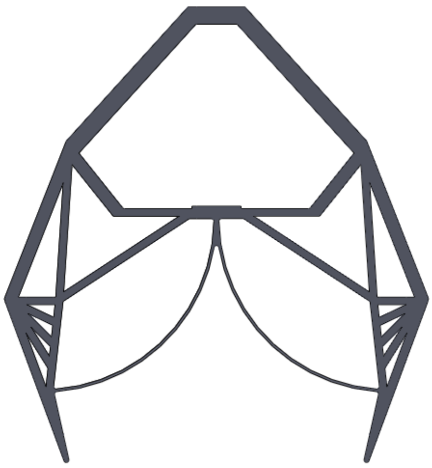

Figure 4.17: Gripper concept 3.3 with preformed arc shaped membranes. After actuation, membrane interference of both sides of the gripper resulted in inconsistent gripper actuation which causes inaccurate object placement.

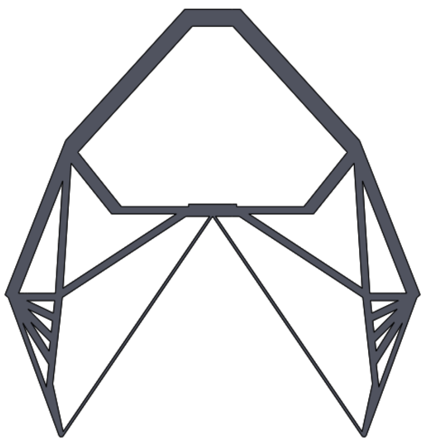

Figure 4.18: Gripper concept 3.4 with line membranes. These membranes are working without complains and will be further developed.

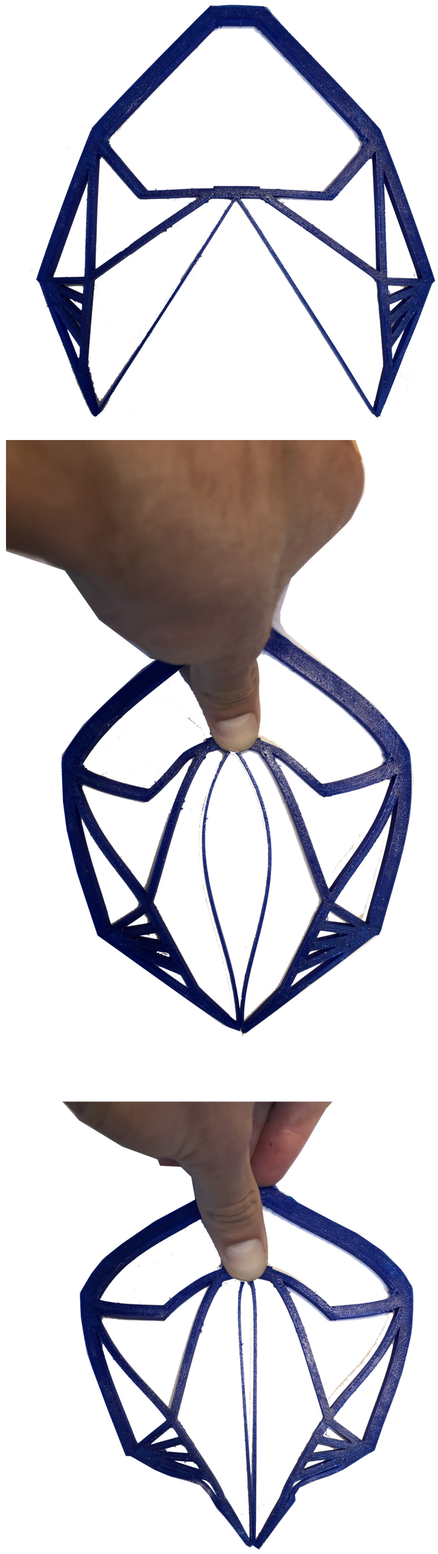

Figure 4.19: 3d printed slice of gripper concept 3.4, top: rest state, center: actuated state with non-tensioned membranes, bottom: actuated state with tensioned membranes.

5

Prototyping

5.1 Proof of concept

With the use of the 3d printed slices, the importance of the fixation point of the compliant mechanism was discovered. To this extent, the relative distance between node 2 and 7 is crucial for the gripping movement. When node 2 is fixed and node 7 is moved upwards, the compliant mechanism is actuated correctly but the tips do not reach under the object. Instead, the tips are touching the chicory approximately half way of the height of the chicory. Therefore, it is essential that node 7 (and 6 and 8) are fixed, and node 2 is moved downwards (figure 4.11). These last mentioned initial conditions are visualised in figure 4.19.

The linear displacement input for the compliant mechanism can be realized with several mechanical components. For example, an electric motor with lead screw, or linear pneumatic cylinder. A lead screw is probably not fast enough and is relatively heavy compared to an aluminium pneumatic cylinder. Therefore, a pneumatic cylinder is used. In first instance, the positioning of a single cylinder on the center line of the gripper was planned. This setup would be similar to the manual actuated 3d printed slices and could be implemented according to the design sketch in figure 5.1. The square block represents the pneumatic cylinder in this case. This setup would be easy to design and prototype. However, when using a single cylinder, the fingers on both sides of the gripper are actuated simultaneously. This is fine for the pick up phase, but leads to problems in the drop off phase. When the chicories have to be positioned side by side (figure 3.4), independent actuation of the gripper fingers is preferable. In the drop off phase, one side of the gripper remains actuated, and the other side is released. With this setup, chicories can be placed side by side, without touching neighboring chicories. This design decision involves at least two pneumatic cylinders for the actuation. A design sketch of one side of this mechanism is shown in figure 5.2. The diamond shaped actuation mechanism is replaces by the pneumatic cylinder. A stiff connection is designed to attach the cylinder to the gripper mechanism. It is not preferred that the the actuation mechanism bends due to the input force of the cylinder at the connection point of the cylinder with the compliant gripper. All energy should be transferred towards the fingers of the gripper to establish the prescribed deformation behaviour.

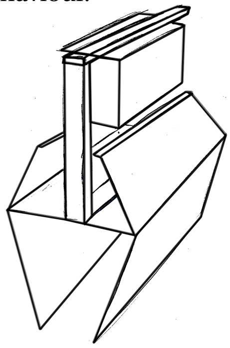

Figure 5.1: Schematic gripper drawing for a working prototype with two sided actuation by a pressure cylinder (square block). The mechanism is actuated by pushing the a piston down.

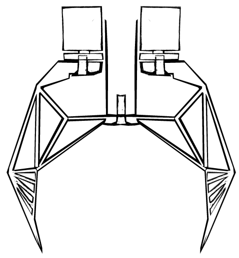

Figure 5.2: Front view drawing of gripper concept 3. This drawing shows a potential setup for a working prototype. The gripper is actuated by pressure cylinders (square blocks) and is fixed by a screw in the middle. The gripper is actuated by pushing the pistons of the cylinders down.

According to the design sketch in figure 5.1 and 5.2, a SolidWorks assembly has been made, figure 5.3 and 5.4. This proof of concept prototype consist of the gripper mechanism depicted in figure 4.19. The compliant mechanism is mounted (fixed) on key nodes 6,7 and 8 (figure 4.11). A bolt and pressure plate combination keeps key nodes 6,7 and 8 fixed in x, y and z direction. Both the gripper and the solid gripper base (gray in figure 5.3) have been 3d printed. To be able to screw the gripper on the base, an insert for a M6 nut has been designed. By using a metal nut, both parts can be assembled decently. The pressure cylinders used in this proof of concept are lightweight FESTO DSNUP-16-50-P-A cylinders.

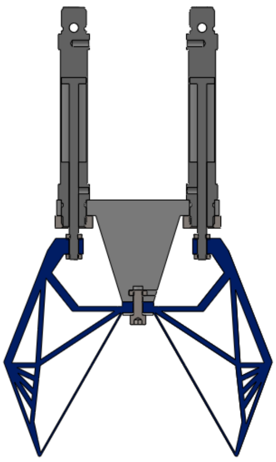

Figure 5.3: 2D schematic view of proof of concept. The cylinder housings are bolted to a base plate and the compliant gripper is connected to the ends of the cylinder pistons. The compliant gripper part is fixed at the middle of the base plate by a screw. The gripper is actuated by pushing the cylinders down.

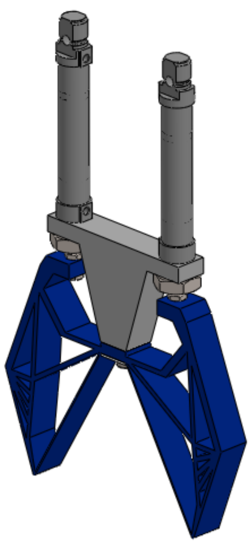

Figure 5.4: 3D schematic view of the SolidWorks model of the proof of concept.

The cylinders have a diameter of 16 mm and produce 120 N in advancing direction and 104 N in returning direction. This force difference for both working directions can be traced back to the principle of $Pressure = Force/Area$ for which the returning direction has less piston surface area due to the presents of the sliding actuation pin. The ANSYS FEM model predicted a required actuation force of just 10 N and a stroke length of 38 mm. This small actuation force is calculated for a gripper without object an without tensioned membranes (figure 4.19). For this proof of concept, complicated contact force analysis for the force between the gripper tips to tension the membrane is not necessary. The required force is strongly dependent on the object diameter, resulting in different input forces to tension the membranes. Therefore, it is important to have over capacity on the cylinder output force. The Festo DSNUP-16-50-P-A cylinders are sufficiently capable for this actuation. Both cylinders have been screwed onto the top of the base of the gripper by an M16 nut (figure 5.3). The piston end of the cylinders have been screwed onto the actuation mechanism of the compliant gripper to transfer the output force of the cylinders into the actuation mechanism of the gripper. After 3d printing and assembling the parts, the first real proof of concept prototype was created (figure 5.5).

Figure 5.5: Proof of concept finished build. After 3D printing the solid and compliant parts, the model is assembled including the pressure cylinders.

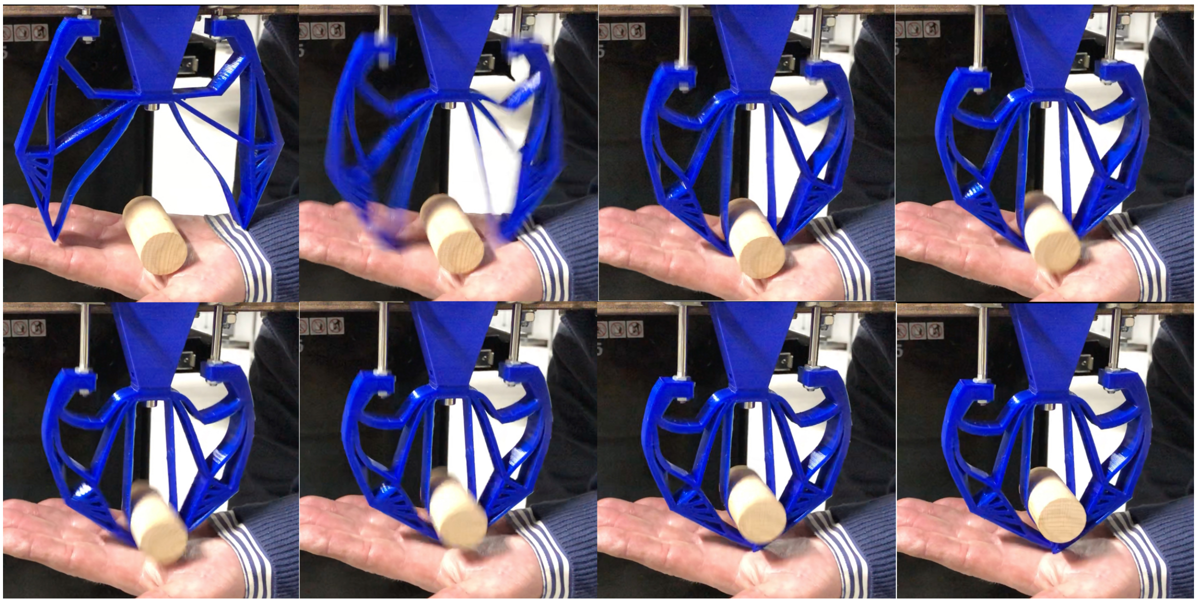

Figure 5.6: Proof of concept gripper with video motion capture. The picture sequence has a chronological order from left to right, top to bottom. Image 1 shows the starting position. Image 2 shows a half closed gripper. Image 3,4 and 5 show a fully closed gripper with further tensioning membranes. Image 6,7 and 8 show the sliding behaviour of the object into the gripper mouth.

To test this proof of concept, both cylinders have been connected to an air compressor and a manual valve via tubes. The manual valve reverses the airflow into the cylinders by flipping the switch. Therefore, a basic test of the pick up and drop of phase could be performed. Both actions look sufficient as visualized in figure 5.6. During the pick up phase, both fingers reached under the object and lifted the object. When the tips of the fingers were closing, the membranes tensioned which caused the object to slide upwards into the gripper. This can be a positive or negative side effect for the damage aversion. This have to be investigated with a full size prototype, which is able to grip a reach chicory. The object used in this proof of concept test is a wooden cylindrical beam of 30 mm diameter. This represents the smallest chicory diameter. Testing with a real chicory will be done with a full size prototype. This proof of concept looked promising enough to build a next version of this concept.

5.2 Full scale prototype

To be able to hold the force requirements, current gripper design with corresponding stiffness is extruded to a gripper depth of 110 mm (figure 4.14). This depth dimension covers the majority of the chicory length sizes. The objects are varying in length up to 200 mm. A gripper depth of 110 mm should be sufficient to cover the belly (middle section) of the chicory. The ends of the chicory are extra fragile and therefore not preferred to grip. By not touching the ends during gripping, the chances of damaging the chicory are further reduced. A first design drawing of the 110 mm extruded gripper concept is shown in figure 5.7. The setup is similar to the proof of concept prototype. The main differences are the depth extrusion and pressure cylinders used. For the extruded prototype, approximately 100 N is needed to actuate the gripper. Using stronger cylinders (FESTO DSN 20-50-PPV) provides over capacity to tweak the correct membrane tension. A 3d SolidWorks model of the 110 mm extruded gripper was created (figure 5.8, 5.9, B.2 and B.3).

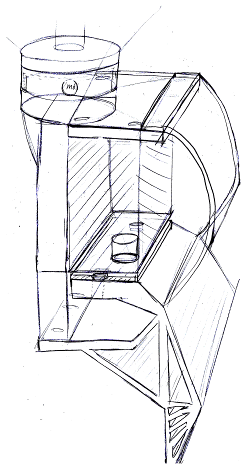

Figure 5.7: A 3D drawing of gripper concept 3 for a working prototype with a rectangular pressure cylinder to actuate the gripper. The cylindrical robot mounting head is shown at the top of the image and a covering membrane over the cylinder could be used protect the cylinders from water or dust.

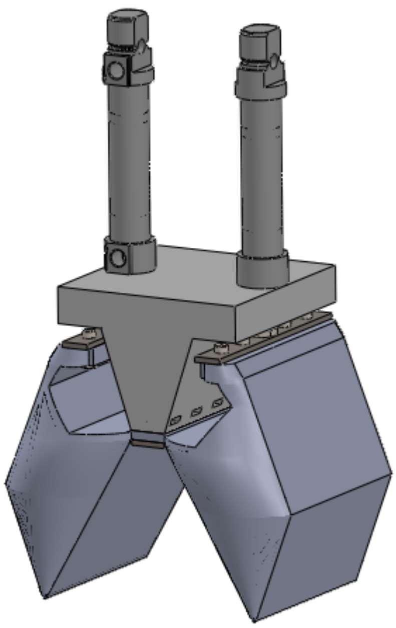

Figure 5.8: Schematic view of prototype 1 in SolidWorks with closed ends to prevent dirt form accumulation between the links.

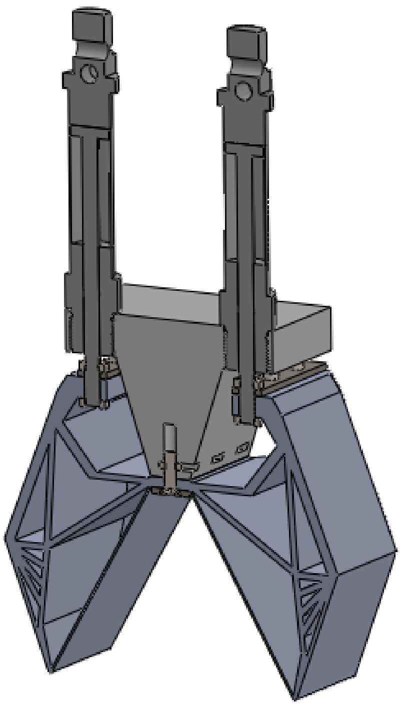

Figure 5.9: Schematic section view of prototype 1 showing the internal structure of the gripper, the cylinders and mounting nuts and bolts.

Table 5.1: E modules of PP and TPU for comparison.

Material:	E modules:
Formfutura polypropylene	320 Mpa
Ninjatek Cheetah TPU	16 Mpa

The base principle of this extruded gripper is similar to the working principle of the proof of concept. The base plate on which the cylinders and compliant gripper are assembled is extruded in depth up to 110 mm and 3D printed M22 screw threads have been integrated to attach the cylinders. The full extruded concept makes use of a mounting plate to keep nodes 6,7 and 8 of the compliant gripper fixed to the base. Similarly, two pressure plates are used to distribute the force of the cylinders over the depth of the actuation mechanism. Without these pressure plates, the gripper would only close in the middle of the gripper (at the cross section of the cylinders). The sides of the gripper should not completely close in that case. The last modification is an aluminium CNC milled robot connector plate at the top of the cylinders. This connector plate has two M6 holes, to be able to attach the gripper to the robot head and two 23 mm holes to attach the pressure cylinders. The end sides of the gripper is closed with a convex surface. This is to prevent the gripper mechanism from catching dirt and grease which could lead to contamination. Unfortunately, the 3D printer failed at 95% during this 3 day printing process. Therefore, one side of the gripper is not closed (figure 5.10). This will effect the measurements in the evaluation phase, if necessary a reprint of this part will be performed. The failed print is expected to be useful nevertheless, because the closed convex surface is contributing minimally to the stiffness of the compliant gripper.

The NinjaTek Cheetah material used for the print is not food safe. This is fine for testing but a problem for real implementation. To solve this potential problem, a food safe, flexible and 3D printable material was found. This polypropylene (PP) plastic is commonly used in food industries. To be specific, the brand name of this material is: Centaur PP - Natural from company Formfutura in Nijmegen (the Netherlands). They have an explicit FDA proof certificate for this 3D printable material. The objects which are printed with this material are however not directly food safe. The material does mostly cover the requirement among the migration limit. In combination with a cleaver food safe design for the gripper, a real implementation could be possible regulation wise. The PP material is stiffer (table 5) compared to the NinjaTek TPU. Therefore, the infill destiny of the 3D printed compliant gripper mechanism was reduced to match the stiffness of the NinjaTek Cheetah TPU material by estimation. A reprinted 110 mm extruded gripper with this PP material on 20% infill is shown in (figure 5.10). Still, the reprinted gripper of the polypropylene feels stiffer than the original TPU material. Nevertheless, this second prototype will be tested and compered.

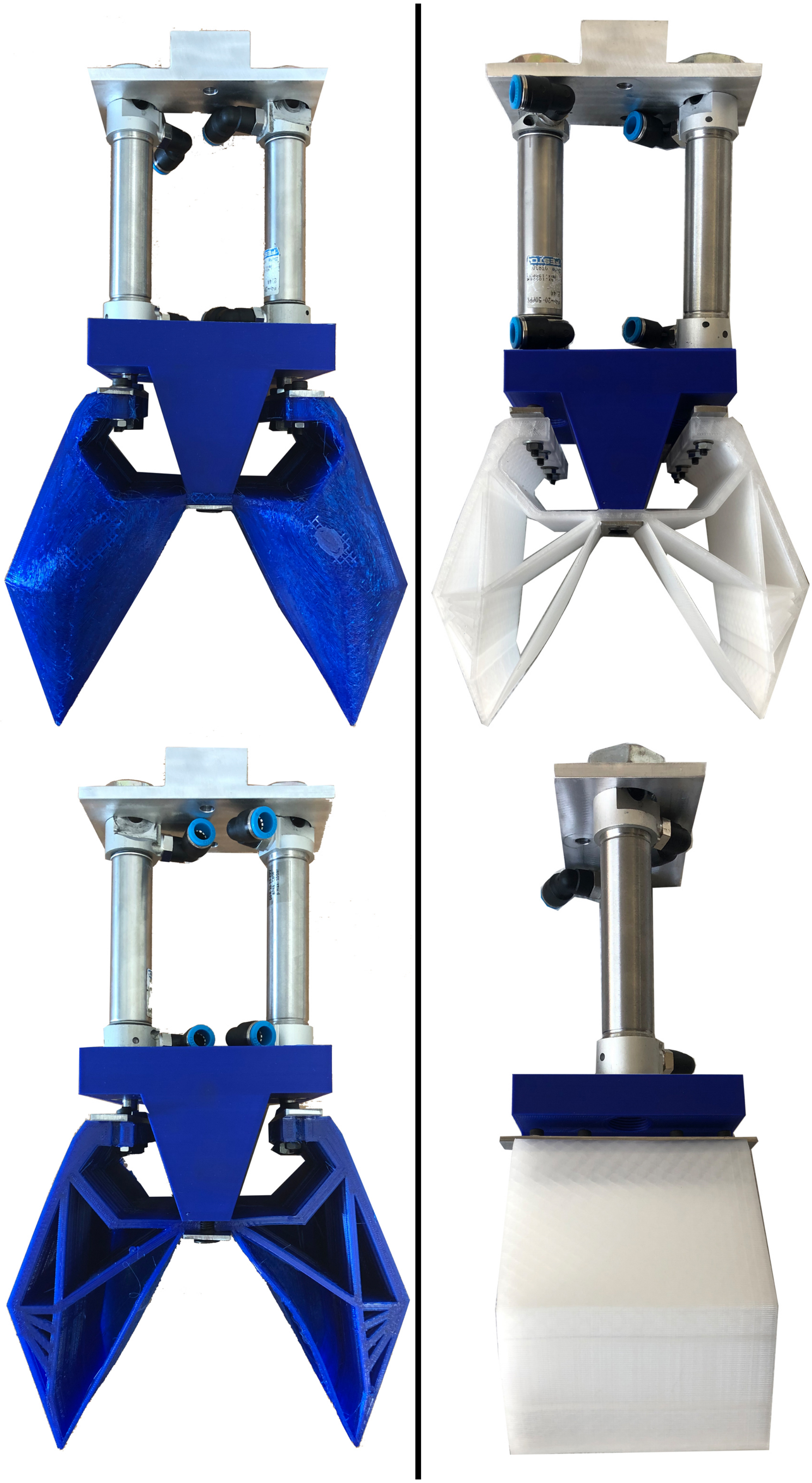

Figure 5.10: Prototype 1 (left) printed with TPU and prototype 2 (right) printed with clear food safe PP material. Both grippers have the same internal linkage structure. Prototype 1 is printed with one closed end due to a print failure and prototype 2 is printed with 20% density infill to reduce the stiffness of the gripper.

5.3 Prototype variants

Two sided actuation to reach under the chicory is not necessarily to grip and hold the object. Inspired by the human hand, which uses the thumb as static finger and the other fingers as curving fingers to reach under the object, an asymmetric gripper (figure 5.11) have been designed. The compliant mechanism of the curving finger (right side of the gripper) is similar to previous prototypes. The thin left side of the gripper creates the possibility to place the chicories side by side without a drop (figure 3.4). This thin finger uses a similar membrane shape adaptive principle as the compliant curving finger. Obviously, the actuated finger is stiffer than the thin finger. To be able to match the load criteria on the thin finger as well, a metal back plate on the outside of this flat finger (figure 5.15) was designed. Similar to previous prototype variants, the membrane of this asymmetric gripper is not tensioned at closed actuation state (figure 5.12). Depending on the object in the gripper, an extra input force is required to tension the membrane on the actuated finger. The static thin finger membrane is initially tensioned by default (figure 5.12). This is not possible at the compliant finger due to tension reduction caused by the actuation movement of the tip of the finger. This asymmetric gripper is designed in two variants. The first variant (figure 5.13) consist of a 110 mm gripper depth for the actuated and static fingers. With this variant, the chicories can be placed side by side with a separation distance equal to the thickness of the thin static finger (figure B.4). The second variant of this asymmetric gripper consist of two actuated fingers and two static thin fingers (figure 5.14). In this setup, the 40 mm space between the static thin fingers (figure B.7) can be used to place the chicories really side to side, almost touching each other as visualized in figure 3.4. By inspecting figure 5.15 the clear differences between the two asymmetric gripper variants is shown.

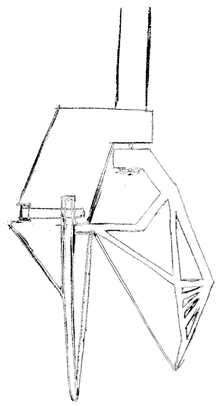

Figure 5.11: Drawing of an asymmetric gripper layout for better side by side drop off of the chicories. The flat finger (left) makes it possible to place the chicory side by side.

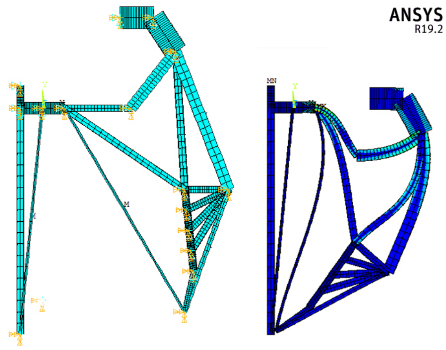

Figure 5.12: Asymmetric gripper modeled in ANSYS to perform a FEM analysis. Left image shows the initial shape, right image shows the deformed shape with stress concentrations indicated in red.

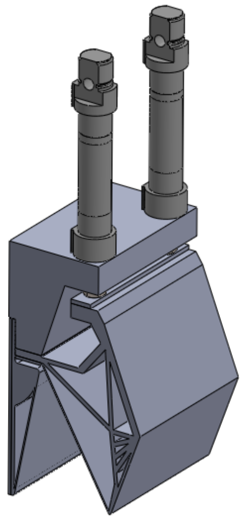

Figure 5.13: Prototype 3 (asymmetric) in 3D SolidWorks view with flat side on the left and compliant side on the right. The gripper is actuated by pressure cylinders.

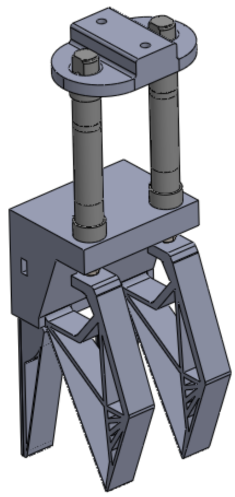

Figure 5.14: Prototype 4 (asymmetric) in 3D SolidWorks view with a four finger design. The two flat fingers (on the back) create the possibility to drop the chicory side by side by positioning the two flat fingers next to the belly of the chicory.

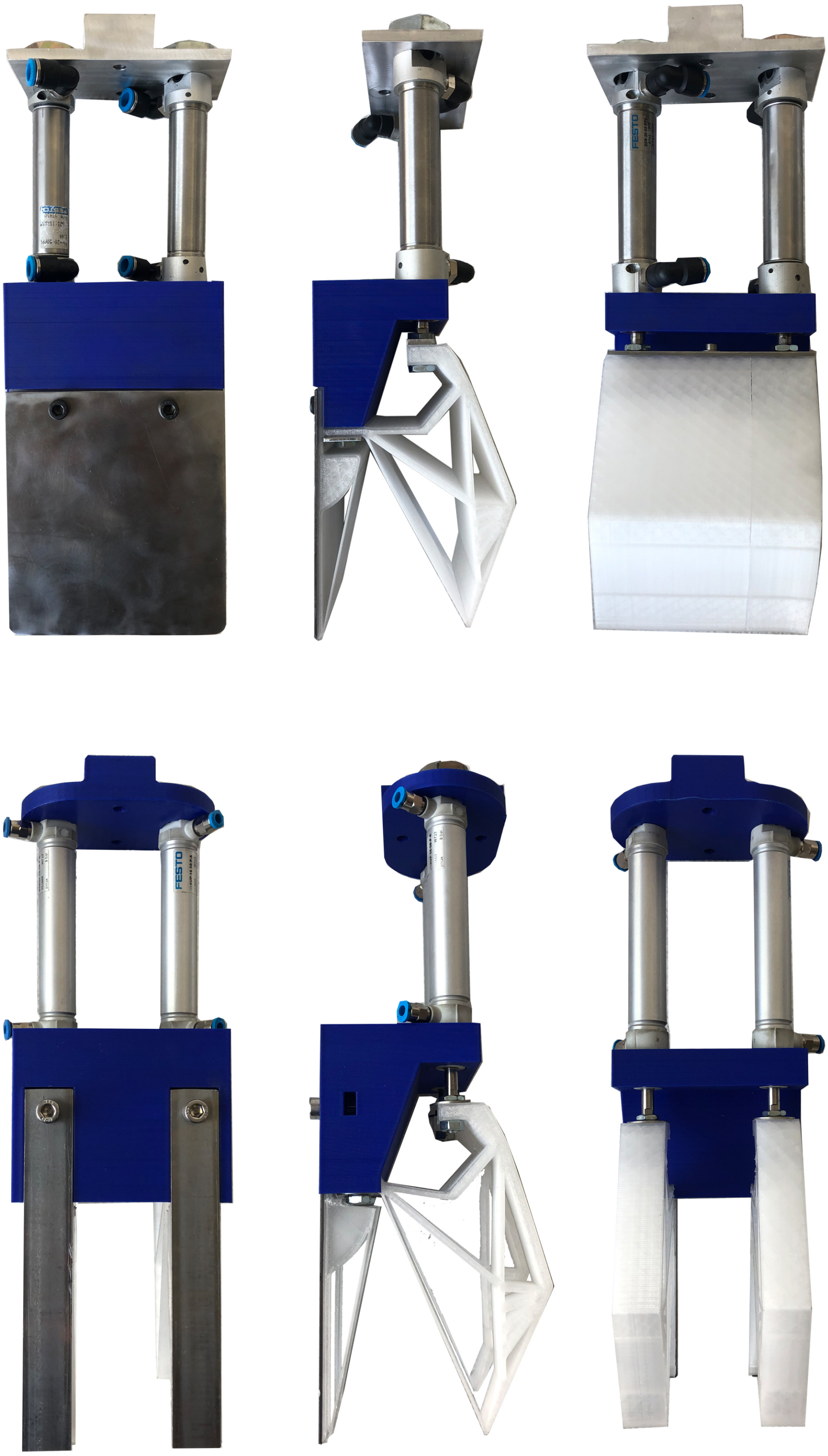

Figure 5.15: Prototype 3 (top) and 4 (bottom) 3D printed and assembled. The first column shows the first side view of the gripper: flat finger side. The second column shows the front view of both gripers and the third column show the other side view. Prototype view consists of four fingers and prototype 3 of two fingers.

5.4 Prototype evaluation

5.4.1 Force experiment

The force experiment setup consists of a mounting frame to hold the gripper steady, a 3 cm diameter cylindrical wooden beam with a 2.7 kg weight attached and an air compressor with compatible tubes (figure 5.16). To start the experiment, the gripper is mounted to the frame by two M6 bolts, similar to the final ABB FlexPicker delta robot. To be able to perform this experiment accurately, the grippers are leveled before testing (figure B.8).The tubes are connected to a manual valve to reverse the actuation direction of the cylinders. The valve is connected to the cylinders with tubes on one side, and to the compressor on the other side. Within this setup, the largest compatible tubes (8 mm inner diameter) are used to provide maximum air flow to reduce actuation times. The wooden cylinder is attached to the 2.7 kg load by a steel cable. This load represents the maximum acceleration force of the object onto the gripper.

When the setup is ready, the pressure into the cylinders is increased until the gripper closes. With this pressure, the load test is performed by gripping the object first, and applying the load subsequently. If necessary, the pressure is increased up until the load criteria is reached with a maximum of 6 bars. Most industrial compressors have a maximum pressure of 6 bars due operation cost savings. The grippers pass the force test when they are able to hold the 2.7 kg load for at least 1.3 seconds in z direction (figure 5.16), x direction (figure 5.17) and negative x direction. Grippers 1 and 2 are symmetric, so the x direction force test is similar to the negative x direction force test. Controversially, grippers 3 and 4 are asymmetric and have been tested in x direction on both sides of the gripper (figure B.9 and B.10).

Finally, all four grippers passed the force experiments. Due to the different diameter cylinders used across the prototypes, different operating pressures for the four prototypes were used (table 5). The operating pressures needed to hold the force requirements are used similarly in the damage test to verify whether the required closing force causes damage on the chicory.

Figure 5.16: Gripper 1 tested in z direction. The gripper is fixed to the frame and a 2.7 kg load is applied on the gripper. Gripper prototypes 1, 2, 3 and 4 are evaluated similarly.

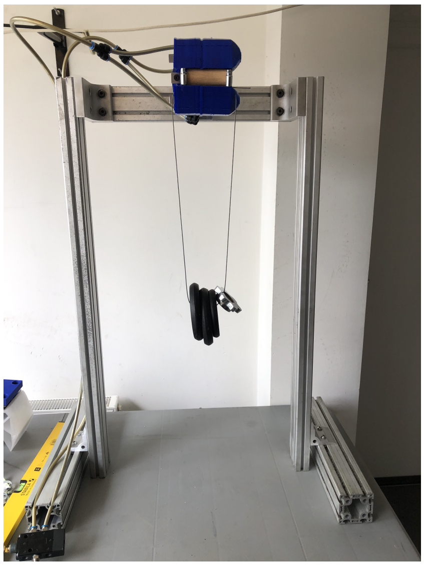

Figure 5.17: Gripper 1 tested in x direction. The gripper is fixed to the frame and a 2.7 kg load is applied on the gripper. Gripper prototypes 1, 2, 3 and 4 are evaluated similarly.

Table 5.2: Pressures and force input per prototype to hold the 2.7 kg load in z direction.

Prototype No.:	Cylinder type:	Pressure input:	Total force input:
1	2x FESTO DSN-20-50-PPV	5 bar	314 N
2	FESTO DSEU-40-40(and 25)-P-A	4 bar	1006 N
3	2x FESTO DSN-20-50-PPV	5 bar	314 N
4	2x FESTO DSNUP-16-50-P-A	4 bar	160 N

5.4.2 Damage experiment

To determine the potential damage caused by the gripper during the gripping movement, four chicory test samples are gripped by each individual gripper concept. The test setup is similar to the force experiment, with a different gripper positioning height relative to the table, figure 5.18. The first three chicories are gripped by the gripper with the corresponding required actuation pressure (table 5). The fourth chicory servers as control sample to be able to separate environmental influences from gripping damage. This is done for all four gripper concepts, figure 5.19, B.11, B.12 and B.13. The chicories are covered with aluminium foil after testing to block incoming light which causes the chicory to colorize green and influence the comparable results. All samples have been photographed all around before the test which is used as reference. After 24 hours and 48 hours, the samples are inspected and photographed again. When the chicory shows damage at 24 hours already, the 48 hour result will be even worse en therefore not relevant. In this case, the 48 hour check will be skipped to speed up the evaluation process. The ultimate goal is to prevent the chicory from any damage for at least 48 hours after sorting. This is the average time form harvesting and sorting towards selling. The results of the damage comparison is inserted in an excel data sheet.

The results of the damage experiment, in which three chicories have been gripped for each gripper concept, are clear (figure 5.20). Gripper concept 1 performed best on the damage test. This is due to the more compliant material used in this prototype. The transparent PP material used in prototype 2,3 and 4 behaved stiffer than expected beforehand. Even after reducing the infill density of the 3D prints of prototype 2,3 and 4, the stiffness remained significantly high, resulting in damaging 88% of the test samples. The stiffness of the grippers require a large input force which translates in a large contact pressure onto the chicory. This results in damaging the chicories. During the upcoming iteration steps, a proper stiffness reduction is required to reach the obtained damage criteria.

Investigating the gripper prototypes with the corresponding test samples individually shows difference in damage onto the chicories. prototype 1 did not show any damage, but seems not sufficiently able to pick up the chicory. This requires a different experimental setup in which the chicory is lifted after gripping. This new setup will be taken into consideration during the evaluation of the iterated gripper concepts.

Looking at the sample results of prototype 2, a large crack in the chicory skin is visible on sample 1, figure 5.21. This is caused by the squeezing force on the sides of the chicory, resulting in high stress concentration at the top side of the chicory, which cracks the skin open. This indicates the demand for a more compliant gripper design which generates less normal force onto the sides of the chicory. In addition, also the third prototype has similar damaged sample results (figure 5.22). Difference in damage due to the thin asymmetric finger of concept 3 was not found.

Prototype 4 shows different damage marks in combination with the cracked skins damage or prototype 2 and 3. Due to the four finger design, the middle section of the chicory (the belly) is not covered by the gripper contact surface. The two actuated fingers cause therefore a cutting edge into the skin of the chicory at the location where the contact surface ends, figure 5.23. This could be solved by a more compliant design, or by a continuous membrane design similar to prototype 3. Which of these two possible solutions works best will be investigated in the iteration phase. Before testing on other requirements as pick up robustness and endurance, the two main criteria on force and damage have to be met prematurely.

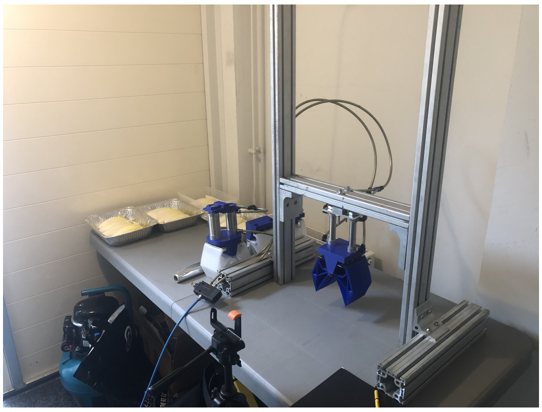

Figure 5.18: Damage experiment setup overview in which the gripper is fixed to the frame and grasps the chicory from the table. The chicory samples are placed in aluminum containers to be able to trace which samples belong to which prototype.

Figure 5.19: Damage experiment performed with gripper prototype 1. This experiment is done with prototype 2, 3 and 4 similarly.

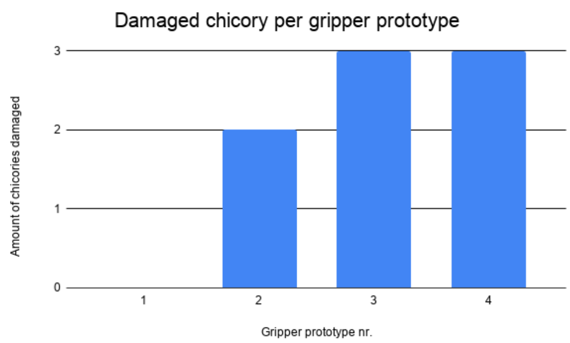

Figure 5.20: Results of damage experiment for prototype 1, 2, 3 and 4. On the x axis the prototype number and on the y axis the amount of chicories damaged.

Figure 5.21: Untouched sample (left) versus damaged chicory sample with crack in the skin (right) caused by prototype 2. The red ovals indicate the damage location before and after gripping.

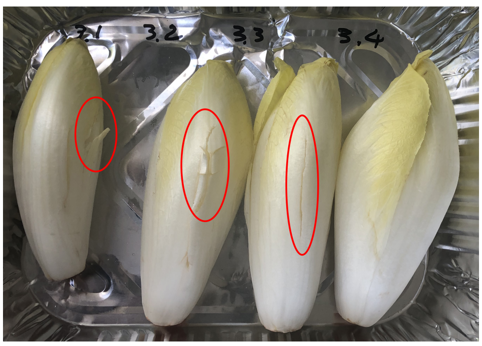

Figure 5.22: Damaged chicory samples with cracks in the skins caused by prototype 3. The red ovals indicate the damage location before and after gripping.

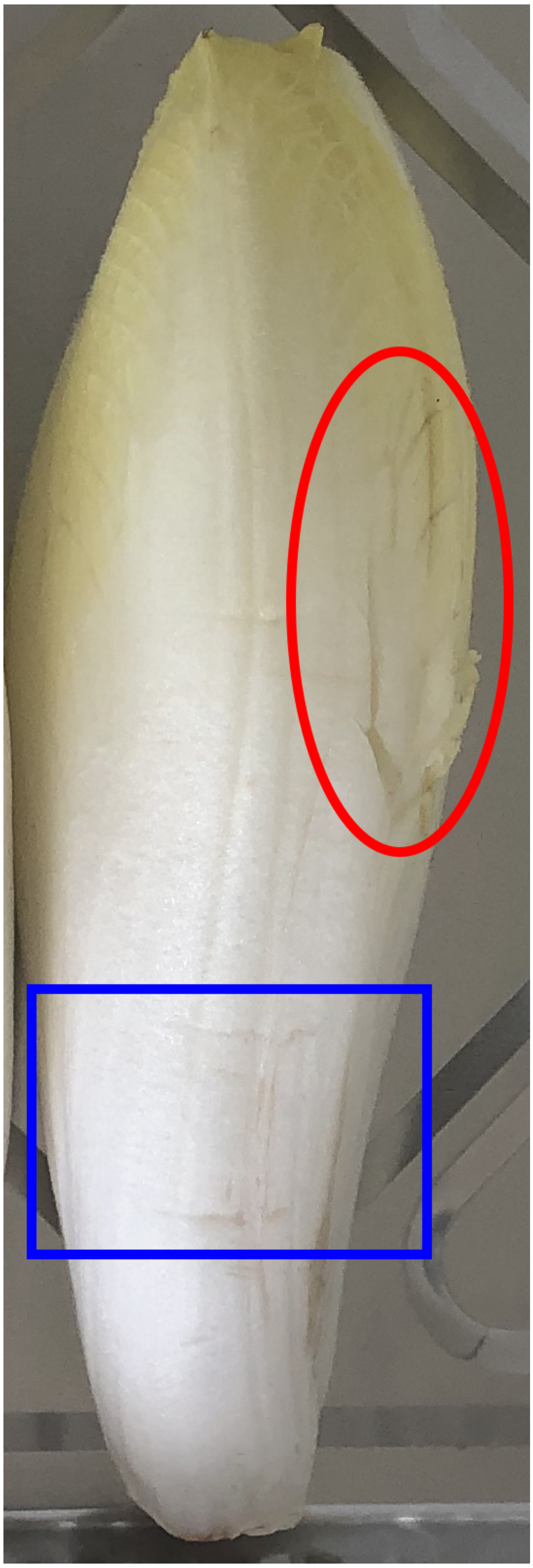

Figure 5.23: Damaged chicory sample with crack (red) and cutting edges (blue) caused by prototype 4.

6

Prototype optimization

6.1 Iteration 1 - stiffness reduction

6.1.1 Design

Looking at the drop off locations of the chicories in side by side configuration, a clear problem occurs with gripper prototypes 1 and 2 (figure 6.1). Due to the double sided actuation, a side by side placement is not possible. The best performance for prototypes 1 and 2 in terms spacing at drop off is ranging into several centimeters. This spacing is required to be maximum 10 mm. Even with tilted gripper configuration (figure 6.1), the chance of touching and damaging the previously placed chicory is assumable. Therefore, these double sided actuation gripper configurations are out of consideration for the gripper design process.

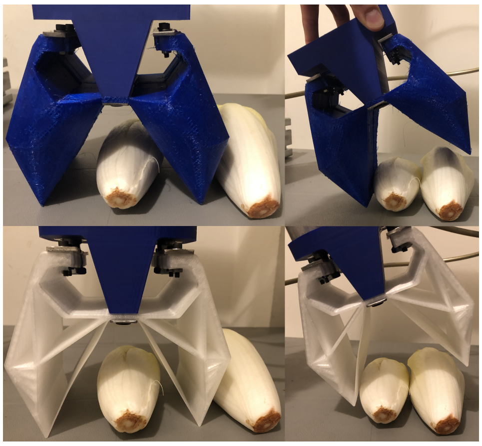

Figure 6.1: Drop off distance for gripper prototype 1 and 2 in normal position (left) and in tilted position (right). Due to the symmetric configuration of these prototypes, dropping of chicories side by side is not possible within 1 cm spacing.

As discussed during the evaluation of prototypes 1, 2, 3 and 4, the stiffness of prototype 1 does not result in any damage. However, the material is not food graded. The material used in prototypes 2,3 and 4 are food graded and 3D printable. To be able to combine the stiffness properties of prototype 1 with the food grade benefits of the PP material, a more compliant design is required. The asymmetric gripper layout results in closer side by side drop off. Looking at these two asymmetric prototypes, concept 4 is easier to prototype due to shorter printing times. Prototype 4 can be printed within 12 hours, whereas prototype 3 takes around two days to complete. Therefore, prototype 4 is optimized in terms of gripping performance as tested in the evaluation phase. When prototype 4 keeps failing on cutting edges after several iterations, the gripper layout will be extruded into a larger contact gripper similar to the setup of concept 3. The design decisions are visualised in figure

To match the stiffness of prototype 1 with the material of prototype 2, the material of both E modules has been inspected (table 5). The PP is 20 times stiffer than the TPU based on E modules comparison. This E modules stiffness increase can be compensated by reducing the heights of the beams in the gripper design. By compensating the area moment of inertia, similar stiffness properties for the gripper can be reached with different materials. The inertia of a rectangular cross-sectional beam is calculated using: $I_{xx} = b * h^3/12$. In general, the displacement of a beam is inversely proportional to the moment of inertia and the E modules. Therefore, the height of the beams (h) for the first design iteration need to be factorized by: $factor = \sqrt[3]{\frac{E_{TPU}}{E_{PP}}} = 0.368$. After multiplying all beam heights with this factor, gripper stiffness of prototype 1 is translated into iteration 1 with PP material. For simplicity, no compensation for the base width of the beams (b) is calculated. The effects of the beam width (b) on the stiffness is limited compared to the effect of the beam heights. Neglecting the stiffness contribution of the base (b) makes extrusion of the design of iteration 1 into a 110 mm depth configuration (similar to prototype 3) easy if cutting edges remain present in the rapid prototype-able four finger gripper design.

To check the stiffness compensating factor calculation, a new gripper design for iteration 1 is modeled in ANSYS APDL. The contact membrane for iteration 1 remains 1 mm in thickness. With the obtained stiffness reduction factor, a membrane thickness of 0.36 mm would be reached. This is to thin to print on a 3D printer with a 0.4 mm nuzzle diameter and is also fragile in terms of layer adhesion. A thin membrane is therefore not beneficial for endurance performance. 1 mm is estimated as sufficient, but this will be investigated with an extensive duration test. By comparing the deformation behaviour (in ANSYS APDL) of iteration 1 with the old design configuration of prototype 1, a sufficient check for the stiffness reduction is performed. Figure 6.2 shows the comparisons in deformation behaviour with equal input force (6N) and equal gripper depth (20 mm for fast computation). The Ninjatek Cheetah material compliant gripper design is similar to the layout of gripper prototype 1, with an asymmetric thin finger substituted instead. So, the overall stiffness of the gripper remains equal with different materials.

After the stiffness reduction, the pick up problem notified during the evaluation of prototype 1 had to be solved. Due to the elastic material behaviour of the Ninjatek Cheetah, prototype 1 seems to lag in performing a gripping motion underneath the chicory. Due to the contact of the chicory with the membrane, a more or less normal force based friction grip was performed (figure 6.3). Although this did not result in damaging the chicory as studied in the evaluation phase, it is not beneficial for the pickup motion of the gripper. To resolve this problem, a repositioning of the connection points of the membrane was performed to create an extended gripper tip which acts like a shovel (figure 6.4).

6.1.2 Evaluation

The new iteration 1 design have been 3D printed and assembled (figure 6.5). To compare iteration 1 with previous prototypes, identical force and damage experiments have been performed as described in the prototype evaluation section. In terms of force performance, this iteration 1 design reaches both force direction requirements. This is as expected due to similar gripper stiffness as prototype 1. The pickup movement is also significantly better in reaching under the object (figure 6.5). Despite, looking at the sample damage results, a new type of damage occurred. Due to the new membrane fixation points of iteration 1, a local pressure point was created at the beginning of the membrane (figure 6.6). This resulted in local dents which are unwanted. In addition, similar to prototype 4 (four finger design gripper before iteration), cutting edges by the membranes are present on the chicory.

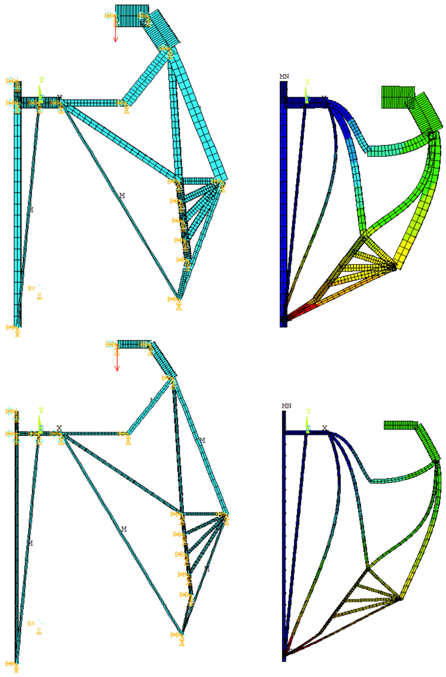

Figure 6.2: Asymmetric design with TPU material (top left) and actuation (top right) versus asymmetric design with PP material (bottom left) and actuation (bottom right) in which colors indicate relative element displacement. Both configurations have similar input forces and result in similar output deformation. The stiffness of these two grippers with different materials is therefore similar.

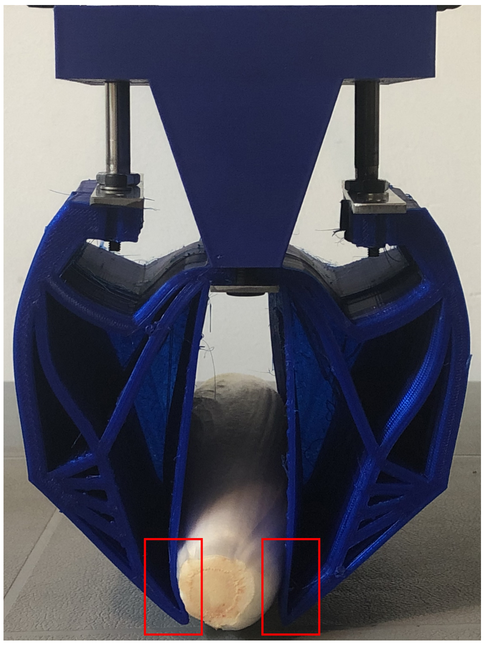

Figure 6.3: Lag of performing a gripping motion underneath the chicory by prototype 1 indicated by the red rectangles.

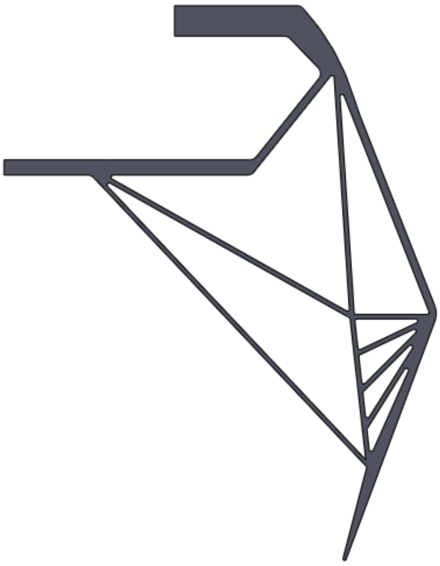

Figure 6.4: Final gripper design for iteration 1 with repositioned membrane, extended gripper tip and implementation of the stiffness reduction factor for the PP material.

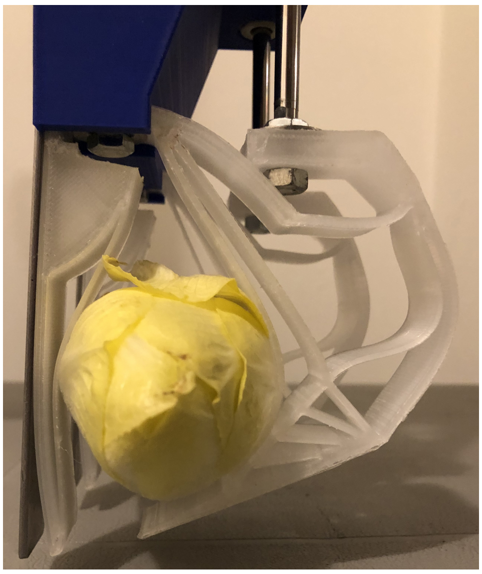

Figure 6.5: Iteration 1 actuated during damage test. The membranes of the compliant finger and the flat finger adapt to the outer shape of the chicory and the extended tip reaches underneath the chicory.

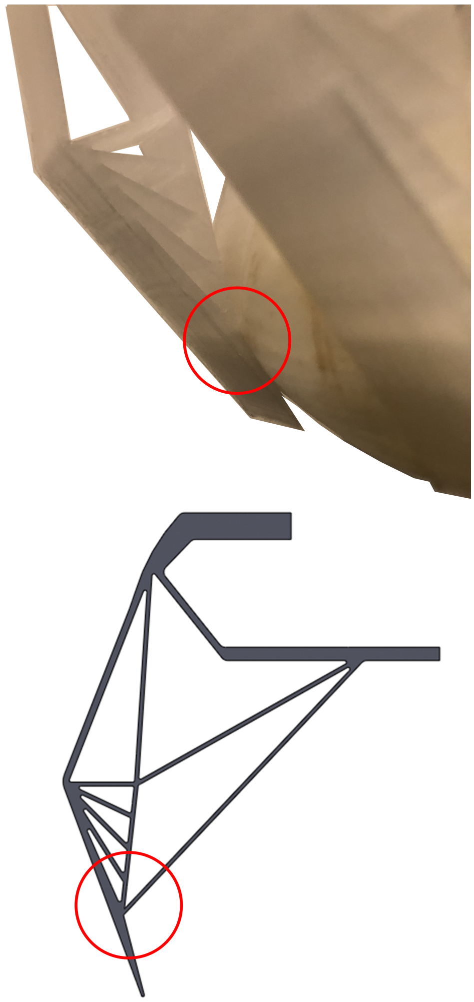

Figure 6.6: Local contact pressure concentration at membrane fixation point of iteration 1 indicated by the red circle. The pressure concentration resulted in damaging the chicory.

6.2 Iteration 2 - tip design

6.2.1 Design

To resolve the problems occurring with iteration 1, a new design has been created: iteration 2 (figure 6.7). The new design consists of a similar membrane which is merged with the tip of the gripper. The convex tip of the gripper with the integrated membrane should pick up the chicory similar to iteration 1. Due to the removal of the membrane fixation point, local contact pressure damage should be avoided. The pre-curvature of the membrane is designed to stimulate the deformation to reach under the object. Also, the links on the outside of the gripper have been replaced with precurved arc form beams to stimulate bending motion under the object. The last modification in iteration 2 is hidden in the compliance of linkage 12-17 (see figure 4.11 respectively). Due to the deformation of this link, extra membrane tension is created when the membrane touches the chicory. This principle is also used in the first proof of concept prototype (figure 4.19).

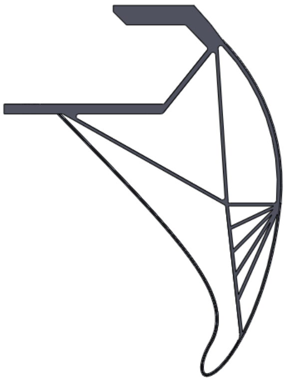

Figure 6.7: Gripper design of iteration 2 with re-designed tip by integrating the membrane with the tip of the gripper.

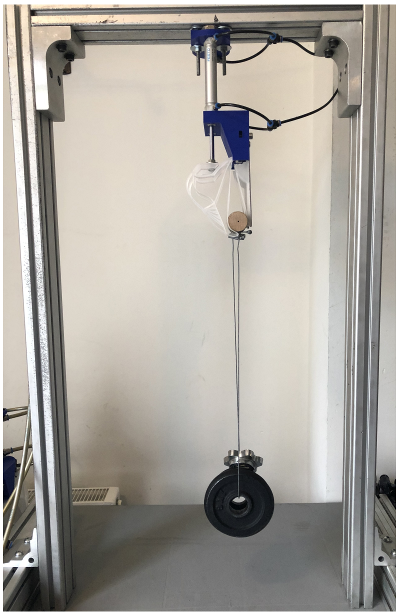

Figure 6.8: Iteration 2 in force experiment. Iteration 2 is able to hold the required 2.7 kg load.

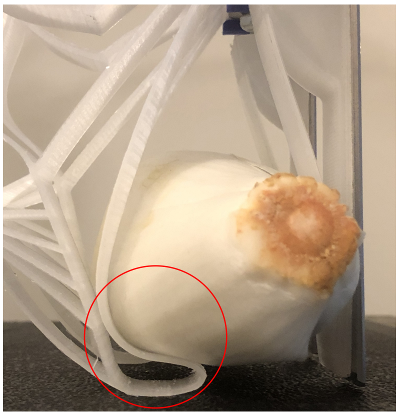

Figure 6.9: Iteration 2 gripping a large diameter chicory. The tip is reaching underneath the large chicory and does not damage the sample.

6.2.2 Evaluation

Again, iteration 2 have been evaluated similar to the previous prototypes as described during the evaluation section of previous prototypes (figure 6.8 and B.15). As depicted in figure 6.8, force requirements have been reached without any problems. Looking at the damage test results, an unexpected distinction in damage occurred among different chicory diameter samples. Large diameter samples had no damage beside some minor cutting edges (not visible on photo). However, small diameter chicories samples exhibited dents due to the larger tip of the gripper. The tip is relatively large compared to the diameter of the small chicories. With large chicories, this tip is sliding underneath the object, but with small chicories, the tip hits the object almost at the center. The damaging behaviour is clarified by comparing figure 6.9 and figure 6.10.

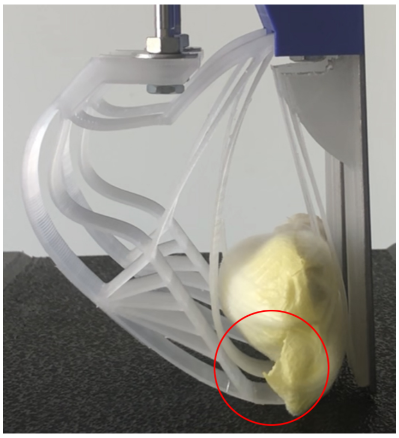

Figure 6.10: Iteration 2 gripping a small diameter chicory. The tip is reaching underneath the small chicory sample but does damage the sample.

6.3 Iteration 3 - membrane design

6.3.1 Design

For iteration 3, just a small change is made compared to iteration 2. A less precurved membrane should solve the problem of hitting the smaller chicories with the tip of the gripper (figure 6.11). To optimize the gripping motion to reach under the object, the underside of the gripper slide over the ground (figure 6.12). Therefore the gripper is positioned slightly lower relatively to the ground. This positioning height can be optimized by trail and error for better tip positioning due to the sliding. The stiffness of this gripper is similar to iteration 2.

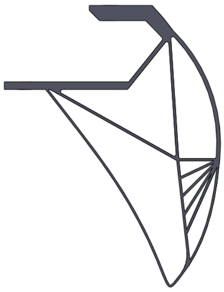

Figure 6.11: Design of iteration 3 with less precurved membrane to slide underneath the chicories and avoid hitting smaller diameter chicories.

Figure 6.12: Underside of the gripper tip of iteration 3 sliding over the ground to reach under the small size chicories. This contributes positively to the pick up performance.

6.3.2 Evaluation

Similar to previous prototypes, iteration 3 have been tested on force and damage requirements. At this point, the importance of gripping the chicory and performing the force experiment simultaneously was discovered. To accomplish this, the experimental procedure of the force experiment was changed. To be able to grip the chicory and apply force on the gripped chicory, the gripper was lifted after gripping and and loaded with 2.7 kg subsequently (figure 6.14). The force application is done by using a modified chicory on which weights were attached (figure B.14). Iteration 3 was able to hold the 2.7 kg loading requirement, similar to previous prototypes with an operation pressure of 2 bars.

Also the damage experiments gained positive results. No damage was present, except for some cutting edges created by the membranes. This is a major breakthrough! Iteration 3 manages to perform an excellent gripping motion for small and large chicories without damage (figure B.16). In addition, a side by side drop off test has been performed (figure 6.13), which is a design requirement for the chicory gripper as well. With this layout, chicories can be placed within 10 mm of spacing. Therefore the drop of requirement is reached.

Figure 6.13: Iteration 3 dropping off chicories side by side on a flowpack which are used for packaging the chicories.

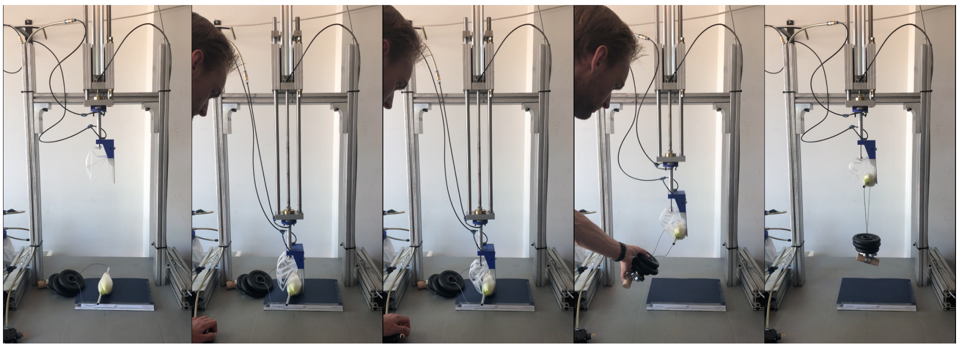

Figure 6.14: New force experiment procedure: 1. Default setup, 2. Gripper moving down, 3. Gripper actuated and gripping the chicory, 4. Moving gripper and chicory up, 5. Apply full load (2.7 kg) on chicory to test the gripper holding force.

6.4 Iteration 4 - scaling

6.4.1 Design

For iteration 4, four design changes are required. First, the compliant gripper needs to be extended to cover the length of the chicory. Secondly, the thin finger side of the gripper needs to be extended along the chicory length as well. In addition, the height of the thin finger needs to be extended downwards as well. In iteration 3, a gab between the tip of the thin finger and the ground was present. This gab is not providing support to the chicory and could potentially result in damaging the chicory. By extending this thin finger downwards, even the smallest chicory will be supported. Finally, the presents of chicories with a diameter up to 9 cm for sale at the supermarket were noticed. Intentionally, the gripper was designed for chicories up to 6 cm in diameter. Because compliant mechanism in general are scalable, a gripper size increase should be possible. However, due to the scaling, a stiffness compensation will be required.

Scaling iteration 3 into iteration 4 and therefore being able to grip the 9 cm diameter chicories, requires a scaling factor in x and y direction (front view) of 1.25×. Scaling the 3D model in SolidWorks can be done using the scale tool. By scaling the model dimensions, not only the grippable object size increases. The height, and width of the beams are scaling proportionally as well. Therefore, stiffness increases unwanted. To illustrate, up-scaling the model with 25% in x and y direction results almost in a gripper stiffness doubling, according to inertia rules:

$$I_{pre-scale} = \frac{b * h^3}{12} \tag{6.1}$$

compared to

$$I_{post-scale} = \frac{b * (1.25 * h)^3}{12} \tag{6.2}$$

resulting in

$$\frac{I_{post-scale}}{I_{pre-scale}} = 1.953 \tag{6.3}$$

To be able to keep the stiffness of the gripper identical to the stiffness of iteration 3, all heights of the scaled gripper beams need to be reduced. This can be done before or after scaling the model. Compensating the heights before scaling was easier to implement in SolidWorks. So, to calculate the pre-scaling stiffness compensating factor, two things need to be taken into account. First, a pre-scaling factor for all beam heights needs to be calculated. Secondly, a cross-sectional base compensating factor needs to be calculated since the gripper is extruded up to full gripper length similar to the pre-iteration design of prototype 3 (5.13). As previously argued, this extrusion along the length of the chicory avoids cutting edges which were present in all four finger layout iteration prototypes. This full size gripper is extruded up to 110 mm. The two compliant fingers in iteration 3 are both 20 mm in depth resulting in a 40 mm wide membrane contact surface. To extend this contact surface along the length of the chicory, a depth increase of

$$Factor_{contactsurface} = \frac{110mm}{20mm + 20mm} = 2.75 \tag{6.4}$$

is required. This factor can be added to the inertia calculation of the scaled model:

$$I_{scaled} = \frac{2.75 * b * (1.25 * h)^3}{12} \tag{6.5}$$

Comparing the default inertia ($I_{default} = \frac{b*h^3}{12}$) with the scaled inertia shows a stiffness increase of 5.371 times compared to the default stiffness:

$$\frac{I_{scaled}}{I_{default}} = \frac{\frac{2.75*b*(1.25*h)^3}{12}}{\frac{b*h^3}{12}} = 5.371 \tag{6.6}$$

To reduce this significant stiffness increase, all heights of the beams need to be multiplied with:

$$Factor_{pre-sclae} = \sqrt[3]{\frac{1}{5.371}} = 0.571 \tag{6.7}$$

before scaling the model. This compensating factor was inserted in the scaled inertia equation:

$$I_{scaled} = \frac{2.75 * b * (0.571 * 1.25 * h)^3}{12} \approx \frac{b * h^3}{12} \tag{6.8}$$

resulting in approximately similar stiffness compared to iteration 3. Applying the scaling factor to all beam heights should result in a membrane thickness of 0.713 mm. This is manually increased up to 1 mm to maintain durability of the membrane, which is the most important chicory contact surface of the gripper.

Iteration 4 has been model using ANSYS APDL to predict the movement of the compliant finger tip toward the thin finger (figure 6.15) and to check for stress concentrations. Stress concentrations are resolved by smoothing the edges at the location of the concentrations. To be able to fully close the gripper, an input force of 25 N is required according to the model. The deformation of this model looks sufficient and was therefore ready to be 3d printed.

Because of the scaling, not only the compliant mechanism is increased in size, also the blue mounting part needed to be changed. For this iteration 4, two Festo DSN-20-50-PPV pressure cylinders were used. The previously iteration used DSNUP-16-50-P-A cylinders, which are capable to actuate the gripper of iteration 4 as well. However, by using different cylinders, iteration 3 remained intact to be able to perform a side by side comparison with iteration 4.

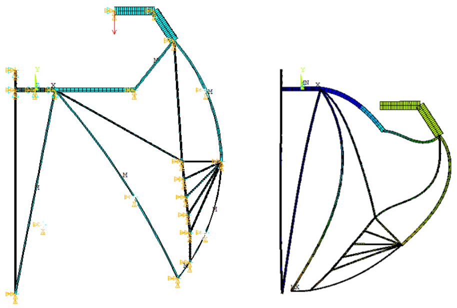

Figure 6.15: Iteration 4 including scaling and stiffness compensating factors. Left image shows the passive state and the right image shows the actuated state of the gripper. The input force is equal to the input force of iteration 3, resulting in similar deformation. Therefore, stiffness of the scales iteration 4 is similar to the iteration 3 design. The color scale represents relative element displacement from blue (small) to red (large displacement).

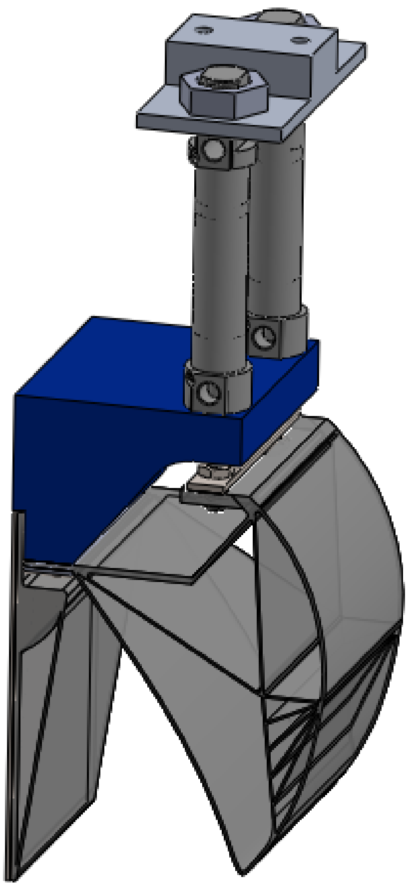

Figure 6.16: Iteration 4 SolidWorks assembly with robot mount plate (top), base plate (blue part), flat finger (left finger) and compliant finger (right finger)

6.4.2 Evaluation

The iteration 4 prototype (figure 6.16), was tested on force and damage similar to the previous prototypes. Iteration 4 is able to grip and hold the 2.7 kg load (2 bars input), and did not damage any of the chicory samples during the damage experiment. Not even a single cutting edge was present. As obtained, iteration 4 is indeed capable of gripping large (up to 9 cm diameter) and small (3 cm diameter) chicories, figure 6.17.

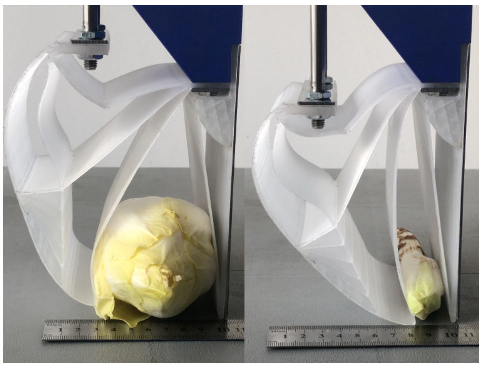

Figure 6.17: Iteration 4 prototype gripping large and small chicories without damage. The left image shows a large chicory and right image shows a small chicory gripped by iteration 4.

For the first time during the iteration process, this prototype was performing as required on the force test and the damage test. Therefore, the next major step in evaluating this gripper prototype can be taken: an endurance test. To be able determine how long the gripper should last in duty, an cost estimation and retail price of the compliant parts of the gripper was made. The non-compliant parts (cylinders, mounting brackets, nuts and bolts), are assumed to last significantly longer than the compliant parts (compliant finger and thin flat finger). Material and production cost taken into account, this gripper to costs 20 euro to produce. Looking at development costs, potential patent fee and other margins, a 200 euro retail price for the compliant parts is estimated. With this retail price, the gripper should last for at least 120.000 gripping repetitions according to the set depreciation requirements of 0.001666 euro per gripping action. Of course, a longer life time should be preferable to increase financial margins on the gripper.

To perform the endurance test, a new test setup was needed. Because an endurance test requires serious air compressor capacities, and the TU Delft was not able to provide this compressor (due to Covid-19 governmental safety precautions TU Delft was closed), the test needed to be performed in a business environment. An offer was received to perform the endurance test at a company named Brokx-schalken BV. By connecting the endurance test setup to the compressor capacities and electronic valves of a metal wire bending machine, the experiment was performed. This machine was producing metal wire products simultaneously with the endurance test. By adding additional commands to operate the electronic valves simultaneously with the production process of the wire bending machine, both processes are controlled by the same machine without interference. Due to the limited product production batch of the machine, an endurance test of 106.000 gripping repetitions could be performed. This should provided a clear indication about the endurance performance of the gripper based on the minimal required life time calculation of 120.000 gripping repetitions.

The setup for this endurance test consists of a frame on which the gripper is mounted (figure B.17). To mimic the chicory, a 40 mm diameter steel cylindrical tube was used. A real chicory would not last during the endurance test obviously. To prevent the metal tube from potentially sliding or rolling out of the gripper pick up range, a wooden box around the cylindrical tube which prevented the tube from rotating and sliding (figure 6.18) was added. The input pressure to the gripper pressure cylinders was regulated by an adjustable air gauge. This gauge is set to 2 bar output pressure, which is corresponding with the required closing force to complete the force experiment. After every 10.000 gripping repetitions, the state of the gripper is checked on potential cracks and busts which indicates failure of the gripper.

During and after the 106.000 gripping repetitions, no cracks or bursts have been found on the compliant gripper parts. The only thing which was slightly worn out, was the metal tube which mimicked the chicory. Some metal dust of the tube was visible on the gripper, but after a clean in the dishwasher, non of there marks where visible on the gripper.

To determine whether the gripper was still capable of holding a 2.7 kg load, four force experiments have been redone similar to the previous force experiments. This time in all possible relevant force directions: negative z direction, x direction, y direction and negative y direction (figure 6.19). The gripper was still able to hold the load, but the input pressure into the cylinders was increased from 2 bar up to 3 bar. This indicates a compliance increase of the gripper over time. This is an expected behaviour of all flexible materials. The compliance increase is however no failure criterion as long as the gripper is able to hold the load with a corresponding pressure increase. The limit of increasing the pressure is reached when the chicories are damaged or when the maximum input pressure of the cylinders is reached. Neither of both cases were present with the 1 bar pressure increase.

In line with the force experiments, all drop off configurations have been mimicked and are displayed in figure 6.20. Due to the flat side of the gripper, chicory can be placed side by side within 10 mm spacing. Looking at the placing of the last chicory in line in the crate, a limitation occurs. Due to the opening space required for the gripper, a small gab occurs between the side of the crate and the last placed chicory.

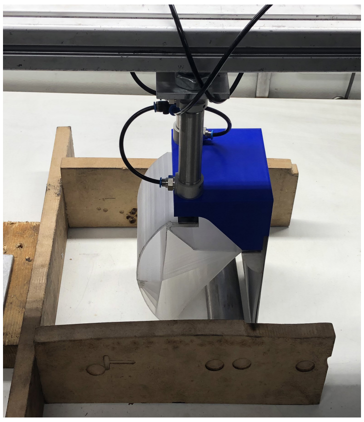

Figure 6.18: Iteration 4 endurance experiment setup close up, including steel cylinder as chicory replacement and a wooden limiting movement frame to keep the cylinder inside the gripper mouth.

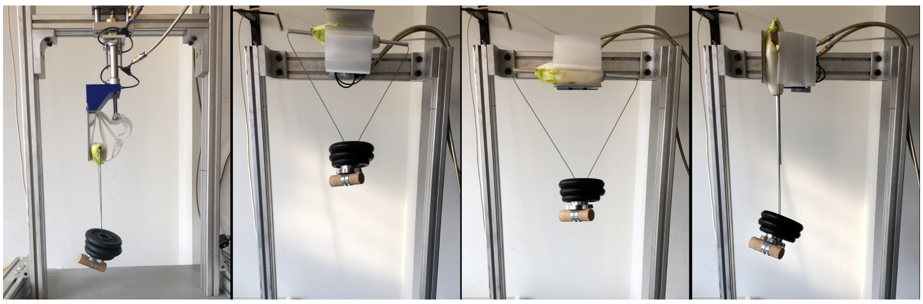

Figure 6.19: Force experiments after the endurance test, from left to right: negative z direction, y direction, negative y direction and x direction. All directions reached the force requirement with 3 bar input pressure.

Related to the endurance testing, a robustness test has been performed. 10,000 gripping cycles of the the endurance test are performed using a real chicory instead of a metal tube (figure B.18). During these 10,000 gripping actions, several chicory samples have been replaced. Within these chicory replacements, several diameter sizes have been placed. Not even a single gripping failure occurred during this 10,000 real chicory gripping actions. Therefore, at least a gripping failure rate of 1/10,000 (0.01%) is reached. This transcends the obtained failure rate noted in the list of gripper design requirements by a factor 10. Therefore, the pickup failure requirements have been met. To extent the robustness test, rotational perturbations have been applied to the real chicory sample during the final gripper repetitions of the endurance test (figure B.19). 100 rotational perturbations have been performed on a large and on a small chicory sample, resulting in not a single gripping failure.

To investigate the closing and opening speed of the gripper, a time series has been made (figure B.20 and B.21). The gripping action has been filmed with a standard 60 frames per second (fps) image rate which is sufficiently fast enough to determine the closing and opening speeds. For the closing movement, the starting frame refers to one frame before the gripper starts closing. The last frame of the series is one frame after the gripper stops closing and the pressure cylinders are completely extended. By analysing the closing speed (figure B.20), the time indicated on the frames starts at 0:00:00:03 (3). This indicates hours:minutes:seconds:milliseconds (frame number of original film), respectively. The time difference between the first and last frame in this time series is 23 milliseconds (ms). The same is done for the opening gripper motion (figure B.21). Which results in a similar speed compared to the closing speed: 23 ms. The required max. pick and place time is 30 ms each. So, both the opening and closing actuation are within the time requirements.

The next step in the evaluation process of iteration 4 refers to food safety. As specified in the design requirement list, a maximum allowable material transfer from gripper to chicory is prescribed. The transfer limit is $60mg/kg$ food according to FDA (and EU) regulations. This limit is specified for potential PP plastic transferring from the gripper into the chicory. To determine the migration rate of gripper iteration 4, 14 chicory samples have been weighted prior testing as reference. Each individual chicory is gripped for 2 seconds and re-weighted afterwards by using the experimental setup of figure 6.21. By subtracting the two weight measures, the transfer rate is calculated. Due to the precision of the scale (0.0001 gram is equal to 0.1 mg), each individual chicory up to a maximum weight of 200 grams can be tested on material migration. To minimize repeatability uncertainties of the scale, every chicory is weighted three times before and after gripping. According to the measurements, transfer rates are calculated. The diameter of the chicory can be dependent on the transfer rate for example. Therefore, depending on the repeatability of the measurements, the highest transfer rate calculated is leading for the final resultant material migration rate.

Ideally, to check whether the material transfer from gripper to chicory is 100%, a weight measure of the gripper is needed as well. Unfortunately, no scale was available with the required maximum load in combination with the required precision to be able to weigh the gripper prototype accurately. Even the compliant parts of the gripper were heavier than 200 grams. By taking the compliant parts of the gripper, a potential material loss during the dissembling process can occur, therefore weighing the full gripper prototype would be preferable. However, because only the chicory weight can be measured, the assumption of 100% material transfer from gripper to chicory had to be made.

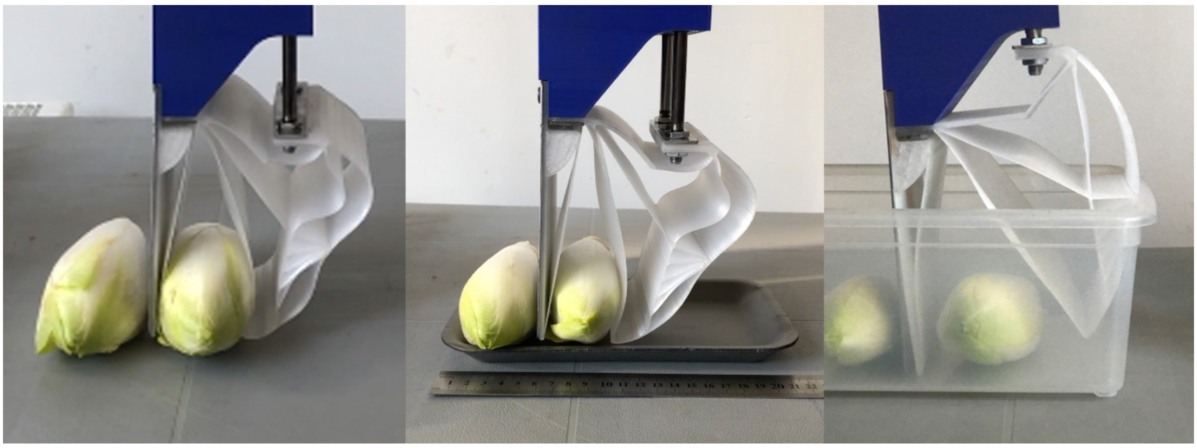

Figure 6.20: Drop off configurations: side by side on flat plane (left), flowpack (middle) and in a crate (right).

So far the theory. By applying the first sample on the scale, strange behaviour of the mass of the chicory was noticed: it continuously decreased in mass! To verify whether the scale had a stabilization issue, a reference mass of 200 gram was applied on the scale. This reference mass was measured accurately (with 0.1 mg precision) within seconds. This reference mass check confirmed that the chicory sample is losing weight continuously. This causes a serious problem for the migration limit measurements. In first instance the plan was to perform three measurements before and after gripping the chicory sample. Due to the instant weight loss of the chicory, this is not an accurate approach. Therefore, the chicory was weighted until it sort of stabilized, followed by a gripping action and a reweighing of the sample rapidly without delays. By performing this measurement on 14 samples, the least measured material transfer after gripping was -92 mg/kg. This shows that the chicory has lost 92 mg/kg sample during the gripping process instead of gained mass by material transfer from the gripper onto the chicory.

To declare this weight loss phenomena, the chicory was assumed to act like a sponge. The chicory is losing water continuously. When pressure is applied on the surface of the chicory, even more water is squeezed out of the chicory. Therefore a significant weight loss is present. Unfortunately, due to this negative material transfer coefficient, no conclusions on the material transfer from gripper to chicory can be made regarding FDA limits. Therefore, the exact same experiment needs to be redone with a analytical scale which is capable of handling a maximum mass up to 2 kg. In this new experiment, not only the chicory samples are weighted after every gripping action, also the entire gripper prototype itself needs to be measured. However, even with this new experimental setup, squeezed water from the chicory onto the gripper can compensate potential plastic particle transfer form the gripper onto the chicory. So even with a new experimental setup, material transfer limits could potentially not be proven.

Due to the unprovability of the transfer rate, the food grade certificate obtained by the material supplier needs to be trusted. This is tricky however. Due to the 3D printing process a texture on the contact membrane is formed. This texture can potentially wear out and result in plastic particles in the food. Therefore, further research of the migration rate is needed.

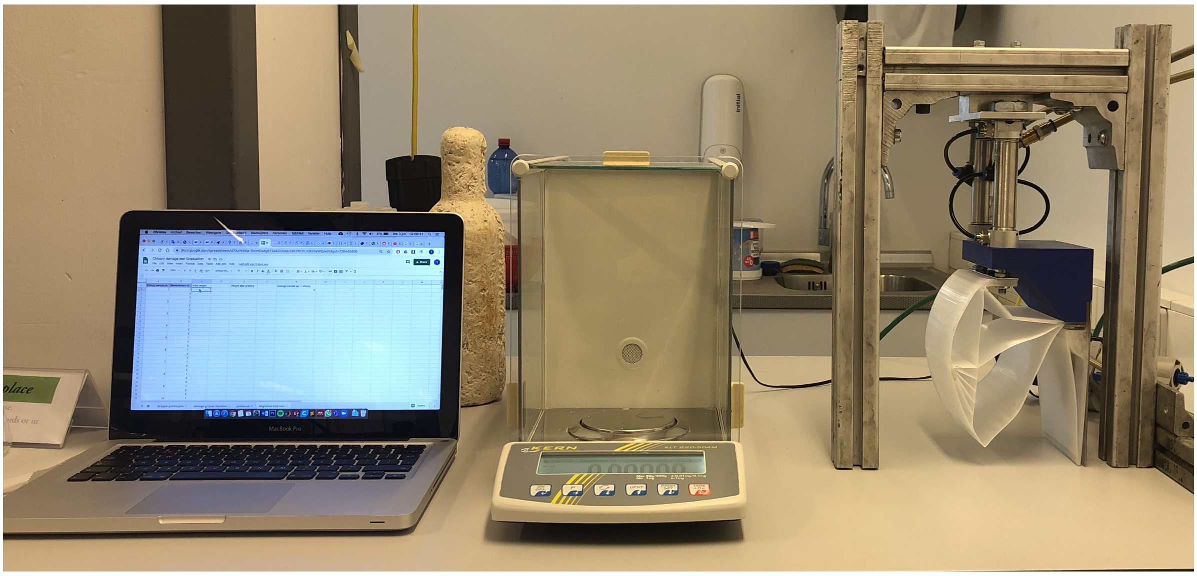

Figure 6.21: Migration limit experimental setup, with a laptop to note the weights measured by the analytical precision scale and gripper iteration 4 in a small test frame to grip the chicory samples individually.

7
Results

7.1 Prototype designs

The analysis phase of this graduation project resulted in a list of nineteen design requirements. Based on these design requirements, nine concept drawings have been made and simulated using ANSYS FEM software. From these drawings and simulations, two concepts have been merged into a proof of concept prototype. The proof of concept has been 3D printed and tested on basic working principles. According to this proof of concept prototype, four full size prototypes have been made taking the design requirements into account. The first four prototypes have been evaluated on force and damage criterion. Force requirements have been reached by all prototypes. However, damage requirements were not reached by three of these four prototypes. Four iteration steps on the gripper design were needed to reach damage and force requirements combined with required pick up performance. An overview of this design process is illustrated in figure 7.1. Iteration 4 was the first iterative prototype which managed to grip without damage and perform a decent pick up of the chicory. With iteration 4, all remaining requirements were evaluated.

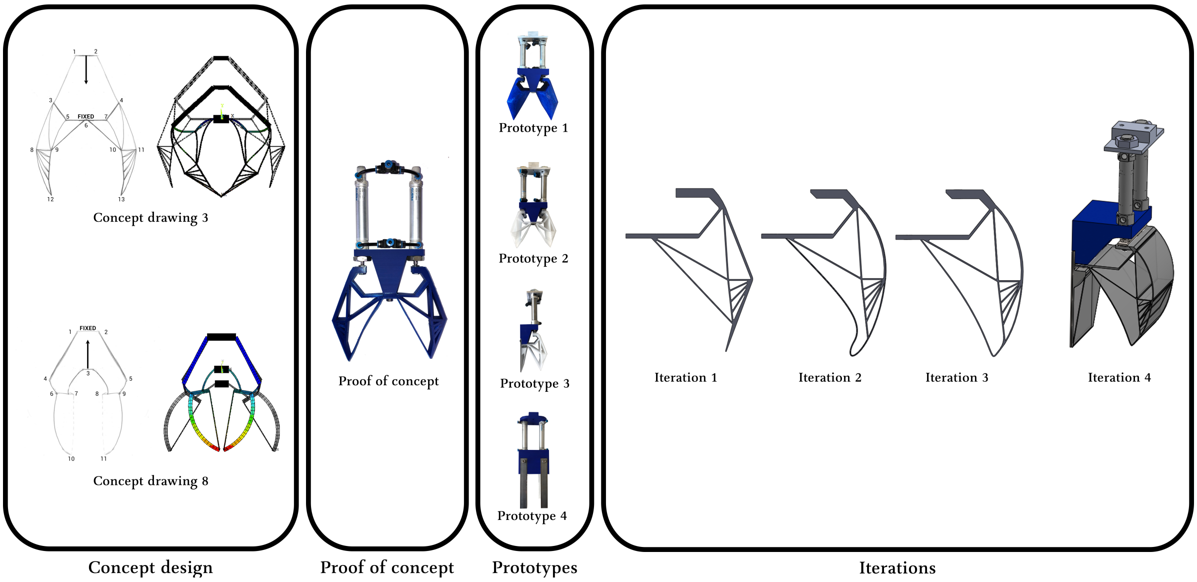

Figure 7.1: Design process from concept drawing to iteration phase. Concepts 3 and 8 have been merged into a proof of concept. The proof of concept is expanded with four working prototypes. Based on the performance of the prototypes, 4 iteration steps have been accomplished.

7.2 Damage avoidance

A damaged chicory can consist of crushing marks, local dents and/or cutting edges. Figure 7.2 illustrates the process of minimizing damage among the prototypes and iterations originating from the first concept drawings. Prototype 1 in figure 7.2 shows 0% damage. This due to the compliance of the ninjatek cheetah material used in this gripper. The PP material was used in prototypes 2, 3 and 4. However, the stiffness of these prototypes was to high, resulting in almost 100% damage. During the iteration steps, a method for stiffness reduction was performed and resulted in a significant stiffness decrease with the PP material. This resulted in removing the crushing damage on the chicories completely (figure 7.2). However, in iteration 1, new damage occurred due to the connection point of the membrane, resulting in local dents (as shown in figure 7.2). Iteration 2 resolved these local dents but created a new type of local damage at smaller sized chicories. Iteration 3 was able to grip the chicories without damage apart from cutting edges. Iteration 4 is a scaled and extruded version of iteration 3. Due to the extruded shape, no cutting edges were present in iteration 4 and no other damages were introduced. No damage on any sample occurred after 24 hours and 48 hours.

7.3 Force efficiency

Iteration 4 is able to pick up small light weight chicories of 40 gram and large chicories up to 300 gram. Related to the weight of the chicory is the ability to hold the chicory while an acceleration force up to 26.5 N is applied on the chicory in (negative) z, (negative and positive) y and (positive) x direction. Iteration 4 is able to withstand these acceleration forces in all obtained directions similar to previous prototypes. To be able to compare all gripper prototypes across this thesis, efficiency is plotted against sample damage in figure 7.3. The efficiency is calculated by

$$Efficiency = \frac{F_{holding}}{F_{input}} \tag{7.1}$$

in which the holding force corresponds to the 2.7 kg load applied on the grippers during actuation. The input force varies across the prototypes. A clear trend is visible in the transition form the prototype phase to the iteration phase. Due to the stiffness reduction in iteration 1, less energy is occupied by the compliant mechanism which results in an efficiency increase. In iteration 2, efficiency remains equal but sample damage decreases. This is due to removal of local pressure spots in iteration 1 (as illustrated in figure 7.2). Iteration 3 results in similar sample damage and similar efficiency. However, the type of damage is changed (figure 7.2). In iteration 4, all damage is prevented due to the extrusion of the contact membrane. Because of the extrusion of the gripper, more energy is required to actuate the gripper. This energy increase results in a lower efficiency but results also in zero sample damage. Even after 106,000 gripping repetitions was iteration 4 still able to hold the 2.7 kg loading. The compliance of the gripper increased during the extensive testing but the holding force has been compensated by increasing the input pressure into the pressure cylinders. An input pressure of 3 bar after 106,000 gripping repetitions still results in a holding force of 26.5 N (2.7 kg). Due to the required force increase, the efficiency decreases from 21% to 14%.

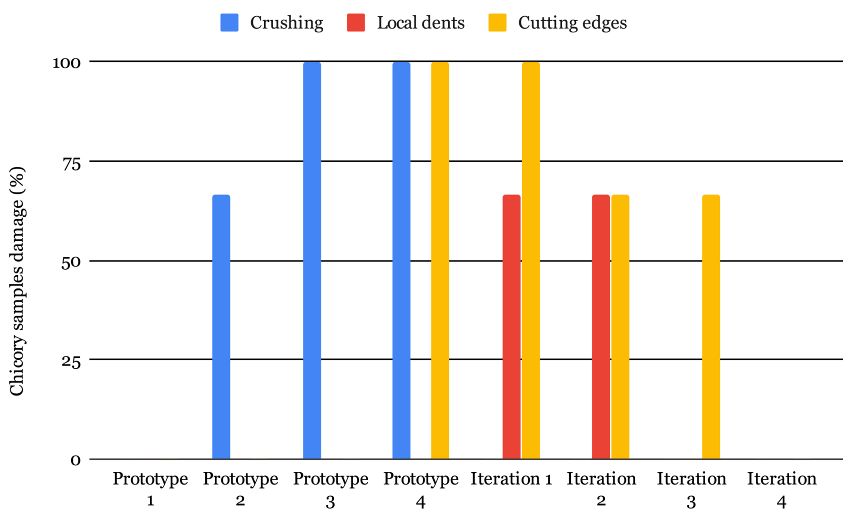

Figure 7.2: Decrease of sample damage with evolving prototypes up to iteration 4. On the x axis all prototypes and on the y axis the amount of damaged chicories.

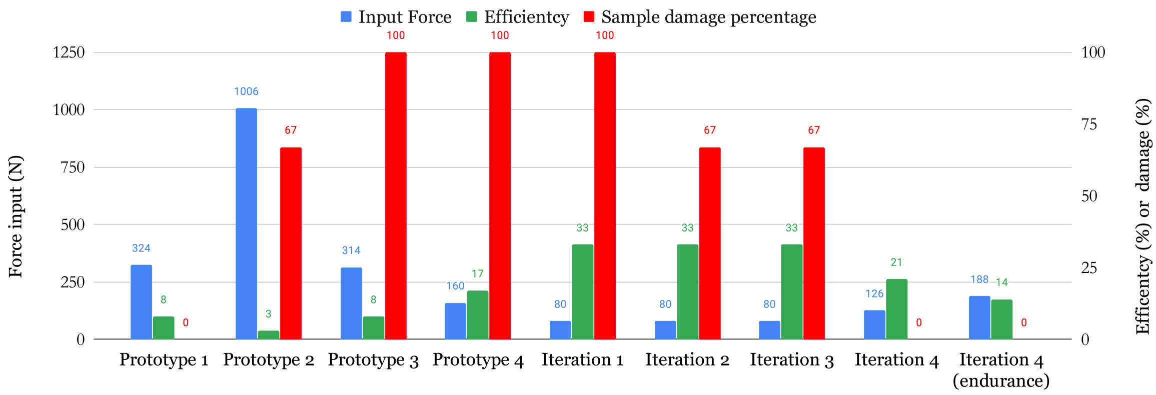

Figure 7.3: Input force compared to efficiency and damage resistance for all prototypes in this report.

7.4 Object variation

The membrane of iteration 4 has a width of 110 mm. Therefore, chicories up to 110 mm are completely covered by the membrane. Larger chicories are not completely covered by the membrane but the membrane covers the majority of the length. These large chicories have a maximum belly length of approximately 80 mm. The membrane is therefore able to cover the belly entirely. The fragile top and bottom of the largest chicories are not covered necessarily to perform a sufficient grip. Therefore, iteration 4 is able to grip all length variations according to the first design requirement. In first instance, the gripper design was specified for chicories with varying diameters form 30 mm up to 60 mm. During the evaluation phase, a significant amount of chicories for sale in the supermarket were noticed which consisted of a diameter up to 90 mm. Therefore, the diameter requirement was increased up to a diameter variation range of 30 mm to 90 mm. To be able to grip this new required diameter, a scaling factor was applied on the compliant gripper during the design process of iteration 4. Due to this scaling, the mouth opening of the gripper was extended to 95 mm. Therefore, iteration 4 is able to grip large chicories up to 90 mm in diameter. Also the smaller size chicories could still be gripped without damage with this scaled model. The 50 mm stroke length of the pressure cylinders cause the gripper to close with a 15 mm gap between the thin finger and the compliant actuated finger. This is the case when the gripper is empty. When a chicory of any diameter size within the required range is gripped, the gripper does not close entirely. The shape adaptive behaviour of the gripper is activated by pushing against the membrane, the tip of the compliant gripper turns inwards which enforces the gripper to curve underneath the chicory. A complete closure of the gripper is not required to hold the chicories, even with the required acceleration forces.

7.5 Endurance and operational speed

During the endurance experiment with iteration 4, the gripper has been actuated 106,000 times. During the last 10,000 gripping cycles, a chicory sample have been placed to test the pick up failure rate. After inserting several chicory sizes without a single pick up failure, the failure rate resulted in 0.01%. This is a factor ten better than intentionally required. The endurance test itself was designed to check whether prototype 4 was profitable in terms of life time expectation. To be profitable, the gripper is allowed to have a maximum depreciation of 0.001666 euro on the retail price per gripping cycle. With the completion of the endurance test of 106,000 gripping repetitions, a retail price of approximately 200 euro is proven to be fair according to the validated life time.

Based on the absence of any wear on iteration 4 after 106,000 gripping repetitions it is plausible that the gripper is able to reach 1 million gripping repetitions without failure. Although, the pressure input needs to be increased according to the increased compliance of the gripper over time. The pressure input with current cylinders is limited to 6 bars. When the gripper compliance increase requires actuation pressures outside the range of the operational pressure of the cylinder to hold the load without damage, the endurance failure criterion is reached. Without a longer endurance test, the expectation can not be proven. Due to planning limitations of this thesis, it was not possible to perform a duration test of 1 million repetitions. Which is unfortunately, because an increased life time of the compliant gripper should result in a higher allowable retail price containing larger profit margins.

Besides endurance, operation speed is an important factor to make this gripper profitable. To be able to return investments of the robot sorting machine, an average pick and place cycle time of 1.2 seconds is required. To be able to translate the chicory within this time frame, a maximum allowable pick and release time is calculated to be 0.3 second each. To verify this pick and release time, a 60 frames per second video was recorded and analysed using video capture software. Both closing and opening times are similar and within limits with 23 ms each (figures B.20 and B.21).

7.6 Pick up and release performance

The surface from which the chicory needs to be picked is a flat conveyor belt. The pick up test proves this requirement to be reachable. Requirements regarding drop off contains three side by side (10 mm spacing max.) configurations: on a flat conveyor belt, on a flowpack and in a transportation crate on top of each other. All three conditions have been tested during the iterative prototype phase and have been accomplished as shown in figure 6.20. A remark about the placement of the final chicory in a side by side placement into a transport crate: due to the volume of the compliant finger, a spacing between the side of the crate and the last chicory in line will occur. This gap can not be filled with a chicory, although it potentially fits the open space, simply because the gripper has no space to open without hitting the side of the crate. The open gap is dependent on the size of the chicories placed and can reach up to a gab of $Gap = Width_{gripper} - Diameter_{chicory}$. With a minimal diameter of 30 mm for the smallest chicory present within the design scope, this results in a maximum gap of $Gap = 130mm - 30mm = 100mm$ between the last placed chicory and the side of the crate. The potential gap does decrease the efficiency of the sorting robot.

Due to the mount plate at the top of the pressure cylinders, two M6 bolts can be fitted to be able to mount the gripper to the robot head. In addition, iteration 4 weighs just 1.3 kg and does not exceed the maximum allowable load of 1.7 kg on the robot. To reach within the full operation space of the robot head, a maximum height of 300 mm is required. Iteration 4 has a height of 350 mm and does therefore not accomplish requirement 15. Although, with small design changes of for example the mounting plate, pressure cylinders or mounting base plate, the height requirement will be within reach for a real production model. In the discussion, several design suggestions will be provided.

7.7 Food safety

Requirement 16 to 19 concern food safety requirements. Gripping the chicory without the use of non-food additives is accomplished. The compliant gripper does not need any additives (except compressed air for actuation) to be able to grip the chicory. To clean the gripper, the PP compliant parts can be placed in a dishwasher without performance decrease. In addition, due to the layout of the assembly, all parts can be removed and replaced or maintained. The materials used within a final product contain stainless steel for all mounting parts and cylinders and PP material for the compliant parts. Stainless steel and PP are both food safe materials. Also the PP manufacturer managed to accomplish FDA food safe requirements for the 3D printing filament. To verify the FDA requirements of the PP material in combination with the obtained design of iteration 4, a migration limit experiment is performed. By weighting the chicories before and after gripping, a potential material transfer from gripper to chicory can be examined. The migration limit of PP material into the chicory is 60 mg/kg food. In this experiment, 14 samples have been weighted and gripped. The weight difference before and after gripping is converted to a transfer rate expressed in mg/kg. The results of the migration experiments are presented in figure 7.4.

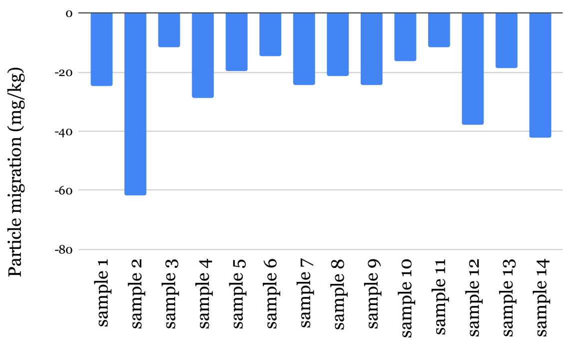

Figure 7.4: Negative material transfer from gripper to chicory. This indicates that the material loss of the chicory due to gripping is larger than the material transfer from gripper to chicory.

Unfortunately, this experiment resulted in useful measurements due to the instant weight reduction of the chicory. During the gripping procedure, even more water is squeezed out the of chicory. This weight loss is larger than the potential material transfer form gripper to chicory. It is even possible that measurement of the material transfer exceeds the migration limit and gets compensated by the amount of water squeezed out of the chicory. This also the result which is visual in figure 7.4 were the material loss causes a negative particle migration. Therefore, no conclusion can be formulated about a migration limit with these measurements.

8
Discussion

8.1 Required improvements

8.1.1 Food safety

According to the results, 17 of the 19 deign requirements for industrial application of the chicory gripper have been reached. After the iterative design process, two design requirements are not explicitly reached by the prototypes. The gripper height needs to be reduced to be able to reach within the full working space of the robot and the migration limit needs additional research.

For the migration limit experiment, an analytical scale with an allowable input load of minimal 1 kg is needed. This scale can be used to determine the weight of the gripper and the chicory individually before and after gripping. A similar experimental setup will be needed. The only difference is the weighting process of the gripper. By comparing the weight variation of the gripper and chicory, more insight in the particle transfer can be gained. However, also with this new setup, material transfer compensation is still possible. When the material transfer (water probably) form the chicory onto the gripper is larger than the migration of PP plastic to the chicory, transfer rates are compensated again. An additional improvement would be to collect and concentrate the water which is squeezed out of the chicory. By evaluating the weight of this lost water, measurements can be compensated. An advanced measurement setup will be required to catch the squeezed water from the chicory.

Elaborating on the food safe requirements, if current 3D printed gripper exceeds the migration limit, a different production technique is needed. The PP material is food safe but the surface texture of the gripper caused by the production technique can be a limiting factor. Therefore, injection moulding can be a suitable option for mass producing the compliant parts of the gripper. Injection moulding results is a smooth contact surface that reduces the particle migration. Similar to current food grade grippers used in industry, injection moulded PP parts are suitable for food handling processes. A different advantage of injection moulding is the dimensional accuracy of the parts and the production speed. Although the compliant parts need extensive cooling within the injection mould, it is nevertheless faster than 3D printing. Due to the extensive cooling, less parts can be moulded per hour and are therefore more expensive. A disadvantage of injection moulding the compliant parts are the investment costs for making the moulds. Due to the complex gripper structure, a complex mould is needed. An injection mould this complex could cost up to 30,000 euro easily. The investment can only be returned when the gripper is produced and sold over 1000 times. A different disadvantage of injection moulding over 3D printing is the loss of form freedom. When a customer wants a slightly different gripper, a 3D printed part can be edited and printed easily. This is not possible with an injection moulded part.

8.1.2 Design improvements

The design of the rigid parts of the gripper need to be manufactured from stainless steel. Stainless steel is a food grade material and is strong enough to handle the load and the actuation forces of the gripper. To reduce weight, two sheet metal parts need to be laser cut and edged to replace the mounting parts of iteration 4. A recommended design for a mass procured gripper is shown in figure 8.1. The previously rigid parts which were 3d printed are replaced by stainless steel parts. Five stainless steel sheet metal parts are present in this design. Starting with the 4 mm thick robot mounting bracket at the top of the gripper, a 4 mm thick base plate to replace the blue 3D printed part, a 2 mm thick pressure plate to distribute the input load on the compliant gripper, a 2 mm thick fixation strip to fix the compliant part and a 3 mm thick back plate to support the thin compliant finger. The thickness of back plate of the thin finger in the iteration 4 prototype was just 2 mm. This resulted in a slightly bended back plate after 100,000 gripping cycles. This new 3 mm thick stainless steel back plate should resolve this problem. However the back plate was slightly bended, this did not significantly reduce the gripper performance. All additional nuts and bolts have to be made from stainless steel as well. The total weight of the this recommended production design is calculated slightly under 1.5 kg and therefore within weight limits. The final design aspect are the pressure cylinders. Regular pressure cylinders make use of oil to lubricate the piston. For food grade applications, a food grade pressure cylinder is required. The performances are similar to the regular cylinder but the materials used are different. The overall material used for these cylinders is stainless steel and they have a special seal to prevent lubricant oil from leaking out the cylinder. All parts combined result in a food grade gripper, ready for mass production.

To reduce the total height of the gripper, all rigid parts have been reduced in height compared to iteration 4 as shown in figure 8.1. Also the new pressure cylinders are smaller and contribute to the height reduction. The final step in reducing the height of the gripper is hidden in the robot mount plate (No. 2 of figure 8.1). This plate lowers the mounting position of the gripper on to the robot head. Therefore, the distance between the robot head and the bottom of the gripper is 292 mm. The spacing between the cylinders facilitates a free rotational movement of the robot head without collision. Also, to position on the mounting holes on the robot mounting plate are aligned with the middle of the opening mouth of the gripper. Therefore, easy programming for the robotic pick and place program is facilitated. When the mounting holes are not aligned with the middle of the gripper mouth, an offset within the pick and place software is required to position the chicory centered in the gripper mouth, this is not preferable.

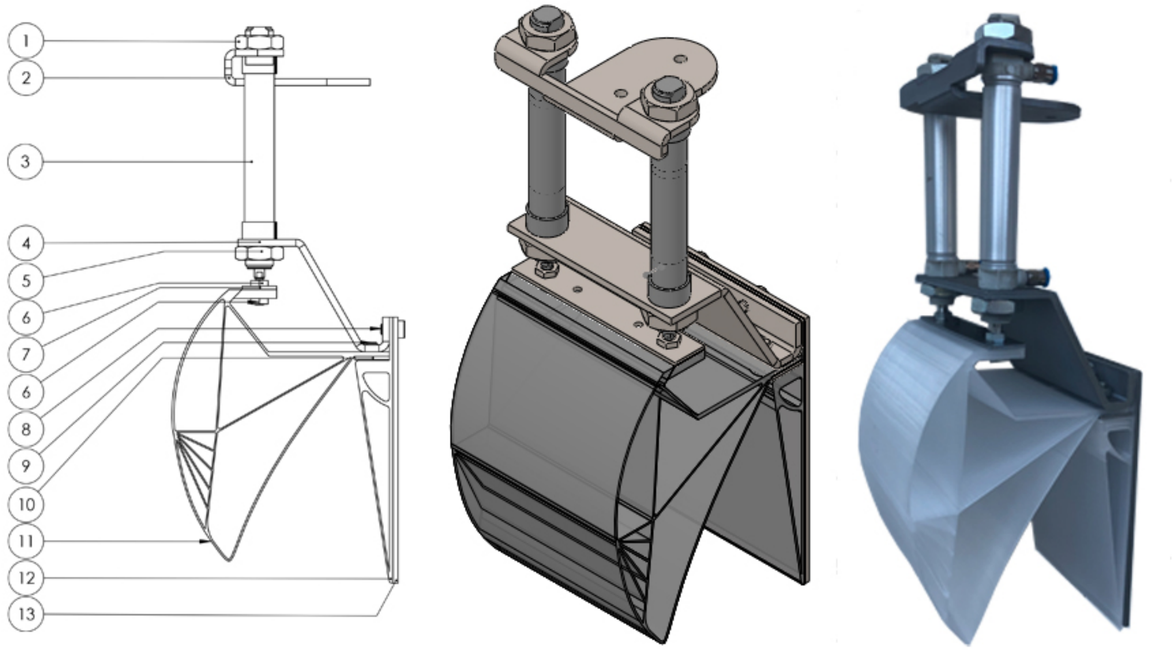

Figure 8.1: Recommended design for mass production, left image front view with part numbers, middle image shows the 3D SolidWorks model and right picture shows a 3D printed model of the recommended design. No. 1. M16 nut, 2. robot mount plate, 3. pressure cylinders, 4. base plate, 5. M16 nut, 6. M6 nut, 7. pressure plate, 8. M6x10 bolt, 9. M6x10 bolt, 10. fixation plate, 11. compliant finger, 12. thin finger, 13. back plate in the left image

8.2 State of the art comparison

By comparing the recommended design of the gripper with current literature, several aspects can be noticed. Gripper B-1 in figure 2.1 (refers to [7]) shows similar crossbars as used in the chicory gripper. In [7], this crossbars are used for shape adaptive behaviour by contact force. The crossbars in the chicory gripper have a stiffening effect to increase the holding force. During the concept phase of this project, similar crossbar shape adaptive structures have been 3D printed and evaluated. The connection points of the crossbars with the outer membranes of the finger result in local pressure damage on the chicory. Inspecting gripper A-II in figure 2.1 ([14]) shows similar performance of a rotating tip with a vertical input displacements on the compliant mechanism. Although the gripper structure differs completely from the chicory gripper, a similar tip displacement can be noticed. In E-II of figure 2.1 ([20] respectively) shows the use of 3D printed elastic material in combination with contact shape adaptive behaviour. This article served as inspiration to use 3D printable material for the prototypes of the chicory gripper. Comparing the actuation mechanism of [33] (E-III of figure 2.1) shows a similar displacement input structure. By reducing the relative distance of the diamond shaped actuation mechanism of the gripper presented in [33], a specific finger displacement was gained. The bar structure of the chicory gripper has some similarities. However, the gripper in [33] used hinge points between the beams and has no shape adaptive membrane. The gripper in [49] (E-IV of figure 2.1) used uniform beam bending similar to the chicory gripper. The bar mechanism of [49] has similarities with the chicory gripper. However, the bars of the chicory gripper are significantly thinner and the gripper of [49] has no membrane to perform a shape adaptive behaviour. Gripper D-VI in figure 2.1 ([86] respectively) does have a membrane structure. The relative large contact surface acts as a membrane on three centered fingers.

The patent literature studied in the state of the art (figure 2.2) shows comparable gripper aspects as well. Gripper D-1 ([84]) for example used uniform beam bending in the gripper structure to create a specific tip motion. Although the three fingered centered design is not suitable for chicory gripping, a design variant of this gripper can potentially be a useful chicory gripper. The most important factor missing in [84] is the ability to create a large contact surface to reduce object damage. Gripper D-10 of figure 2.2 ([11]) shows a membrane to be able increase the contact surface. The chicory gripper uses similar principle with a completely different design to be able to achieve other design requirements for the robotic sorting process as well. Gripper A-11 ([42]) is used for precise finger tip gripping but uses a comparable bar mechanism to prescribe the displacement of the tips. Similar principle is used in the chicory gripper with completely different design criteria. Finally, gripper E-10 of figure 2.2 ([42]) uses rotating tips to pick up the object. This effect is created by beam deformation in the chicory gripper in stead of rotating hinges as used in [42].

Overall, compliant grippers in academic literature show similarities in different aspects of the chicory gripper. However, no specific application for chicory gripping existed. The design of a membrane to be able to adapt to the shape of the object is not innovative on itself. But the application on chicories with an asymmetric gripper layout and a 110 mm extended object contact surface, acting as a membrane, was not yet present in the state of the art overview of the literature and patents. The combination of all design aspects makes the overall design of the chicory gripper an innovative contribution to the academic research on compliant fruit and vegetable gripping.

8.3 Patent request

In order to make the gripper profitable with mass production, a decent amount of gripper sells is required. Investigating the number of chicory farmers in the Netherlands results in approximately 10 registrations. A large chicory farmer produces up to 9 million chicories per year. Assuming that just two of the total chicory farmers in Holland are willing to invest in a robotic sorting line, results in 18 million sorting actions. When a compliant 3D printed finger survives duty for 500,000 sorting actions, approximately 36 grippers have to be produced every year. Assuming that the static parts and the cylinders of the gripper are lasting for years, only the compliant parts need to be replaced. With an operational life time of 500,000 gripping cycles, a retail price of approximately 800-1000 euros is allowable. This retail prices leaves margin for financing a patent request to protect the design of the gripper. Investigating the patents of compliant grippers in figure 2.2 shows no clear similar design as discussed in the state of the art comparison. However, further research by the European Patent Office will be required. Due to the retail margins, a patent investment could be returned within approximately 2 to 3 years (with retail in Holland only). The disadvantage of a patent request is the longer time to market. Due to the research and patent registration time by the EPO, the time to market is approximately 2 years. Currently, chicory farmers are looking for an automation option and several agriculture automation companies are researching the possibilities of chicory gripping. With a time to market of 2 years, it is assumable that different unpatented gripping solutions are introduced on the market prematurely. Furthermore, the power of compliant gripping is not specified in the specific design of the chicory gripper presented in this thesis. Compliant mechanisms can be adapted easily to new required design criteria. This is the real benefit of compliant gripping. By changing links, hinges or material, a completely different performance can be gained. Therefore, the sense of patenting this specific design is questionable.

8.4 Reflection

Reflecting on the design process of this shape adaptive compliant chicory gripper, several aspects could have been done in more detail. During the evaluation of the concept drawings and decision making process, a more measurable performance metric could have been used. The main aspects for the decision making of the concepts referred to tip movement to reach underneath the object and damage avoidance. By exporting data from the FEM model about the tip movement and the ability of reaching under the object, a more statistical decision could be made. The same holds for the shape adaptation and damage avoidance performance of the gripper. By performing an automated contact analysis in ANSYS, more quantitative insights could have been gained. These results could have been taken into account in the decision making process.

During the prototyping phase, the PP material was introduced. To transfer the stiffness of the previously used TPU material into the PP material, a 20% infill density of the 3D prints was introduced. This did not work out as expected. Instead stiffness reduction factors on the heights of the beams should have been introduced. This was however done during the iteration phase and worked out as calculated. A FEM calculation with a 20% infill structure is very computational, and therefore probably not very accurate with short run times. With the stiffness reduction due to the reduced heights of the beams, the modeling was easier and more accurate. A final remark about this project is the ability to test the gripper is a real robot setup. According to the covid-19 safety precautions of the dutch government, no testing in industry or academic environment was possible. Nevertheless, the theoretical force and handling requirements have been simulated by experiments. A real test with visual feedback on the robotic sorting system needs to be performed before the gripper can be classified as reliable.

8.5 Conclusions

With this thesis, the opportunities for compliant grippers in agricultural industries has been demonstrated. The application for robotic sorting of chicories is just one of the possibilities. A comparable compliant gripper can be used for different types of fruits and vegetables, for example: lettuce, cabbage or corn. Specially vegetables with leaves on the outside are suited for mechanical compliant grippers. Due to the unlimited form freedom of compliant mechanisms, grippers can be designed with a large variety of requirements for a large variety of applications. In this specific application on chicory gripping, 19 design requirements were set and 17 of the requirements have been reached by the created prototypes. Two remaining requirements on material transfer limits and overall gripper height can be reached with additional research.

Bibliography

[1] Robert Howe Aaron Dollar. Robust compliant adaptive grasper and method of manufacturing same. 2007-11-05. Patent Application Publication No. WO2008058061A2. WO patent office.

[2] Matthew D. Ellis Aaron Geisberger. Storing mechanical potential in a mems device using a mechanically multi-stable mechanism. 2002-09-10. Patent Application Publication No. US7012491B1. US patent office.

[3] Muddasar Anwar, Toufik Al Khawli, Irfan Hussain, Dongming Gan, and Federico Renda. Modeling and prototyping of a soft closed-chain modular gripper. *Industrial Robot*, 46(1):135–145, 2019. ISSN 0143991X. doi: 10.1108/IR-09-2018-0180.

[4] Kazuo Yokoyama Atsushi Ono. Laminated-type multi-joint portion drive mechanism and manufacturing method therefor, grasping hand and robot arm provided with the same. 2005-08-09. Patent Application Publication No. US7258379B2. US patent office.

[5] Dominik Diensthuber Axel Thallemer. Gripper device for gripping objects. 2012-11-27. EP Patent No. 2735406A1. EP patent office.

[6] Chen Xiaohong Chen Rui Xiao Fangjie Bai Long, Deng Yupeng. The electrostatic absorption flexible grips of marmem driving. 2018-06-08. CN Patent No. 108687794A. CN patent office.

[7] Christian Ivan Basson, Glen Bright, and Anthony John Walker. Testing flexible grippers for geometric and surface grasping conformity in reconfigurable assembly systems. *South African Journal of Industrial Engineering*, 29(1):128–142, 2018. ISSN 22247890. doi: 10.7166/29-1-1874.

[8] Bruno Belzile and Lionel Birglen. A compliant self-adaptive gripper with proprioceptive haptic feedback. *Autonomous Robots*, 36(1-2):79–91, 2014. ISSN 09295593. doi: 10.1007/s10514-013-9360-1.

[9] K. Bengtsson. Irb 360-8/1130, irb 360-6/1600 , abb robots. https://library.e.abb.com/public/5089951be174befec1257c430032d757/IRB%20360-Range.pdf, 2013. Accessed: 06-11-2019.

[10] Santosh D B Bhargav. DETC2013-12179. pages 1–10, 2016.

[11] Lionel Birglen. Mechanical finger for grasping apparatus. 2015-09-11. Patent Application Publication No. WO2016037288A1. WO patent office.

[12] Lionel Birglen and Francois Herbecq. Self-adaptive compliant grippers capable of pinch preshaping. *Proceedings of the ASME Design Engineering Technical Conference*, 7(PARTS A AND B):249–257, 2009. doi: 10.1115/DETC2009-87067.

[13] Sung Soo Kim Seok Won Lee Chang Hwan LIM, Chang Eun Lee. Cable conveying apparatus. 2018-02-27. Patent Application Publication No. US20190240830A1. US patent office.

[14] Rui Chen, Ruizhou Song, Zhuo Zhang, Long Bai, Fuqiang Liu, Pei Jiang, Dirk Sindersberger, Gareth J. Monkman, and Jianglong Guo. Bio-Inspired Shape-Adaptive Soft Robotic Grippers Augmented with Electroadhesion Functionality. *Soft Robotics*, 6(6):701–712, 2019. ISSN 21695180. doi: 10.1089/soro.2018.0120.

[15] Ren Tao Chen Yonghua. A kind of soft drive unit of energy pre-storage. 2017-08-08. CN Patent No. 107433611A. CN patent office.

[16] Javier Martin Christine Rotinat-Libersa, Belen Solano. Integrated mecatronic structure for portable manipulator assembly. 2011-09-30. Patent Application Publication No. US20130298759A1. US patent office.

[17] Jason Dearden, Clayton Grames, Brian D. Jensen, Spencer P. Magleby, and Larry L. Howell. Inverted L-arm gripper compliant mechanism. *Journal of Medical Devices, Transactions of the ASME*, 11(3), 2017. ISSN 1932619X. doi: 10.1115/1.4036336.

[18] Zengya Dong, Guohua Gao, Hao Wang, and Yunsong Du. Study on Deformation and Contact Force Stability of a Novel Flexible Self-Adaptive Picking Manipulator. *Proceedings of 2018 2nd IEEE Advanced Information Management, Communicates, Electronic and Automation Control Conference, IMCEC 2018*, (Imcec):759–763, 2018. doi: 10.1109/IMCEC.2018.8469512.

[19] Mario Doria and Lionel Birglen. Design of an underactuated compliant gripper for surgery using nitinol. *Journal of Medical Devices, Transactions of the ASME*, 3(1):1–7, 2009. ISSN 19326181. doi: 10.1115/1.3089249.

[20] Khaled Elgeneidy, Peter Lightbody, Simon Pearson, and Gerhard Neumann. Characterising 3D-printed soft fin ray robotic fingers with layer jamming capability for delicate grasping. *RoboSoft 2019 - 2019 IEEE International Conference on Soft Robotics*, pages 143–148, 2019. doi: 10.1109/ROBOSOFT.2019.8722715.

[21] Aline Defranceski Feras Alzoubi, Herman Huber. Handling device and method for monitoring a handling procedure. 2016-09-01. EP Patent No. 3290167A1. EP patent office.

[22] Jan Cornelis Flikweert. Gripper, use of a gripper, and a product processing system. 2009-09-28. NL Patent No. 2003558C2. NL patent office.

[23] Hermann-Josef Frings. Medical gripping tool. 2013-07-25. DE Patent No. 102013107972A1. DE patent office.

[24] Stergios Ganatsios, Alina Spanu, Octavian Dontu, Daniel Besnea, and Gheorghe I. Gheorghe. CAD analysis applied to self-centering compliant grippers. *Applied Mechanics and Materials*, 327:305–309, 2013. ISSN 16609336. doi: 10.4028/www.scientific.net/AMM.325-326.305.

[25] Wang Hao Ren Han Li Lianshi Zheng Yuhang Gao Guohua, Dong Zengya. One kind pneumatically swallows type flexible manipulator. 2017-08-28. CN Patent No. 107414882A. CN patent office.

[26] L Garcia, M Naves, and D M Brouwer. 3D-printed flexure-based finger joints for anthropomorphic hands*. In *IEEE/RSJ International Conference on Intelligent Robots and Systems (IROS)*, pages 1437–1442, 2018. ISBN 9781538680933.

[27] Anmelder Gleich. Building block for building elastic elements. 2014-10-13. DE Patent No. 102014014891A1. DE patent office.

[28] SAGROSS DESIGNOFFICE GmbH. Arrangement for the variable deformation of handling devices, tools and other mechanical constructions. 2016-05-09. DE Patent No. 202016003086U1. DE patent office.

[29] Kwang-Gyu Lim Hae-Kwon Lee. Screw fastening apparatus using the collaborative robot. 2018-02-08. KR Patent No. 101882646B1. KR patent office.

[30] Karin Hoetmer, Just L. Herder, and Charles J. Kim. A Building Block Approach for the design of statically balanced compliant mechanisms. *Proceedings of the ASME Design Engineering Technical Conference*, 7 (PARTS A AND B):313–323, 2009. doi: 10.1115/DETC2009-87451.

[31] Mingxian Huang, Qinghua Lu, Weilin Chen, Jian Qiao, and Xingyao Chen. Design, analysis, and testing of a novel compliant underactuated gripper. *Review of Scientific Instruments*, 90(4), 2019. ISSN 10897623. doi: 10.1063/1.5088439.

[32] Lu Qinghua Huang Mingxian. A kind of clamp assemblies and flexible retainer. 2018-08-21. CN Patent No. 108839046A. CN patent office.

[33] Mirna Issa, Dalibor Petkovic, Nenad D. Pavlovic, and Lena Zentner. Sensor elements made of conductive silicone rubber for passively compliant gripper. *International Journal of Advanced Manufacturing Technology*, 69(5-8):1527–1536, 2013. ISSN 02683768. doi: 10.1007/s00170-013-5085-8.

[34] Nagarjun Jawahar, Sangamitra Manoharan, and Harish Chandran. Compliant Mechanisms - Integration of Micro Gripping Device with Positioner Using Topological Optimization. *SAE Technical Papers*, 2015-April(April):2–6, 2015. ISSN 01487191. doi: 10.4271/2015-01-0499.

[35] Bianca Homberg Joseph Delpreto Alex Shafer Jeffrey Bingham, Taylor Alexander. Sensorized robotic gripping device. 2018-12-11. Patent Application Publication No. WO2019118383A1. WO patent office.

[36] Eduard Schweigert Jens Gräßle. Gripper and method of manufacturing a gripper. 2016-06-21. EP Patent No. 3138669A2. EP patent office.

[37] Dr. Sdahl Michael Johannes Mühlschlegel. gripper. 2011-02-15. DE Patent No. 102011011255A1. DE patent office.

[38] Elias Knubben Johannes Stoll. Gripping equipment for gripping e.g. solar cell, has adjusting device attached to system portion for deformation of system portion between resting and function positions and between function and resting positions with action of forces. 2012-01-20. DE Patent No. 102012001095A1. DE patent office.

[39] Klaus Junginger. Device for gripping marking caps. 2018-11-05. DE Patent No. 202018106283U1. DE patent office.

[40] Gerrit Augustinus Kragten Justus Laurens Herder, Peter Steutel. Underactuated grasper. 2010-07-29. NL Patent No. 2005168C2. NL patent office.

[41] S. Kota, K. J. Lu, Z. Kreiner, B. Trease, J. Arenas, and J. Geiger. Design and application of compliant mechanisms for surgical tools. *Journal of Biomechanical Engineering*, 127(6):981–989, 2005. ISSN 01480731. doi: 10.1115/1.2056561.

[42] Yaroslav Tenzer Lael Odhner, Leif Jentoft. Compliant adaptive robot grasper. 2016-03-04. Patent Application Publication No. WO2016141266A1. WO patent office.

[43] Kameron C. Chan Federico Parietti Lawrence Zachary Bright, Jeffrey Ackerman Curhan. Flexure gripping device. 2019-03-07. Patent Application Publication No. US20190275683A1. US patent office.

[44] Hans Tokpa Leidenfrost. End effector. 2018-11-30. Patent Application Publication No. WO2019108952A1. WO patent office.

[45] Shuguang Li, John J Stampfli, Helen J Xu, Elian Malkin, Evelin Villegas Diaz, Daniela Rus, and Robert J Wood. A Vacuum-driven Origami " Magic-ball " Soft Gripper. pages 7401–7408, 2019.

[46] Xiong Li, Wenjie Chen, Wei Lin, and Kin Huat Low. A Variable Stiffness Robotic Gripper Based on Structure-Controlled Principle. *IEEE Transactions on Automation Science and Engineering*, 15(3):1104–1113, 2018. ISSN 15455955. doi: 10.1109/TASE.2017.2732729.

[47] He Fuben Zhang Hongzhe Su Mengmeng Liang Yande, Wang Ruifeng. A kind of flatly moving type robot flexibility paw. 2017-04-11. CN Patent No. 106881726A. CN patent office.

[48] Jürgen Lieb. Holding device for holding objects. 2013-08-14. DE Patent No. 102013013555A1. DE patent office.

[49] Chih Hsing Liu, Chen Hua Chiu, Ta Lun Chen, Tzu Yang Pai, Yang Chen, and Mao Cheng Hsu. A soft robotic gripper module with 3d printed compliant fingers for grasping fruits. *IEEE/ASME International Conference on Advanced Intelligent Mechatronics, AIM*, 2018-July:736–741, 2018. doi: 10.1109/AIM.2018.8452420.

[50] Chih Hsing Liu, Guo Feng Huang, Chen Hua Chiu, and Tzu Yang Pai. Topology Synthesis and Optimal Design of an Adaptive Compliant Gripper to Maximize Output Displacement. *Journal of Intelligent and Robotic Systems: Theory and Applications*, 90(3-4):287–304, 2018. ISSN 15730409. doi: 10.1007/s10846-017-0671-x.

[51] Wang Bo Wang Haiqi Xie Yuming Wang Piao Liu Heping, Liu Zheng. A kind of flexibility clamping jaw. 2018-05-22. CN Patent No. 108638115A. CN patent office.

[52] Luo Dujin. Bionic flexible manipulator. 2017-02-27. CN Patent No. 106826902A. CN patent office.

[53] Nils Mallitzki. Container clamp for holding and guiding containers. 2014-11-03. EP Patent No. 3215444A1. EP patent office.

[54] David Youmans Marc Strauss. Preshaping for underactuated fingers. 2016-02-22. Patent Application Publication No. US9914214. US patent office.

[55] Maxime Beck Mathieu Grossard. Clip-type gripping device and system comprising such devices. 2017-03-07. FR Patent No. 3063668A1. FR patent office.

[56] Benoit Perochon Maxime Beck, Mathieu Grossard. Passive automatic tripping gripping device. 2017-11-29. FR Patent No. 3074077A1. FR patent office.

[57] Stefan Saller Metin Dr. Giousouf, Ruwen Kaminski. Holding device for fixing objects. 2011-03-23. EP Patent No. 2502714A1. EP patent office.

[58] Andrija Milojević, Sebastian Linß, Žarko Ćojbašić, Heikki Handroos, Lauri Luostarinen, and Lena Zentner. Adaptive Soft Robotic Gripper Based on Shape Morphing Compliant System. *2018 International Conference on Reconfigurable Mechanisms and Robots, ReMAR 2018 - Proceedings*, 2018. doi: 10.1109/REMAR.2018.8449831.

[59] Murakatsu Naoki. Electric tweezers. 2003-05-26. CN Patent No. 100408273C. CN patent office.

[60] Naoki Muramatsu. Microactuator. 1997-12-15. Patent Application Publication No. US20030110874A1. US patent office.

[61] Martin Neusser. Single-piece objects gripper device for use in mounting machine for mounting electronic components on printed circuit board, has gripper element actively connected with pliers element for gripping objects during actuation of membrane. 2012-02-03. DE Patent No. 102012100916A1. DE patent office.

[62] Duc Chuong Nguyen, Thanh Vu Phan, and Huy Tuan Pham. Design and Analysis of a Compliant Gripper Integrated with Constant-Force and Static Balanced Mechanism for Micro Manipulation. *Proceedings 2018 4th International Conference on Green Technology and Sustainable Development, GTSD 2018*, 2: 291–295, 2018. doi: 10.1109/GTSD.2018.8595638.

[63] Kaidi Nie, Weiwei Wan, and Kensuke Harada. An Adaptive Robotic Gripper with L-Shape Fingers for Peg-in-Hole Tasks. *IEEE International Conference on Intelligent Robots and Systems*, pages 4022–4028, 2018. ISSN 21530866. doi: 10.1109/IROS.2018.8594370.

[64] D Petkovi and N D Pavlovi. Mechanisms, Transmissions and Applications. 3:143–150, 2012. doi: 10.1007/978-94-007-2727-4. URL `http://link.springer.com/10.1007/978-94-007-2727-4`.

[65] Dalibor Petkovic, Mirna Issa, Nenad D. Pavlovic, and Lena Zentner. Passively adaptive compliant gripper. *Applied Mechanics and Materials*, 162:316–325, 2012. ISSN 16609336. doi: 10.4028/www.scientific.net/AMM.162.316.

[66] Chem Safety Pro. Food contact science and testing: What are oml, sml and qm? 2018. Accessed: 06-11-2019 via https://www.chemsafetypro.com/Topics/Food_Contact/Food_Contact_Science_and_Testing_.

[67] Kai Dipl.-Ing. Wegener Ralf Dipl.-Ing. Becker, Florian Dipl.-Ing. Simons. Finger-like gripping device, comprising several lateral elements movable joined with transversal elements and springs. 2005-03-07. DE Patent No. 102005010380A1. DE patent office.

[68] Ramon Dipl.-Ing. Hofer Ralf Dipl.-Ing. Becker, Andrzej Dipl.-Ing. Grzesiak. Gripper device in form of artificial hand, has two fingers attached at frame and is formed like hinge and can bend in area around finger in assigned movement plane. 2006-02-28. DE Patent No. 102006009559B3. DE patent office.

[69] Santosh Bhargav D. B. Ramnath Babu T. J. Sample manipulator. 2017-08-08. Patent Application Publication No. WO2018073833A1. WO patent office.

[70] Santosh Bhargav D. B. Ramnath Babu T. J. Method for regulating a sample manipulator. 2017-08-08. Patent Application Publication No. WO2018122863A1. WO patent office.

[71] Brian Dunne Daniel Nelson Mason Mc Innis David Bullock Russ Mitchell, Brandon Evers. Produce orientor. 2019-03-08. Patent Application Publication No. WO2019177680A1. WO patent office.

[72] Jason A. Chrisos Ryan R. Knopf, Joshua Aaron Lessing. Gripper with tunable compliance for dexterous object manipulation. 2019-06-26. Patent Application Publication No. US20190387678A1. US patent office.

[73] Masahiro Shiomi. Robot and robot hand. 2012-12-14. EP Patent No. 2604398A2. EP patent office.

[74] Masahiro Shiomi. Gripping apparatus, robot, and gripping method. 2014-10-24. Patent Application Publication No. US20150115636A1. US patent office.

[75] Chien-Ching Chiu Shyh-Chour Huang. Microgripper device for a micro-mechanism. 2004-09-01. Patent Application Publication No. US20060043749A1. US patent office.

[76] Peter Steutel, Gert A Kragten, and Just L Herder. Design of an underactuated finger with a monolithic structure and largely distributed compliance. In *Proceedings of the ASME Design Engineering Technical Conference*, volume 2, pages 355–363, 2010. ISBN 9780791844106. doi: 10.1115/DETC2010-28127.

[77] Sun Tao, He Zhiyuan, Song Yimin. Flexible mechanical hand claw capable of achieving passive enveloping. 2015-05-18. CN Patent No. 104889980A. CN patent office.

[78] One Of A Kind Technologies. Crux agribotics - sortipack tomatoes.

[79] Jung Yuan Wang and Chao Chieh Lan. A constant-force compliant gripper for handling objects of various sizes. *Journal of Mechanical Design, Transactions of the ASME*, 136(7):1–10, 2014. ISSN 10500472. doi: 10.1115/1.4027285.

[80] Wang Wenqing. Mechanical clamping jaw for clamping egg-shaped object. 2016-06-14. CN Patent No. 105904479A. CN patent office.

[81] Paul H. Adams William Harrington, Robert F. Smith. Reaching and grasping tool with improved gripping heads. 2017-12-19. EP Patent No. 3338952A1. EP patent office.

[82] Hasenpusch Wolfgang. Concentric gripper. 2001-15-10. DE Patent No. 20107907U1. DE patent office.

[83] Yu Weidong, Wang Hao, Chen Genliang, Xu Xun, Tang Chuyu, Pan Hao. Clamp for precise devices. 2016-10-25. CN Patent No. 106393166A. CN patent office.

[84] Yuan Qingdan, Xi Zhigang. Flexible three-finger clamp holder having touch sensing function. 2016-10-11. CN Patent No. 106346510A. CN patent office.

[85] Tang Yue. A kind of flexible mechanical arm and its control method of cooperating. 2018-11-22. CN Patent No. 109202873A. CN patent office.

[86] Aurelian Zapciu, George Constantin, and Diana Popescu. Adaptive robotic end-effector with embedded 3D-printed sensing Circuits. *MATEC Web of Conferences*, 121:1–8, 2017. ISSN 2261236X. doi: 10.1051/matecconf/201712108008.

[87] Yang Zheng, Lin Cao, Zhiqin Qian, Ang Chen, and Wenjun Zhang. Topology optimization of a fully compliant prosthetic finger: Design and testing. *Proceedings of the IEEE RAS and EMBS International Conference on Biomedical Robotics and Biomechatronics*, 2016-July:1029–1034, 2016. ISSN 21551774. doi: 10.1109/BIOROB.2016.7523766.

A

Appendix A

Literature study as a reference for the relevance of the subject of this thesis, starts on the next page.

State of the art adaptive shape gripping for automated agricultural industries

Thomas Hester, Gerwin Smit and Paul Breedveld
Delft university of technology - BioMechanical Engineering

22-01-2020

CONTENTS

***Abstract*—Traditional grippers consisted of rigid fingers, designed for specific objects. The inability of gripping different shaped and sized objects makes them useless in modern times. Demand for adaptive grippers is increasing. Especially agricultural industries require gentle and adaptive gripping to speed up sorting and harvesting processes. This state of the art provides a classification structure of adaptive gripping. Therefore, selection criteria of adaptive gripping have been set. Three levels of selection were discussed along with several examples for non adaptive repelled end groups. The selected adaptive grippers were classified in four categories. This selection and classification process serves inspirational purposes for new adaptive gripper development within agricultural industries. Adaptive grippers are mainly used for industrial, agricultural and prosthetic applications. Grippers within these three application fields have been analysed on fundamental working principles and subdivided within the classification structure. 175 relevant articles were filtered, selected and classified. This resulted in seven end groups. Three non adaptive and four adaptive gripping end groups. With these end groups, several analysis have been performed. Quantitative inquiry of publications among these end groups showed several research trends over the years.**

Keywords: Gripper, end-effector, robotic hand, harvest, adaptive, flexible, compliant, under-actuated, agricultural, fruit, vegetable, industry, prosthetic.

I. INTRODUCTION

A. Background

Adaptive shape gripping is a principle of object grasping without essential presents of friction forces. The gripper adaptively encloses the contours of the object to create a normal force which supports the object. These grippers are used in industrial and prosthetic industries. Recently, the demands for adaptive shape grippers in agricultural industries were growing. Especially gripping of fruits and vegetables requires force and shape adaptive gripping for efficient robotic sorting or harvesting applications.

B. Problem definition

Within gripping, three principles are known: grasping, suction and adhesion based gripping. Suction based gripping is perfectly suited for specific smooth surfaced objects, but gripping vegetables with leaves (chicory, cabbage or lettuce for example) is hard. The outside leaves attach to the suction actuator but can not hold the load of the entire object taking acceleration forces applied by the sorting or harvesting robot into account. Adhesion based grippers in general complicate food handling regulations because of adhesion additives or micro structures in which product residues remain. Grasping principles prevail after all. Because agricultural food varies in shape and size, adaptive grippers are required. Lag of inspiration for innovative adaptive shape grippers applied in agricultural industries, obstructs robotic fruit and vegetable food handling.

C. Goal

This state of the art provides a selection criteria overview of grippers in general specified towards an classification of adaptive shape gripping. The classification is based on fundamental working principles among these grippers.

II. Method

A. Literature search

All academic literature used in this study was gathered using the scopus search engine. To search for adaptive grippers within current literature, three search groups have been created. The first group consisted of all relevant synonyms for gripper and gripping: gripp*, grasp*, ”end-effector”, ”end effector”, ”robotic hand” and ”harvest”. The asterisks represent all possible word extensions and citation marks refer to an explicit string in between the marks. The second group represented all relevant synonyms for adaptive, using queries: ”adaptive”, ”flexible”, ”compliant”, ”under actuated” and ”under-actuated”. The third search group specified the application fields of the grippers, using queries: agri*, agro*, fruit*, vegetable*, prosthetic* and industr*. This group combines three specific application fields: prostheses, agricultural industries and industry in general. The first four search queries refer to the explicit application field on which this study is specified: gripping of agricultural food. To extent this core application field, an extra adaptive gripping application was taken into account by introducing prostheses. Because the human hand is extremely adaptive during grasping, prostheses in general have been taken into account. Lastly, industrial applications were included because grippers are widely used in industrialized (production) environments containing an increasing amount of robotic manipulated grippers. A visualisation of the search groups is presented in table II-A. These search groups were used to search within titles, abstracts and keywords.

Several other application fields for grippers are known. For example: medical and micro (electronic) grippers. These applications have not been taken into account due to irrelevant and non comparable gripper and object dimensions.

	AND $\rightarrow$		
OR $\downarrow$	gripp*	underactuat*	agri*
	grasp*	under-actuat*	agro*
	”end effector”	”adaptive”	fruit*
	”end-effector”	”flexible”	vegetable*
	”robotic hand”	”compliant”	prosthetic*
	”harvest”		industr*

TABLE II.1: Search groups in matrix format, horizontally combined with AND structure, vertically combined using an OR structure

Searching within titles, abstracts and keywords of the articles resulted in 2,528 English results. Research areas as business and management or physics and astronomy were included in the search as well. Therefore, three relevant subject areas have been selected to specify the search. Engineering, Materials Science, Agricultural and Biological Sciences. 2,053 articles remained. Among these articles, several results contained a theoretical control-system and simulation based approach which translates sensor data via a feedback-loop into an adaptive (normal) force gripper. These concepts of adaptive gripping are not taken into account. In this study, the mechanism design principles of adaptive grippers have the main focus. Therefore an extra filter was applied on the remaining 2,053 results which excluded all control and simulation titled articles. The resulting 1,495 articles have been accessed and evaluated manually, based on abstract inspection.

TITLE-ABS-KEY(gripp* OR grasp* OR ”end effector” OR ”end-effector” OR ”robotic hand” OR ”harvest” AND (under-actuat* OR underactuat* OR adaptive OR flexible OR compliant) AND (agri* OR agro* OR fruit* OR vegetable* OR prosthetic* OR industr*)) AND NOT (TITLE(control*)) AND NOT (TITLE (simulat*)) AND (LIMIT-TO (SUBJAREA, ”ENGI”) OR LIMIT-TO

(SUBJAREA, "AGRI") OR LIMIT-TO (SUBJAREA, "MATE")) AND (LIMIT-TO (LANGUAGE, "English"))

B. Inclusion and exclusion criteria

The evaluation process to determine whether an article should be included or excluded is based on the presents of a suggested or tested gripper design, finger design or mechanism design. At least one specific gripper part or principle was required to pass the inclusion criteria. Articles containing control algorithms and gripper simulation only were excluded form this study. 176 unique and relevant results remained after manual title and abstract evaluation. Articles for which abstract evaluation was not sufficient, the full content has been assessed.

The filtered articles have been published form 1982 until 2020. Because the articles potentially contain more than one gripper and/or multiple application purposes, more grippers than articles are present in this study. The 175 articles represent grippers among three application fields as specified in the search query.

III. Selection of adaptive grippers

A. Overview

To investigate the evolution and contribution of the different application fields over time, a time line visualisation was made (figure III.1). Analysing this time line in general shows a significant increase of adaptive gripping articles in the last two decades. The agricultural grippers have a noticeable increase in the last decade. However, contribution of all three application fields individually, increased similar and proportional to the total adaptive gripping articles.

Making a classification structure of grasp-based grippers requires a prior selection procedure toward adaptive shape locking grippers. This selection consists of three levels which subdivide the core working principles of each gripper. The first level subdivides different force application principles: friction based gripping and shape lock gripping. Gripping based on friction forces, compensate load forces due to normal forces translated into friction. Shape lock gripping compensates load forces directly by using the normal forces as supporting and load carrying counter forces. Therefore, no friction forces are required. Shape locking will be specified in deeper selection levels. The second level of the classification subdivides the relative grip size of the shape lock: local or overall shape lock. Local shape locking grips a specific part of the object only. Overall shape locking grips the overall outer contours of the object. To this extent, overall shape locking will be subdivided further in level three in which the ability of gripping different sized and shaped objects was determined. This resulted in a partition of rigid or adaptive structured grippers. To be able to grip and hold shape and size varying fruits and vegetables, adaptive structures are most promising and therefore further elaborated in a classification structure.

B. Selection process

a) Friction based or shape locking - level 1: Grasping can be divided in two main groups, friction based and shape locking based gripping. Friction based grippers make use of normal forces to establish a sufficient friction force to hold an object. The normal forces create a friction force relative to the friction coefficient corresponding to the gripper and object material specifications. High friction coefficients increase the performance of the friction based grippers in general. In shape locking, normal forces on the object do not necessarily establish a friction force to hold the object but, create a support force around the contours of the object. This support forces compensate the gravitational and acceleration forces directly. Controversially, low friction coefficients in shape locking grippers can even be preferable to enforce decent positioning of the object into the gripper.

Friction based grippers are the first end group of this selection structure (figure III.2). A typical friction based gripper, described by Bergelin is called "parallel jaw gripper" [1]. This gripper uses two (rotational) friction pads to create two contact points on the object. A linear actuator positions the pads onto the object. During activation of the linear actuator, two springs are compressed and generate a normal force on the object via the pads. These normal forces generate a friction force to hold the object, as visualized in figure III.4.

A different friction based gripper by Lochte in 2014 [2] used spherical particles in an air tight bag to create contact area with the object. The medium inside the bag is removed by the vacuum after positioning the bag onto the object. Due to this vacuum, a normal force is created and translated in to a friction force (figure III.5). Other friction based grippers can be found in: [3]–[30]

Shape locking grippers perform an enclosure of the object contours as depicted in figure IV.3 and IV.6. This gripping principle does not require friction forces but support the object via normal forces around the outer contours. This shape locking principle will be subdivided in level 2.

b) Local or overall shape lock - level 2: Elaborating on shape locking, a local and overall shape lock was subdivided. A local shape lock performs a shape lock grip on a specific part of the object and an overall shape

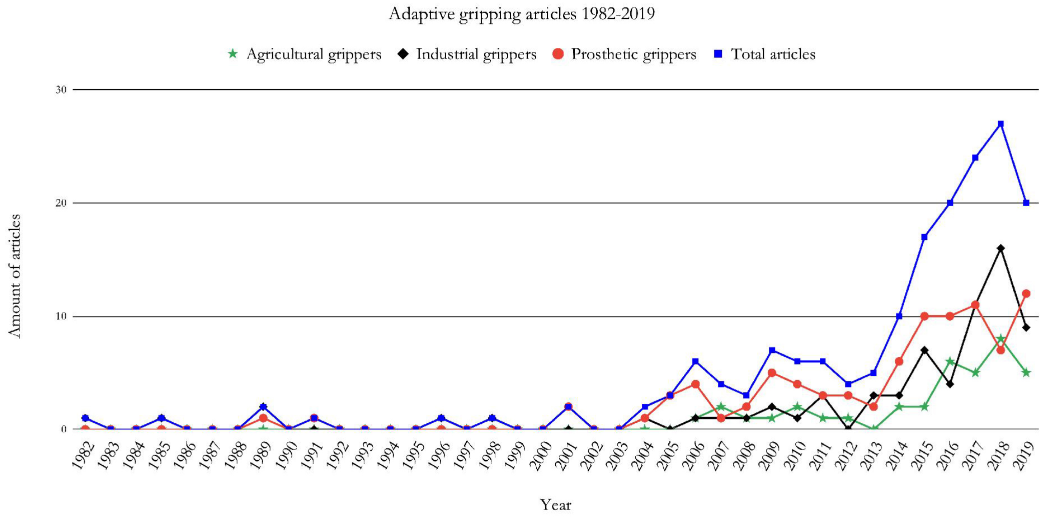

Fig. III.1: Filtered adaptive gripping literature from 1982 to 2019 among agricultural, industrial and prosthetic gripper articles relative to the total articles used in this study.

lock encloses the overall outside contours of the object. Gripping convex shapes (as most fruits and vegetables are) with a local shape lock is basically a friction based grip due to the absence of notches. Therefore local shape locking is only used for industrial applications. Performing an overall shape lock on the object reduces internal and surface stresses due to the larger contact area. This reduces risk on potential object damage.

A typical local shape lock gripper of Chen [3] is depicted in figure III.6. This gripper performs a local shape lock on the mushroom shaped hub at the top of the cylindrical object. The closing mechanism has cylindrical concave shaped finger tips to shape lock the cylindrical hub locally. Local shape lock grippers are the second end group of this classification structure as depicted in figure III.2. Similar local shape lock grippers can be found in: [4]–[6], [31]

Overall shape lock grippers support the majority of the outer contours as depicted in figure IV.4, IV.5, IV.3 and IV.6. More overall shape lock grippers will be discussed in selection level 3.

c) Rigid or adaptive structure - level 3: The overall shape lock can be performed by a rigid or adaptive structure. Rigid structures consist of at least two non-deformable fingers which do not alter shape during gripping a variety of different shaped objects. However, adaptive structures do change finger shape or configuration while performing gripping actions on different shaped objects. To grip size and weight varying objects without damage, an adaptive shape lock is preferred.

A typical rigid structure gripper is shown in figure III.7. The rigid fingers enclose the outer shape of the spherical object but do not adapt among the contours of different shaped objects.

The rigid structure gripper is the third end group of this classification. Similar rigid structure grippers categorized in this end group can be found in: [3], [4], [8], [9], [27], [32], [33]

The adaptive structures as depicted in figure IV.3 and IV.6, are extensively subdivided in the classification structure. The gripper in figure IV.6 for example, was tested with several objects. Each object resulted in a different states of the gripper finger. This gripper is therefore an adaptive structure. Non-adaptive end groups discussed in level 1,2 and 3 can be deeper classified beyond the scope of this study.

IV. Classification of adaptive grippers

A. Overview

Within adaptive gripping a subdivision of the core working principle can be made. Adaptive structures are divided in hinged structures or elastic structures. Hinge

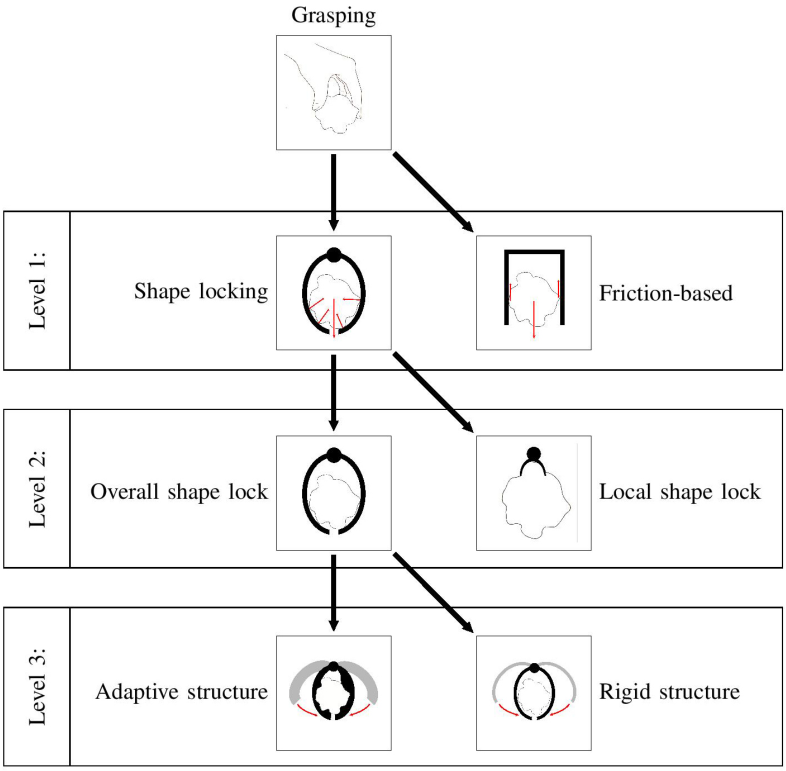

Fig. III.2: Selection toward adaptive gripping in three selection levels with three non adaptive gripping end groups.

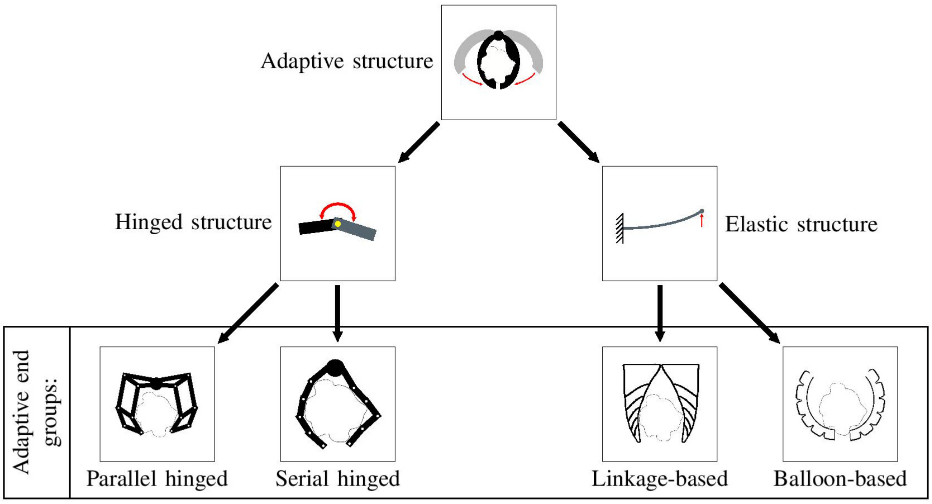

Fig. III.3: Classification of adaptive grippers resulting in four end groups.

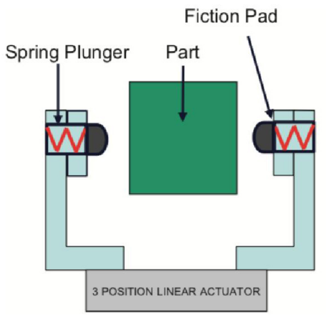

Fig. III.4: Friction based gripper of Bergelin [1] using friction pads and compression springs to generate a normal force resulting in a friction based grip.

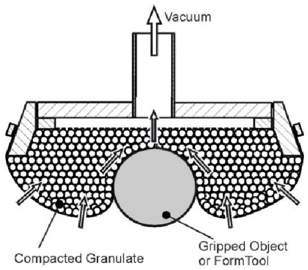

Fig. III.5: Friction based gripper of Lochte [2] using granular particle jamming and vacuum techniques to create a normal force resulting in friction.

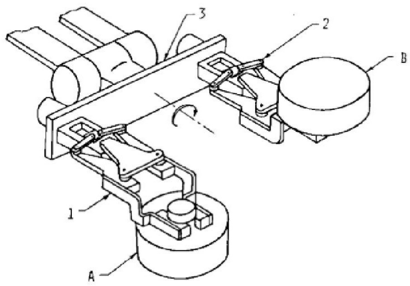

Fig. III.6: Double local shape lock gripper described by Chen to unload an object (A) form a lathe using the left gripper (1) while using the right gripper (2) to mount a second object (B) on the same lathe by rotating the wrist (3), according to [3].

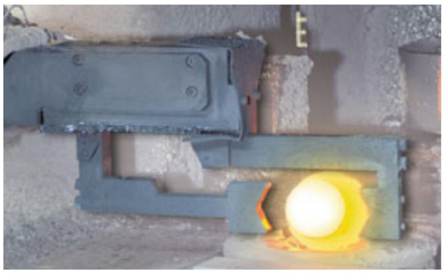

Fig. III.7: Rigid structure gripper by [5] for gripping a hot cast-iron rot for transportation toward a cooling container.

structures fold rigid body parts around the object to establish a shape lock and elastic structures perform material deformation while adaptive shape locking the object contours, as shown in figure III.3. Typical hinged structures are shown in figure IV.1, IV.2 and IV.3. Typical elastic structures are depicted in figure IV.6 and IV.7. Elaborating on these two adaptive mechanisms, hinge structures consist of serial or parallel hinged fingers and flexing structures consist of linkage-based or balloon-based fingers. This classification resulted in four adaptive gripper end groups, forming the core of this article. The classification structure is visualised in figure III.3.

B. *Serial hinged*

Within the hinged structures serial hinged structures can be subdivided. A typical serial hinged structure is shown in figure IV.1. The hinges are positioned in serial order in line with each other. These hinges are bend due to a cable displacement generated by the movement of the manual operated bar sliding mechanism. The cables inside the fingers are positioned off centre towards the side of the hand. Therefore, a moment is generated on the hinges during activation, resulting in the bending movement of the fingers.

A more industrial and agricultural oriented serial hinged gripper (figure IV.2) is described in [35]. Again, the hinges within one finger are positioned in series. The electric motors drive a pulley wheel connected to a tendon. This tendon is guided through the inside of the fingers. By winding up the tendon, an open gripper state is created. This process loads rotation springs located in the finger joints. To close the gripper, tendon tension is released and the torsion springs are unloaded. To adapt on the varying fruit sizes, index and middle finger (figure IV.2) are able to pivot.

Similar serial hinged grippers are discussed in [3], [5], [8], [36]–[93]

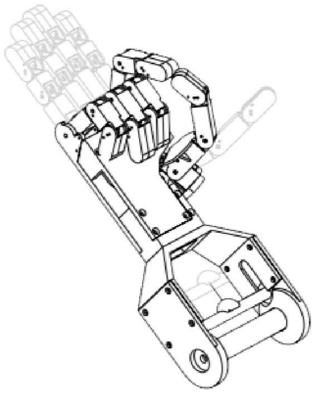

Fig. IV.1: Serial hinged adaptive hand in open (faded image) and closed state, activated by a cable displacement due to translation of the siding rot at the handle bar. [34]

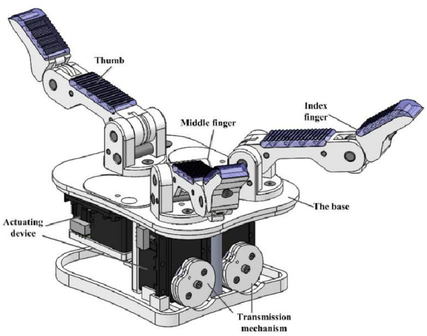

Fig. IV.2: Serial hinged adaptive fruit picker by [35] activated by cable displacement and active torsion springs in the hinges.

C. Parallel hinged

Parallel hinged grippers consist of fingers with hinges positioned next to and above each other. The majority of parallel hinged adaptation mechanism used leaver mechanisms to rotate rigid body parts of each finger. The parallel hinges act as rotation point serving this leaver. Therefore, parallel hinged mechanisms are possibly able to rotate around there instant axis of rotation which is not located at the position of the hinge. With this principle, mechanical leavers were created to adapt the finger structure.

A clear parallel hinged structure was used in [94]. The linear displacement of the gripper base results in contact forces between the rigid body parts of the gripper and the object. These contact forces enforce a rotation of the rigid body parts in the fingers. Due to the parallel hinge structure, an adaptive mechanism is formed, resulting in a contour following adaptive shape lock.

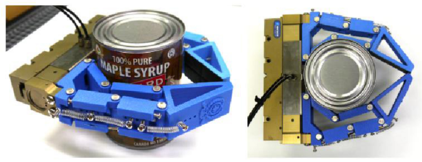

Fig. IV.3: Parallel hinged adaptive structure [94] consisting of rigid bodies connected by hinges positioned in parallel.

A different parallel hinged gripper is described by Liang in 2019 [29]. The pin array structure (figure IV.4 and IV.5) acts as an adaptive shape locking gripper which encloses the object by sliding pins onto the object surface. Inspecting the mechanism underneath the white shell, reveals the parallel hinged structure. The pins are forced in closed position due to a spring (no. 3 in figure IV.5). The rope (no. 4) is winded around the winding wheel (no. 8) and an retracted movement is created resulting in an open gripper state. The parallel pin array and parallel winding wheels (hinges) form the basis for a parallel structure. Depending on the type of object, this gripper can also perform a friction based grip. Therefore, Liang's pin array gripper is categorized in both, the friction based end group and the parallel hinged end group. Other parallel hinged grippers can be found in: [3], [8], [30], [41], [79], [95]–[130]

Fig. IV.4: Parallel hinged adaptive pin array structure consisting of three parallel arrays [29].

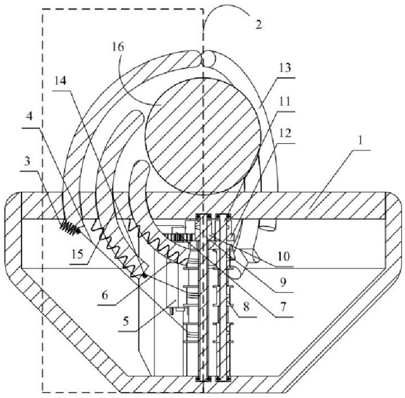

Fig. IV.5: Pin array mechanism: 1: base, 2: bar group assembly, 3: main spring, 4: rope, 5: motor, 6: reducer, 7: transition gear, 8: winding wheel, 9: auxiliary shaft, 10: auxiliary gear, 11: middle shaft, 12: middle gear, 13: circular sliding bar, 14: auxiliary spring, 15: sliding slut, 16: object. All according to: [29].

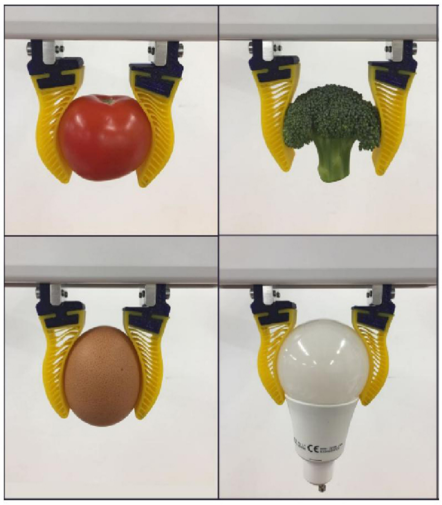

Fig. IV.6: Linkage-based elastic adaptive structure [131] consisting of deformable fingers and interconnecting horizontal structures used to grip different shaped and sized objects among different application purposes.

D. Linkage-based

The linkage-based end group consist of grippers which deform due to object contact forces or intrinsic input forces. Several linkage-based grippers are known as compliant mechanisms. Grippers consisting of multiple elastic parts, linked together, are able to perform similar to these compliant mechanisms. To this extent, linkage-based grippers published in [131], consist of single part 3D-printed elastic fingers which deform due to object contact forces. Therefore, the structure in the finger deforms according to the shape of the object as shown in figure IV.6.

A different linkage-based gripper is published in [132]. This gripper, consist of dielectric elastic actuators (DEAs) acting as single elastic links. The dielectric elastomer membrane is positioned in between two flexible electrodes. Voltage applied to the electrodes generate a Maxwell pressure which reduces the membrane thickness. This thickness reduction results in internal stresses which cause the bending movement of the fingers, according to [132]. Other linkage-based grippers are presented in [6], [55], [79], [93], [133]–[165]

E. Balloon-based

Within elastic structures, a balloon-based category has been subdivided. This gripper type is actuated by inflation, causing elastic material deformation. Therefore, expansion of the fluid-chambers generate a bending movement of the finger. Due to contact forces of the object and isobar fluid pressure, a contour following shape lock is established.

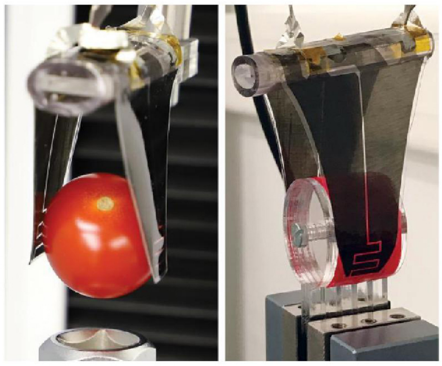

Fig. IV.7: Linkage-based structure using DEAs acting as single elastic link [132].

A classical balloon-based elastic structure is presented in [166]. This deep sea coral gripper is inflated with pressurized air, resulting in expansion of the pressure chambers of the balloon-based fingers. This expansion causes curvature of the fingers, resulting in adaptive shape locking the coral. A different balloon-based gripper (figure IV.9) is discussed in [167]. The rotational expansion chamber shown in figure IV.10, causes a rotation and translation of the finger. Air compression inside the chamber creates shape adaptation during enclosure of the object. Other balloon-based grippers can be found in [6], [31], [37], [46], [47], [79], [168]–[174]

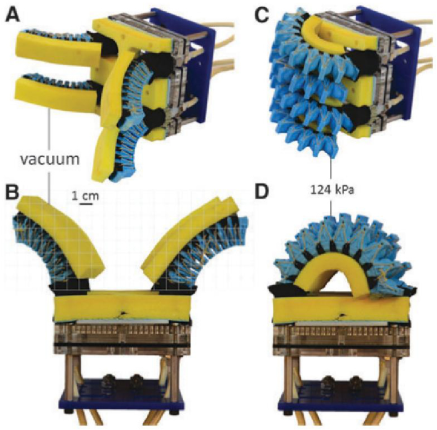

Fig. IV.8: Balloon-based inflated coral gripper consisting of four pressure actuated fingers with foam protection to reduce damage on the coral [166].

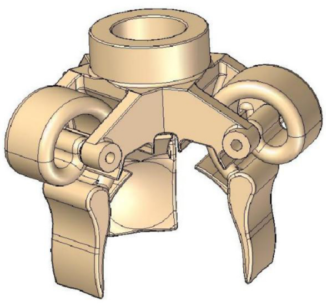

Fig. IV.9: Balloon-based inflated fruit gripper [167] with rotational expansion chambers for adaptive shape locking

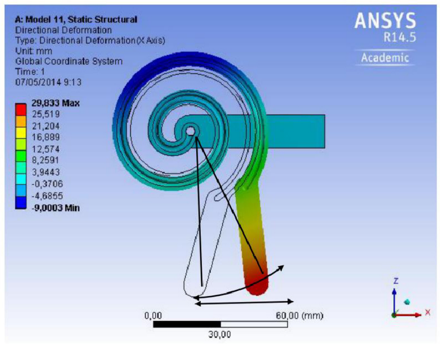

Fig. IV.10: Balloon-based inflated rotating mechanism [167], neutral state in transparent silhouette and actuated chamber in displacement gradient colors.

V. Discussion

After selecting and classifying the articles, tends among the end groups can be extracted. Figure V.3 shows a peak of parallel hinged grippers in 2006. This peak is mainly caused by publications of the Harbin Institute of Technology (China) during IEEE international conference on Robotics, Biometics, Mechatronics and Automation. From 2006 onward an overall increase in serial hinged grippers can be seen. This trend is traced back to prosthesis application development (figure III.1 and V.4). From 2014 onward, an expansion of linkage-based elastic grippers is noticed. This end group is equally applied in agricultural, industrial and prosthetic applications (figure V.4). Never the less, a steep decline in publications for this linkage-based end group occurred in 2019. Analysing the amount of agricultural gripper applications (figure V.4), linkage-based elastic grippers appear to be dominant in this sector. Friction-based grippers are mainly used in non adaptive industrial grippers. The amount of publications of these grippers experienced a peak in 2016 but declined in recent years (figure V.3). Balloon-based grippers are mainly used for agricultural purposes as depicted in figure V.4.

Reflecting on the presented selection and classification structure, several grippers consisted of multiple working principles. Articles with multiple different grippers or with equally dominant mechanisms are placed in multiple end groups. Articles [3]–[6], [8], [9], [27], [29]–[31], [37], [41], [46], [47], [55], [79], [93], [175] consist of redundant end group. Looking at [47] for example, two fundamental mechanisms are discovered. A serial hinged and balloon-based structure have been integrated (figure V.1). In addition, [23], [28], [43], [67], [79], [85], [94], [95], [107], [113], [123], [131], [132], [136], [160]–[162], [164], [165], [170], [175] consist of redundant industrial, agricultural or prosthetic application purposes. For example: [156]–[158], [164], are classified in both agricultural and industrial applications. This linkage-based elastic gripper, shown in figure V.2, was used for gripping fruit and boxes. Fruit refers to agricultural application and boxes to industrial warehouse purposes.

Therefore, this gripper was included in agricultural and industrial applications.

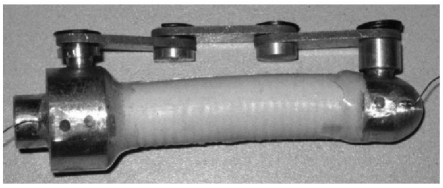

Fig. V.1: Serial hinged and balloon-based mechanism integration by [47], with four metal hinges to connect three rigid body parts in series, actuated using the expanding balloon (in white).

Fig. V.2: Linkage-based agricultural and industrial gripper by [156] with a topology optimized finger to adapt among different shaped objects in several application purposes.

VI. Conclusions

This state of the art overview of adaptive shape grippers described a selection and classification system in which grippers of 175 articles have been analysed. Scopus search engine was used to find adaptive gripping articles among three application purposes: agricultural, industrial and prosthesis grippers. The selection procedure resulted in three non adaptive end groups: friction based, local shape lock and rigid structure grippers. The classification of adaptive structure grippers resulted in and four end groups: serial hinged, parallel hinged, linkage-based and balloon-based grippers. Among these groups, 160 adaptive gripper mechanisms and 43 non adaptive grippers mechanisms were evaluated. The serial hinged end group was dominant: 63 grippers, followed by parallel hinged (n=43), linkage-based (n=39), friction based (n=30), balloon-based (n=15), rigid structure (n=8) and local shape lock (n=5). Typical examples for each end group have been explained and additional references were provided. These examples may serve as inspiration for new innovative adaptive shape grippers. In combination with the discussed trend lines, specific applications can be served.

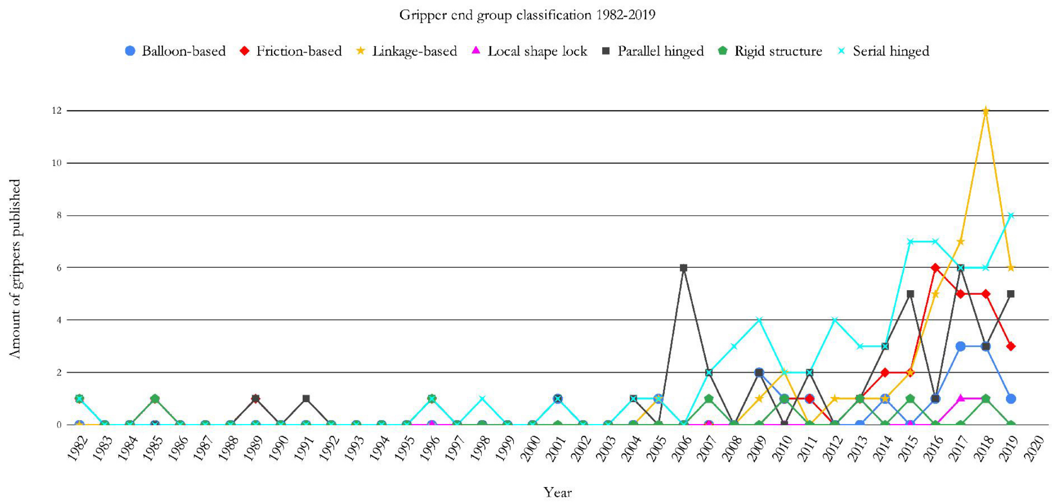

Fig. V.3: Progress of the amount of publications for each end group per year from 1982 to 2019.

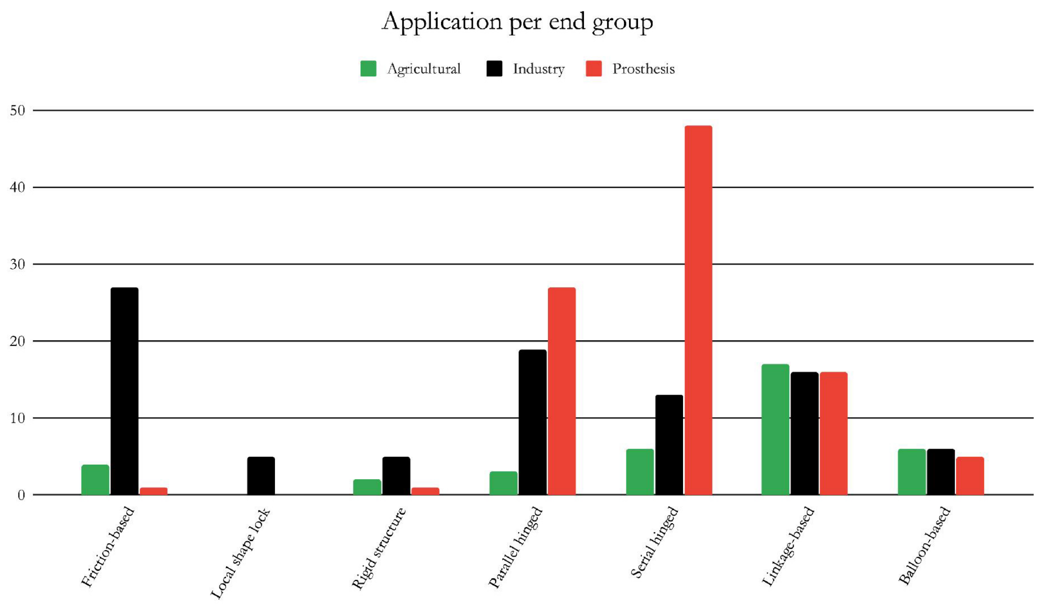

Fig. V.4: End group comparison of agricultural, industrial and prosthesis applications.

REFERENCES

[1] B. Bergelin, B. Slaboch, J. Sun, and P. A. Voglewede. A handy new design paradigm. *Mechanical Sciences*, 2(1):59–64, 2011.

[2] Christian Löchte, Holger Kunz, Raphael Schnurr, Sören Langhorst, Franz Dietrich, Annika Raatz, Klaus Dilger, and Klaus Dröder. Form-flexible handling and joining technology (formhand) for the forming and assembly of limp materials. *Procedia CIRP*, 23(C):206–211, 2014.

[3] Fan Yu Chen. Gripping mechanisms for industrial robots An overview. *Mechanism and Machine Theory*, 17(5):299–311, 1982.

[4] Christer Johansson, Nils Mårtensson, and Gunnar Sohlenius. Grippers, Tools and Fixtures for Flexible Automated Assembling. *CIRP Annals - Manufacturing Technology*, 34(1):21–24, 1985.

[5] Penisi Osvaldo Hugo. Visual Servo Control of Robot Grasping in Robotics. *Handbook of Robotic Grasp*, 10(June 2014):107–131, 2013.

[6] Dongsheng Liu, Hongbin Zang, Jiangmin Tuo, Nana Zhu, Bing Liao, Tao He, and Lei Hu. A Flytrap-inspired Soft Manipulator Driven by Single Airbag*. *2018 WRC Symposium on Advanced Robotics and Automation, WRC SARA 2018 - Proceeding*, pages 165–171, 2018.

[7] O Masory, J W Song, and H J Liu. A 2-DOF ACTIVE COMPLIANT GRIPPER FOR ROBOTIC APPLICATIONS. *Journal of Mechanical Working Technology Elsevier Science Publishers B N., Amsterdam*, 20:315–327, 1989.

[8] Philippe Gorce and Jean Guy Fontaine. Design methodology approach for flexible grippers. *Journal of Intelligent and Robotic Systems: Theory and Applications*, 15(3):307–328, 1996.

[9] Wei Chen Lee and Chih Wei Wu. A novel design of a prosthetic hand. *Conference Proceedings - IEEE International Conference on Systems, Man and Cybernetics*, pages 1821–1824, 2010.

[10] Manuel A. Armada, Alberto Sanfeliu, and Manuel Ferre. Robot2013: First iberian robotics conference: Advances in robotics, volume 2. *Advances in Intelligent Systems and Computing*, 253:153–167, 2014.

[11] Fei Chen, Luca Carbonari, Carlo Canali, Mariapaola D'imperio, and Ferdinando Cannella. Design of a novel dexterous robotic gripper for in-hand twisting and positioning within assembly automation. *Assembly Automation*, 35(3):259–268, 2015.

[12] Holger Kunz, Christian Löchte, Franz Dietrich, Annika Raatz, Fabian Fischer, Klaus Dröder, and Klaus Dilger. Novel form-flexible handling and joining tool for automated preforming. *Science and Engineering of Composite Materials*, 22(2):199–213, 2015.

[13] Chih Chieh Chen and Chao Chieh Lan. An accurate force regulation mechanism for handling fragile objects using pneumatic grippers. *IEEE/ASME International Conference on Advanced Intelligent Mechatronics, AIM*, 2016-Septe:389–394, 2016.

[14] Atsushi Kakogawa, Hiroyuki Nishimura, and Shugen Ma. Underactuated modular finger with pull-in mechanism for a robotic gripper. *2016 IEEE International Conference on Robotics and Biomimetics, ROBIO 2016*, pages 556–561, 2016.

[15] Nahian Rahman, Luca Carbonari, Darwin Caldwell, and Ferdinando Cannella. Manipulation & workspace analysis of Dexclar: A newly formed DEXterous gripper. *2016 IEEE International Conference on Robotics and Biomimetics, ROBIO 2016*, pages 1876–1881, 2016.

[16] Mădălin Petru Sbanca and Gheorghe Leonte Mogan. Advances in Robot Design and Intelligent Control. *Advances in Intelligent Systems and Computing*, 371:47–57, 2016.

[17] E. Vitzrabin and Y. Edan. Changing Task Objectives for Improved Sweet Pepper Detection for Robotic Harvesting. *IEEE Robotics and Automation Letters*, 1(1):578–584, 2016.

[18] Guohua Wang, Yabo Yu, and Qingchun Feng. Design of End-effector for Tomato Robotic Harvesting. *IFAC-PapersOnLine*, 49(16):190–193, 2016.

[19] Myoung Su Choi, Dong Hyuk Lee, Hyeonjun Park, Young Jin Kim, Ga Ram Jang, Yong Deuk Shin, Jae Han Park, Moon Hong Baeg, and Ji Hun Bae. Development of multi-purpose universal gripper. *2017 56th Annual Conference of the Society of Instrument and Control Engineers of Japan, SICE 2017*, 2017-Novem:1421–1424, 2017.

[20] Shiuh Jer Huang, Wei Han Chang, and Jui Yiao Su. Intelligent robotic gripper with adaptive grasping force. *International Journal of Control, Automation and Systems*, 15(5):2272–2282, 2017.

[21] Nahian Rahman, Carlo Canali, Darwin G Caldwell, and Ferdinando Cannella. Dexterous gripper synthesis from modular finger approach. In *Proceedings of the ASME Design Engineering Technical Conference*, volume 9, pages 9–13, 2017.

[22] Giulio Rosati, Simone Minto, and Fabio Oscari. Design and construction of a variable-aperture gripper for flexible automated assembly. *Robotics and Computer-Integrated Manufacturing*, 48(March):157–166, 2017.

[23] Jeffrey M. Krahn, Francesco Fabbro, and Carlo Menon. A soft-touch gripper for grasping delicate objects. *IEEE/ASME Transactions on Mechatronics*, 22(3):1276–1286, 2017.

[24] Chih Chieh Chen and Chao Chieh Lan. An Accurate Force Regulation Mechanism for High-Speed Handling of Fragile Objects Using Pneumatic Grippers. *IEEE Transactions on Automation Science and Engineering*, 15(4):1600–1608, 2018.

[25] Toshihiro Nishimura, Masanari Tennomi, Yosuke Suzuki, Tokuo Tsuji, and Tetsuyou Watanabe. Lightweight, High-Force Gripper Inspired by Chuck Clamping Devices. *IEEE Robotics and Automation Letters*, 3(3):1354–1361, 2018.

[26] Pei Chen Wu, Nan Lin, Ting Lei, Qian Cheng, Jin Ze Wu, and Xiao Ping Chen. A New Grasping Mode Based on a Sucked-type Underactuated Hand. *Chinese Journal of Mechanical Engineering (English Edition)*, 31(1), 2018.

[27] Jennifer Kwiatkowski, Jean Philippe Roberge, Nicholas A. Nadeau, Louis L'Écuyer-Lapierre, and Vincent Duchaine. An Extrinsic Dexterity Approach to the IROS 2018 Fan Robotic Challenge. *IEEE International Conference on Intelligent Robots and Systems*, pages 4139–4144, 2018.

[28] Shuguang Li, John J. Stampfli, Helen J. Xu, Elian Malkin, Evelin Villegas Diaz, Daniela Rus, and Robert J. Wood. A vacuum-driven origami 'magic-ball' soft gripper. *Proceedings - IEEE International Conference on Robotics and Automation*, 2019-May:7401–7408, 2019.

[29] Bo Liang and Wenzeng Zhang. A novel universal gripper with multi-layer circular sliding bars. *Proceedings of MARSS 2019: 4th International Conference on Manipulation, Automation, and Robotics at Small Scales*, pages 1–5, 2019.

[30] Bo Liang and Wenzeng Zhang. CSB-II Hand: A universal griper with circular sliding bars. *2019 4th IEEE International Conference on Advanced Robotics and Mechatronics, ICARM 2019*, pages 727–731, 2019.

[31] Rahim Mutlu, Charbel Tawk, Gursel Alici, and Emre Sariyildiz. A 3D printed monolithic soft gripper with adjustable stiffness. *Proceedings IECON 2017 - 43rd Annual Conference of the IEEE Industrial Electronics Society*, 2017-Janua:6235–6240, 2017.

[32] Jizhan Liu, Pingping Li, and Zhiguo Li. A multi-sensory end-effector for spherical fruit harvesting robot. *Proceedings of the IEEE International Conference on Automation and Logistics, ICAL 2007*, pages 258–262, 2007.

[33] Qingchun Feng, Xiaonan Wang, Guohua Wang, and Zhen Li. Design and test of tomatoes harvesting robot. *2015 IEEE International Conference on Information and Automation, ICIA 2015 - In conjunction with 2015 IEEE International Conference on Automation and Logistics*, (August):949–952, 2015.

[34] Eric Le Carpentier, Yannick Aoustin, Eloise Matheson, and Adrien Leon. An Anthropomorphic Underactuated Hand with 15. In *IEEE International Conference on Robotics and Automation*, page 11, 2008.

[35] Xin Song, Huiyong Shan, Hua Liu, and Junwang Guo. An underactuated end-effector design for fruit picking. *International Conference on Mechatronics and Machine Vision in Practice M2VIP 2016 - Proceedings of 23rd*, 2017.

[36] Fabio Leoni, Massimo Guerrini, Cecilia Laschi, Davide Taddeucci, Paolo Dario, and Antonina Starita. Implementing robotic grasping tasks using a biological approach. *Proceedings - IEEE International Conference on Robotics and Automation*, 3(May):2274–2280, 1998.

[37] S. Schulz, C. Pylatiuk, and G. Bretthauer. A new ultralight anthropomorphic hand. *Proceedings - IEEE International Conference on Robotics and Automation*, 3:2437–2441, 2001.

[38] Christian Pylatiuk, Stefan Schulz, Artem Kargov, and Georg Bretthauer. Two multiarticulated hydraulic hand prostheses. *Artificial Organs*, 28(11):980–986, 2004.

[39] Paolo Dario, Maria Chiara Carrozza, Eugenio Guglielmelli, Cecilia Laschi, Arianna Menciassi, Silvestro Micera, and Fabrizio Vecchi. Robotics as a future and emerging technology: Biomimetics, cybernetics, and neuro-robotics in European projects. *IEEE Robotics and Automation Magazine*, 12(2):29–45, 2005.

[40] Michele Guarnieri, Inoh Takao, Edwardo F. Fukushima, and Shigeo Hirose. HELIOS VIII search and rescue robot: Design of an adaptive gripper and system improvements. *IEEE International Conference on Intelligent Robots and Systems*, pages 1775–1780, 2007.

[41] B. Almasri and F. B. Ouezdou. New design of one motor driven under actuated humanoid hand. *IEEE International Conference on Intelligent Robots and Systems*, pages 1491–1496, 2007.

[42] Marco Controzzi, Christian Cipriani, and M. Chiara Carrozza. Mechatronic design of a transradial cybernetic hand. *2008 IEEE/RSJ International Conference on Intelligent Robots and Systems, IROS*, pages 576–581, 2008.

[43] Rosidah Sam and Samia Nefti. Design and development of flexible robotic gripper for handling food products. *2008 10th International Conference on Control, Automation, Robotics and Vision, ICARCV 2008*, (December):1684–1689, 2008.

[44] Vishalini Bundhoo, Edmund Haslam, Benjamin Birch, and Edward J. Park. A shape memory alloy-based tendon-driven actuation system for biomimetic artificial fingers, part I: Design and evaluation. *Robotica*, 27(1):131–146, 2009.

[45] Changhyun Cho, Youngho Lee, and Munsang Kim. Underactuated hand with passive adaptation. *IEEE International Symposium on Industrial Electronics*, (ISlE):995–1000, 2009.

[46] Immanuel Nicolas Gaiser, Christian Pylatiuk, Stefan Schulz, Artem Kargov, Reinhold Oberle, and Tino Werner. The fluidhand III: A multifunctional prosthetic hand. In *Journal of Prosthetics and Orthotics*, volume 21, pages 91–96, 2009.

[47] Shaoming Qian, Libin Zhang, Qinghua Yang, Guanjun Bao, Zhiheng Wang, and Liyong Qi. Research on adaptive multi-contract grasping model of flexible pneumatic finger. *2009 IEEE International Conference on Mechatronics and Automation, ICMA 2009*, pages 2823–2828, 2009.

[48] T. Laliberté, M. Baril, F. Guay, and C. Gosselin. Towards the design of a prosthetic underactuated hand. *Mechanical Sciences*, 1(1):19–26, 2010.

[49] Martin Wassink, Raffaella Carloni, and Stefano Stramigioli. Compliance analysis of an under-actuated robotic finger. *2010 3rd IEEE RAS and EMBS International Conference on Biomedical Robotics and Biomechatronics, BioRob 2010*, (3):325–330, 2010.

[50] Nayan M. Kakoty and Shyamanta M. Hazarika. Biomimetic design and development of a prosthetic hand: Prototype 1.0. *15th National Conference on Machines and Mechanisms, NaCoMM 2011*, pages 1–8, 2011.

[51] Arnold Kalmbach, Supervisor Prof, and Gregory Dudek. Design of an Underactuated Robot Hand with an Adduction Movement Mechanism in a Palm Keisuke. In *IEEE Conference on Systems, Process and Control (ICSPC 2015)*, number December, page 2011, 2011.

[52] Mathieu Baril. ON THE DESIGN OF MECHANICALLY PROGRAMMABLE UNDERACTUATED ANTHROPOMORPHIC ROBOTIC AND PROSTHETIC GRIPPERS. In *ASME 2012 International Design Engineering Technical Conferences & Computers and Information in Engineering Conference*, pages 1–10, 2012.

[53] Daniel A. Bennett, Skyler A. Dalley, and Michael Goldfarb. Design of a hand prosthesis with precision and conformal grasp capability. *Proceedings of the Annual International Conference of the IEEE Engineering in Medicine and Biology Society, EMBS*, pages 3044–3047, 2012.

[54] Zengqiang Li, Jun Zhang, and Guangyuan Liu. Analysis of adaptability of manipulator for grasping apple by cable-driven pneumatic pressure. *Applied Mechanics and Materials*, 120:389–392, 2012.

[55] Mogeeb A. El-Sheikh, Mona F. Taher, and Sayed M. Metwalli. New optimum humanoid hand design for prosthetic applications. *International Journal of Artificial Organs*, 35(4):251–262, 2012.

[56] Mathieu Baril, Thierry Laliberté, Clément Gosselin, and François Routhier. On the design of a mechanically programmable underactuated anthropomorphic prosthetic gripper. *Journal of Mechanical Design, Transactions of the ASME*, 135(12), 2013.

[57] Young June Shin, Soohyun Kim, and Kyung S. Kim. *Design of prosthetic robot hand with high performances based on novel actuation principles*, volume 46. IFAC, 2013.

[58] Yi Wei Liu, Fei Feng, and Yi Fu Gao. HIT prosthetic hand based on tendon-driven mechanism. *Journal of Central South University*, 21(5):1778–1791, 2014.

[59] Baiyang Sun, Caihua Xiong, Wenrui Chen, Qiaofei Zhang, Liu Mao, and Qin Zhang. A novel design method of anthropomorphic prosthetic hands for reproducing human hand grasping. *2014 36th Annual International Conference of the IEEE Engineering in Medicine and Biology Society, EMBC 2014*, pages 6215–6221, 2014.

[60] Kai Xu, Huan Liu, Yuheng Du, and Xiangyang Zhu. Design of an underactuated anthropomorphic hand with mechanically implemented postural synergies. *Advanced Robotics*, 28(21):1459–1474, 2014.

[61] Ewa Niewiadomska-Szynkiewicz and Andrzej Sikora. Progress in Automation, Robotics and Measuring Techniques. *Advances in Intelligent Systems and Computing*, 351:181–190, 2015.

[62] Guanjun Bao, Pengfei Yao, Shibo Cai, Shenshun Ying, and Qinghua Yang. Flexible pneumatic end-effector for agricultural robot: Design & experiment. *2015 IEEE International Conference on Robotics and Biomimetics, IEEE-ROBIO 2015*, pages 2175–2180, 2015.

[63] Nawid Jamali, Marco Maggiali, Francesco Giovannini, Giorgio Metta, and Lorenzo Natale. A new design of a fingertip for the iCub hand. *IEEE International Conference on Intelligent Robots and Systems*, 2015-Decem:2705–2710, 2015.

[64] J. L. Ramirez, A. Rubiano, N. Jouandeau, M. N. El Korso, L. Gallimard, and O. Polit. Hybrid kinematic model applied to the under-actuated robotic hand prosthesis ProMain-I and experimental evaluation. *IEEE International Conference on Rehabilitation Robotics*, 2015-Septe:301–306, 2015.
[65] Cesare Rossi, Sergio Savino, Vincenzo Niola, and Stefano Troncone. A study of a robotic hand with tendon driven fingers. *Robotica*, 33(5):1034–1048, 2015.
[66] Kai Xu, Huan Liu, Zenghui Liu, Yuheng Du, and Xiangyang Zhu. A single-actuator prosthetic hand using a continuum differential mechanism. *Proceedings - IEEE International Conference on Robotics and Automation*, 2015-June(June):6457–6462, 2015.
[67] Dayao Liang, Wenzeng Zhang, Zhenguo Sun, and Qiang Chen. PASA finger: A novel parallel and self-adaptive underactuated finger with pinching and enveloping grasp. *2015 IEEE International Conference on Robotics and Biomimetics, IEEE-ROBIO 2015*, pages 1323–1328, 2015.
[68] Hussein Mnyusiwalla, Philippe Vulliez, Jean Pierre Gazeau, and Saïd Zeghloul. A New Dexterous Hand Based on Bio-Inspired Finger Design for Inside-Hand Manipulation. *IEEE Transactions on Systems, Man, and Cybernetics: Systems*, 46(6):809–817, 2016.
[69] Vincenzo Niola, Cesare Rossi, and Sergio Savino. A model for the grasping analysis of an underactuated finger driven by unextensible tendon. *MATEC Web of Conferences*, 76:1–5, 2016.
[70] M. Phlernjai, T. Takayama, and T. Omata. Passively switched cable-driven transmission for high-speed/high-force robot finger. *Advanced Robotics*, 30(24):1559–1570, 2016.
[71] Parag Khanna, Khushdeep Singh, K. M. Bhurchandi, and Shital Chiddarwar. Design analysis and development of low cost underactuated Robotic hand. *2016 IEEE International Conference on Robotics and Biomimetics, ROBIO 2016*, pages 2002–2007, 2016.
[72] Charalambos Konnaris, Constantinos Gavriel, Andreas A.C. Thomik, and A. Aldo Faisal. EthoHand: A dexterous robotic hand with ball-joint thumb enables complex in-hand object manipulation. *Proceedings of the IEEE RAS and EMBS International Conference on Biomedical Robotics and Biomechatronics*, 2016-July:1154–1159, 2016.
[73] Philippe Wenger, Christine Chevallereau, Doina Pisla, Hannes Bleuler, and Aleksandar Rodić. New trends in medical and service robots: Human centered analysis, control and design. *Mechanisms and Machine Science*, 39:249–263, 2016.
[74] Jun Zhang and Guangyuan Liu. Self-adaption grasping force analysis for an apple sorting hand-claw with robustness. *Robotica*, 34(4):723–737, 2016.
[75] Neeraj Mishra and Anand Vaz. Bond graph modeling of a 3-joint string-tube actuated finger prosthesis. *Mechanism and Machine Theory*, 117:1–20, 2017.
[76] Giovanni Boschetti and Giuseppe Carbone. Dynamic Analysis of Handcycling. *International Journal of Mechanics and Control*, 18(2):1, 2017.
[77] J. L. Ramírez, A. Rubiano, N. Jouandeau, L. Gallimard, and O. Polit. Artificial muscles design methodology applied to robotic fingers. *Computational Methods in Applied Sciences*, 43:209–225, 2017.
[78] Amirul Syafiq Sadun, Jamaludin Jalani, and Jumadi Abdul Sukor. Modbus RTU protocol and arduino IO package: A real time implementation of a 3 finger adaptive robot gripper. *MATEC Web of Conferences*, 108:3–7, 2017.
[79] Daniel R. Ramírez Rebollo, Pedro Ponce, and Arturo Molina. From 3 fingers to 5 fingers dexterous hands. *Advanced Robotics*, 31(19-20):1051–1070, 2017.
[80] Saber Mahboubi, Steven Davis, and Samia Nefti-Meziani. Variable stiffness robotic hand for stable grasp and flexible handling. *IEEE Access*, 6:68195–68209, 2018.
[81] Yusuke Nemoto, Kazunori Ogawa, and Masahiro Yoshikawa. F3Hand: A Five-Fingered Prosthetic Hand Driven with Curved Pneumatic Artificial Muscles. *Proceedings of the Annual International Conference of the IEEE Engineering in Medicine and Biology Society, EMBS*, 2018-July:1668–1671, 2018.
[82] Mišel Cevzar, Tadej Petrič, and Jan Babič. Advances in Service and Industrial Robotics. *Mechanisms and Machine Science*, 49(Raad):797–804, 2018.
[83] C. L. Semasinghe, R. K.P.S. Ranaweera, J. L.B. Prasanna, H. M. Kandamby, D. G.K. Madusanka, and R. A.R.C. Gopura. HyPro: A Multi-DoF Hybrid-Powered Transradial Robotic Prosthesis. *Journal of Robotics*, 2018, 2018.
[84] Jason Spiliotopoulos, George Michalos, and Sotiris Makris. A reconfigurable gripper for dexterous manipulation in flexible assembly. *Inventions*, 3(1), 2018.
[85] Jingwei Su and Wenzeng Zhang. PISA finger: A novel parallel and self-Adaptive underactuated finger with a single chain transmission mechanism. *2017 IEEE International Conference on Robotics and Biomimetics, ROBIO 2017*, 2018-Janua(51575302):455–462, 2018.
[86] Huan Liu, Kai Xu, Bruno Siciliano, and Fanny Ficuciello. The MERO hand: A mechanically robust anthropomorphic prosthetic hand using novel compliant rolling contact joint. *IEEE/ASME International Conference on Advanced Intelligent Mechatronics, AIM*, 2019-July:126–132, 2019.
[87] Lucas Gerez, Junan Chen, and Minas Liarokapis. On the Development of Adaptive, Tendon-Driven, Wearable Exo-Gloves for Grasping Capabilities Enhancement. *IEEE Robotics and Automation Letters*, 4(2):422–429, 2019.
[88] Katharina Hermann, Rafael Hostettler, Markus Zimmermann, and Anand Vazhapilli Sureshbabu. A joint-selective robotic gripper with actuation mode switching. *IEEE International Conference on Automation Science and Engineering*, 2019-Augus:1532–1539, 2019.
[89] Michael T. Leddy and Aaron M. Dollar. Stability optimization of two-fingered anthropomorphic hands for precision grasping with a single actuator. *Proceedings - IEEE International Conference on Robotics and Automation*, 2019-May:451–457, 2019.
[90] Chad G. Rose and Marcia K. O'Malley. Hybrid Rigid-Soft Hand Exoskeleton to Assist Functional Dexterity. *IEEE Robotics and Automation Letters*, 4(1):73–80, 2019.
[91] Wooseok Ryu, Deaho Kim, Youngjin Choi, and Sungon Lee. Development of Prosthetic Finger with Actuator. *2019 16th International Conference on Ubiquitous Robots, UR 2019*, pages 313–318, 2019.
[92] Xu Yong, Xiaobei Jing, Xinyu Wu, Yinlai Jiang, and Hiroshi Yokoi. Design and implementation of arch function for adaptive multi-finger prosthetic hand. *Sensors (Switzerland)*, 19(16), 2019.
[93] Yoshiko Yabuki, Kazumasa Tanahashi, Yasuhiro Mouri, Yuta Murai, Shunta Togo, Ryu Kato, Yinlai Jiang, and Hiroshi Yokoi. Development of new cosmetic gloves for myoelectric prosthetic hand using superelastic rubber. *Robotics and Autonomous Systems*, 111:31–43, 2019.
[94] Lionel Birglen. Enhancing versatility and safety of industrial grippers with adaptive robotic fingers. *IEEE International Conference on Intelligent Robots and Systems*, 2015-Decem:2911–2916, 2015.
[95] Miodrag Rakić. Multifingered robot hand with selfadaptability. *Robotics and Computer Integrated Manufacturing*, 5(2-3):269–276, 1989.
[96] Richard M. Crowder. An anthropomorphic robotic end effector. *Robotics and Autonomous Systems*, 7(4):253–268, 1991.

[97] N. Dechev, W. L. Cleghorn, and S. Naumann. Multiple finger, passive adaptive grasp prosthetic hand. *Mechanism and Machine Theory*, 36(10):1157–1173, 2001.

[98] Minzhou Luo, Tao Mei, Xiaohua Wang, and Yong Yu. Grasp characteristics of an underactuated robot hand. *Proceedings - IEEE International Conference on Robotics and Automation*, 2004(3):2236–2241, 2004.

[99] Giorgio Figliolini and Pierluigi Rea. Overall design of Ca.U.M.Ha. robotic hand for harvesting horticulture products. *Robotica*, 24(3):329–331, 2006.

[100] D.W. Zhao, L. Jiang, H. Huang, M.H. Jin, and H.G. Cai. Development of a Multi-DOF Anthropomorphic prosthetic hand. In *IEEE International Conference on Robotics and Biomimetics*, pages 878–883, 2006.

[101] Hai Huang, Li Jiang, Yiwei Liu, Linqi Hou, Hegao Cai, and Hong Liu. The mechanical design and experiments of HIT/DLR prosthetic hand. *2006 IEEE International Conference on Robotics and Biomimetics, ROBIO 2006*, (50435040):896–901, 2006.

[102] H. Huang, L. Jiang, D. W. Zhao, J. D. Zhao, H. G. Cai, H. Liu, P. Meusel, B. Willberg, and G. Hirzinger. The development on a new biomechatronic prosthetic hand based on under-actuated mechanism. *IEEE International Conference on Intelligent Robots and Systems*, (50435040):3791–3796, 2006.

[103] Zhao Jingdong, Jiang Li, Shi Shicai, Cai Hegao, Liu Hong, and Hirzinger Gerd. A five-fingered underactuated prosthetic hand system. *2006 IEEE International Conference on Mechatronics and Automation, ICMA 2006*, 2006(50435040):1453–1458, 2006.

[104] Minzhou Luo, Wei Lu, Bingyu Sun, and Tao Mei. Autonomous grasping of a space robot multisensory gripper. *IEEE International Conference on Intelligent Robots and Systems*, pages 1014–1019, 2006.

[105] G. Figliolini and P. Rea. Ca.U.M.Ha. robotic hand (cassino-underactuated-multifinger-hand). *IEEE/ASME International Conference on Advanced Intelligent Mechatronics, AIM*, pages 1–6, 2007.

[106] Yuwang Liu, Hongguang Wang, Bin Li, and Weijia Zhou. The underactuation and motion-coupling in robotic fingers and two new 1-dof motion-coupling anthropomorphic fingers. *2008 IEEE International Conference on Robotics and Biomimetics, ROBIO 2008*, pages 1573–1578, 2009.

[107] Lionel Birglen. Type synthesis of linkage-driven self-adaptive fingers. *Journal of Mechanisms and Robotics*, 1(2):1–9, 2009.

[108] P. J. Kyberd, A. Clawson, and B. Jones. The use of underactuation in prosthetic grasping. *Mechanical Sciences*, 2(1):27–32, 2011.

[109] C. Meijneke, G. A. Kragten, and M. Wisse. Design and performance assessment of an underactuated hand for industrial applications. *Mechanical Sciences*, 2(1):9–15, 2011.

[110] Louis Alain Larouche and Lionel Birglen. Assisted design of linkage-driven adaptive soft fingers. *Industrial Robot*, 40(4):337–346, 2013.

[111] Giorgio Figliolini and Pierluigi Rea. Mechatronic design and experimental validation of a novel robotic hand. *Industrial Robot*, 41(1):98–108, 2014.

[112] Xinjun Sheng, Lei Hua, Dingguo Zhang, and Xiangyang Zhu. Design and testing of a self-adaptive prosthetic finger with a compliant driving mechanism. *International Journal of Humanoid Robotics*, 11(3):1–18, 2014.

[113] D. S.V. Bandara, R. A.R.C. Gopura, G. Kajanthan, M. Brunthavan, and H. I.M.M. Abeynayake. An under-actuated mechanism for a robotic finger. *4th Annual IEEE International Conference on Cyber Technology in Automation, Control and Intelligent Systems, IEEE-CYBER 2014*, (c):407–412, 2014.

[114] Jinchang Fan, Canjun Yang, Qian Bi, and Hao Gu. Design of a low-cost underactuated finger for positioning or pinching thin objects. *IEEE/ASME International Conference on Advanced Intelligent Mechatronics, AIM*, 2015-Augus:1108–1113, 2015.

[115] M.W.M. Groenewegen, Milton E. Aguirre, and Just L. Herder. DESIGN OF A PARTIALLY COMPLIANT, THREE-PHALANX UNDERACTUATED PROSTHETIC FINGER. In *ASME 2015 International Design Engineering Technical Conferences & Computers and Information in Engineering Conference IDETC/CIE 2015*, pages 1–7, 2015.

[116] Nurdos Omarkulov, Kuat Telegenov, Maralbek Zeinullin, Ainur Begalinova, and Almas Shintemirov. Design and analysis of an underactuated anthropomorphic finger for upper limb prosthetics. *Proceedings of the Annual International Conference of the IEEE Engineering in Medicine and Biology Society, EMBS*, 2015-Novem:2474–2477, 2015.

[117] Kuat Telegenov, Yedige Tlegenov, and Almas Shintemirov. A low-cost open-source 3-D-printed three-finger gripper platform for research and educational purposes. *IEEE Access*, 3:638–647, 2015.

[118] Aukeehoon Kim, Aujaemin Lee, Audonghyun Hwang, and Auminkyu Kim. A feasibility test of underactuated robotic prosthetic fingers actuated by shape memory alloy. *Proceedings of the IEEE RAS and EMBS International Conference on Biomedical Robotics and Biomechatronics*, 2016-July:554–560, 2016.

[119] D. S.V. Bandara, R. A.R.C. Gopura, K. T.M.U. Hemapala, and Kazuo Kiguchi. Development of a multi-DoF transhumeral robotic arm prosthesis. *Medical Engineering and Physics*, 48:131–141, 2017.

[120] Ming Cheng, Li Jiang, Ni Fenglei, Shaowei Fan, Yuan Liu, and Hong Liu. Design of a highly integrated underactuated finger towards prosthetic hand. *IEEE/ASME International Conference on Advanced Intelligent Mechatronics, AIM*, pages 1035–1040, 2017.

[121] Kyung Yun Choi, Aadeel Akhtar, and Timothy Bretl. A compliant four-bar linkage mechanism that makes the fingers of a prosthetic hand more impact resistant. *Proceedings - IEEE International Conference on Robotics and Automation*, pages 6694–6699, 2017.

[122] R. A.R.C. Gopura, D. S.V. Bandara, N. P.A. Gunasekera, V. H. Hapuarachchi, and B. S. Ariyarathna. A prosthetic hand with self-adaptive fingers. *2017 3rd International Conference on Control, Automation and Robotics, ICCAR 2017*, pages 269–274, 2017.

[123] Bruno Belzile and Lionel Birglen. Optimal design of self-adaptive fingers for proprioceptive tactile sensing. *Journal of Mechanisms and Robotics*, 9(5), 2017.

[124] Ivan I. Borisov, Oleg I. Borisov, Vladislav S. Gromov, Sergey M. Vlasov, and Sergey A. Kolyubin. The UHVAT Gripper: Usable Holding Versatile Adjustable Tool to Grasp Different Objects∗. *IFAC-PapersOnLine*, 51(11):722–727, 2018.

[125] Chao Luo and Wenzeng Zhang. A flexible self-adaptive underactuated hand with series passive joints. *Industrial Robot*, 45(4):516–525, 2018.

[126] Chao Luo and Wenzeng Zhang. A Linear-parallel and Self-adaptive Underactuated Hand with Parallel Pulleys and Active Linkage. In *ICARM 2018 - 2018 3rd International Conference on Advanced Robotics and Mechatronics*, pages 775–780, 2018.

[127] R. P.D.D. Chamara and R. A.R.C. Gopura. An Under-Actuated Mechanism for Anthropomorphic Robotic Prosthetic Hand. *2019 5th International Conference on Control, Automation and Robotics, ICCAR 2019*, pages 162–166, 2019.

[128] Gu Cheol Jeong, Yeoeun Kim, Wooseong Choi, Gangyong Gu, Hyun Joo Lee, Man Bok Hong, and Keehoon Kim. On the design of a novel underactuated robotic finger prosthesis for partial hand amputation. *IEEE International Conference on Rehabilitation Robotics*, 2019-June:861–867, 2019.

[129] S. R. Kashef, M. Davari, and A. Akbarzadeh. A robust design of a prosthetic finger and its dynamic analysis. *Proceedings of the 6th RSI International Conference on Robotics and Mechatronics, IcRoM 2018*, (IcRoM):135–140, 2019.

[130] S. Reza Kashef, Samane Amini, and Alireza Akbarzadeh. Robotic hand: A review on linkage-driven finger mechanisms of prosthetic hands and evaluation of the performance criteria. *Mechanism and Machine Theory*, 145:103677, 2020.

[131] Khaled Elgeneidy, Peter Lightbody, Simon Pearson, and Gerhard Neumann. Characterising 3D-printed soft fin ray robotic fingers with layer jamming capability for delicate grasping. *RoboSoft 2019 - 2019 IEEE International Conference on Soft Robotics*, pages 143–148, 2019.

[132] Vito Cacucciolo, Jun Shintake, and Herbert Shea. Delicate yet strong: Characterizing the electro-adhesion lifting force with a soft gripper. *RoboSoft 2019 - 2019 IEEE International Conference on Soft Robotics*, pages 108–113, 2019.

[133] Jingzhou Yang, Karim Abdel-Malek, and Jason Potratz. Design and prototyping of an active hand prosthetic device. *Industrial Robot*, 32(1):71–78, 2005.

[134] Mahmoud Helal, Liguo Chen, Lining Sun, and Tao Chen. Topology optimization of a three-dimension compliant microgripper using multiobjective compliance. *Proceedings - 2009 IITA International Conference on Control, Automation and Systems Engineering, CASE 2009*, pages 124–127, 2009.

[135] Peter Steutel, Gert A Kragten, and Just L Herder. Design of an underactuated finger with a monolithic structure and largely distributed compliance. In *Proceedings of the ASME Design Engineering Technical Conference*, volume 2, pages 355–363, 2010.

[136] Chih Hsing Liu and Kok Meng Lee. Explicit finite element analysis of a flexible multibody dynamic system with highly damped compliant fingers. *IEEE/ASME International Conference on Advanced Intelligent Mechatronics, AIM*, pages 43–48, 2010.

[137] Stergios Ganatsios, Alina Spanu, Octavian Dontu, Daniel Besnea, and Gheorghe I. Gheorghe. CAD analysis applied to self-centering compliant grippers. *Applied Mechanics and Materials*, 327:305–309, 2013.

[138] Laiqua Khalid, Olivera Stojadinovic, and Marjana Tomic-Canic. Post-operative wound care and dressings. *Handbook of Lasers in Dermatology*, pages 425–435, 2014.

[139] Nagarjun Jawahar, Sangamitra Manoharan, and Harish Chandran. Compliant Mechanisms - Integration of Micro Gripping Device with Positioner Using Topological Optimization. *SAE Technical Papers*, 2015-April(April):2–6, 2015.

[140] George P. Kontoudis, Minas V. Liarokapis, Agisilaos G. Zisimatos, Christoforos I. Mavrogiannis, and Kostas J. Kyriakopoulos. Open-source, anthropomorphic, underactuated robot hands with a selectively lockable differential mechanism: Towards affordable prostheses. *IEEE International Conference on Intelligent Robots and Systems*, 2015-Decem:5857–5862, 2015.

[141] Joseph R. Davidson, Abhisesh Silwal, Cameron J. Hohimer, Manoj Karkee, Changki Mo, and Qin Zhang. Proof-of-concept of a robotic apple harvester. *IEEE International Conference on Intelligent Robots and Systems*, 2016-Novem:634–639, 2016.

[142] Mogeeb A. El-Sheikh. Fibonacci-compliant finger design. *International Journal of Artificial Organs*, 39(9):491–496, 2016.

[143] J. Hemming, B. A.J. Van Tuijl, W. Gauchel, and E. Wais. Field test of different end-effectors for robotic harvesting of sweet-pepper. *Acta Horticulturae*, 1130:567–574, 2016.

[144] Rahim Mutlu, Gursel Alici, Marc In het Panhuis, and Geoffrey M. Spinks. 3D Printed Flexure Hinges for Soft Monolithic Prosthetic Fingers. *Soft Robotics*, 3(3):120–133, 2016.

[145] Yang Zheng, Lin Cao, Zhiqin Qian, Ang Chen, and Wenjun Zhang. Topology optimization of a fully compliant prosthetic finger: Design and testing. *Proceedings of the IEEE RAS and EMBS International Conference on Biomedical Robotics and Biomechatronics*, 2016-July:1029–1034, 2016.

[146] Matteo Cianchetti and Arianna Menciassi. Soft Robotics: Trends, Applications and Challenges. *Biosystems and Biorobotics*, 17:75–85, 2017.

[147] Joseph R Davidson and Mo Changki. Mechanical Design and Initial Performance Testing of an Apple-PICKING END-EFFECTOR. In *ASME 2015 International Mechanical Engineering Congress and Exposition*, pages 1–9, 2015.

[148] Van Ho and Shinichi Hirai. Design and Analysis of a Soft-Fingered Hand With Contact Feedback. *IEEE Robotics and Automation Letters*, 2(2):491–498, 2017.

[149] A. Milojević, N. D. Pavlović, S. Linß, M. Tomić, N. T. Pavlović, and H. Handroos. A concept of adaptive two finger gripper with embedded actuators. *Mechanisms and Machine Science*, 45:239–250, 2017.

[150] Wei Wang and Sung Hoon Ahn. Shape Memory Alloy-Based Soft Gripper with Variable Stiffness for Compliant and Effective Grasping. *Soft Robotics*, 4(4):379–389, 2017.

[151] Aurelian Zapciu, George Constantin, and Diana Popescu. Adaptive robotic end-effector with embedded 3D-printed sensing Circuits. *MATEC Web of Conferences*, 121:1–8, 2017.

[152] Zengya Dong, Guohua Gao, Hao Wang, and Yunsong Du. Study on Deformation and Contact Force Stability of a Novel Flexible Self-Adaptive Picking Manipulator. *Proceedings of 2018 2nd IEEE Advanced Information Management, Communicates, Electronic and Automation Control Conference, IMCEC 2018*, (Imcec):759–763, 2018.

[153] L Garcia, M Naves, and D M Brouwer. 3D-printed flexure-based finger joints for anthropomorphic hands*. In *IEEE/RSJ International Conference on Intelligent Robots and Systems (IROS)*, pages 1437–1442, 2018.

[154] Xiaobei Jing, Xu Yong, Lan Tian, Shunta Togo, Yinlai Jiang, Hiroshi Yokoi, and Guanglin Li. Development of Tendon Driven Under-Actuated Mechanism Applied in an EMG Prosthetic Hand with Three Major Grasps for Daily Life. *IEEE International Conference on Intelligent Robots and Systems*, pages 2774–2779, 2018.

[155] Michael T. Leddy and Aaron M. Dollar. Preliminary Design and Evaluation of a Single-Actuator Anthropomorphic Prosthetic Hand with Multiple Distinct Grasp Types. *Proceedings of the IEEE RAS and EMBS International Conference on Biomedical Robotics and Biomechatronics*, 2018-Augus:1062–1069, 2018.

[156] Chih Hsing Liu, Chen Hua Chiu, Ta Lun Chen, Tzu Yang Pai, Mao Cheng Hsu, and Yang Chen. Topology optimization and prototype of a three-dimensional printed compliant finger for grasping vulnerable objects with size and shape variations. *Journal of Mechanisms and Robotics*, 10(4):1–9, 2018.

[157] Chih Hsing Liu, Chen Hua Chiu, Ta Lun Chen, Tzu Yang Pai, Yang Chen, and Mao Cheng Hsu. A soft robotic gripper module with 3d printed compliant fingers for grasping fruits. *IEEE/ASME International Conference on Advanced Intelligent Mechatronics, AIM*, 2018-July:736–741, 2018.

[158] Chih Hsing Liu, Ta Lun Chen, Tzu Yang Pai, Chen Hua Chiu, Wei Geng Peng, and Mao Cheng Hsu. Topology Synthesis, Prototype, and Test of an Industrial Robot Gripper with 3D Printed Compliant Fingers for Handling of Fragile Objects. *2018 WRC Symposium on Advanced Robotics and Automation, WRC SARA 2018 - Proceeding*, pages 129–134, 2018.

[159] G. Salvietti, Z. Iqbal, I. Hussain, D. Prattichizzo, and M. Malvezzi. The Co-Gripper: A Wireless Cooperative Gripper for Safe Human Robot Interaction. *IEEE International Conference on Intelligent Robots and Systems*, pages 4576–4581, 2018.

[160] Christian Ivan Basson, Glen Bright, and Anthony John Walker. Testing flexible grippers for geometric and surface grasping conformity in reconfigurable assembly systems. *South African Journal of Industrial Engineering*, 29(1):128–142, 2018.

[161] Andrija Milojević, Sebastian Linß, Žarko Ćojbašić, Heikki Handroos, Lauri Luostarinen, and Lena Zentner. Adaptive Soft Robotic Gripper Based on Shape Morphing Compliant System. *2018 International Conference on Reconfigurable Mechanisms and Robots, ReMAR 2018 - Proceedings*, 2018.

[162] Wei Zhang, Jonathan Hong, Saad Ahmed, Zoubeida Ounaies, and Mary Frecker. Parametric Design of a Soft Gripper Actuated Using the Electrostrictive PVDF-based Terpolymer. *ASME 2018 Conference on Smart Materials, Adaptive Structures and Intelligent Systems, SMASIS 2018*, 1:1–10, 2018.

[163] George P. Kontoudis, Minas Liarokapis, and Kyriakos G. Vamvoudakis. A compliant, underactuated finger for anthropomorphic hands. *IEEE International Conference on Rehabilitation Robotics*, 2019-June:682–688, 2019.

[164] Chih Hsing Liu, Mao Cheng Hsu, Yang Chen, Wei Ting Chen, and Ta Lun Chen. A topology-optimized 3D printed compliant finger with flex sensor for adaptive grasping of unknown objects. *IEEE/ASME International Conference on Advanced Intelligent Mechatronics, AIM*, 2019-July:92–97, 2019.

[165] Charbel Tawk, Geoffrey M. Spinks, Marc In het Panhuis, and Gursel Alici. 3D printable vacuum-powered soft linear actuators. *IEEE/ASME International Conference on Advanced Intelligent Mechatronics, AIM*, 2019-July:50–55, 2019.

[166] Kevin C. Galloway, Kaitlyn P. Becker, Brennan Phillips, Jordan Kirby, Stephen Licht, Dan Tchernov, Robert J. Wood, and David F. Gruber. Soft Robotic Grippers for Biological Sampling on Deep Reefs. *Soft Robotics*, 3(1):23–33, 2016.

[167] Carlos Blanes, Martín Mellado, and Pablo Beltran. Novel additive manufacturing pneumatic actuators and mechanisms for food handling grippers. *Actuators*, 3(3):205–225, 2014.

[168] Stefan Schulz, Christian Pylatiuk, Markus Reischl, Jan Martin, Ralf Mikut, and Georg Bretthauer. A hydraulically driven multifunctional prosthetic hand. *Robotica*, 23(3):293–299, 2005.

[169] A. Pettersson, S. Davis, J. O. Gray, T. J. Dodd, and T. Ohlsson. Design of a magnetorheological robot gripper for handling of delicate food products with varying shapes. *Journal of Food Engineering*, 98(3):332–338, 2010.

[170] Andrzej Grzesiak, Ralf Becker, and Alexander Verl. The Bionic Handling Assistant: A success story of additive manufacturing. *Assembly Automation*, 31(4):329–333, 2011.

[171] Hongying Zhang, Yiqiang Wang, Michael Yu Wang, Jerry Ying Hsi Fuh, and A. Senthil Kumar. Design and Analysis of Soft Grippers for Hand Rehabilitation. In *ASME 2017 12th International Manufacturing Science and Engineering Conference*, number June, 2017.

[172] Yang Chen, Shaofei Guo, Cunfeng Li, Hui Yang, and Lina Hao. Size recognition and adaptive grasping using an integration of actuating and sensing soft pneumatic gripper. *Robotics and Autonomous Systems*, 104:14–24, 2018.

[173] Geneviève Miron, Benjamin Bédard, and Jean Sébastien Plante. Sleeved bending actuators for soft grippers: A durable solution for high force-to-weight applications. *High-Throughput*, 7(3), 2018.

[174] Panagiotis Sotiropoulos, Maximo A. Roa, Murilo F. Martins, Werner Fried, Hussein Mnyusiwalla, Pavlos Triantafyllou, and Graham Deacon. A Benchmarking Framework for Systematic Evaluation of Compliant Under-Actuated Soft End Effectors in an Industrial Context. *IEEE-RAS International Conference on Humanoid Robots*, 2018-Novem:650–657, 2019.

[175] Zahra Samadikhoshkho, Kourosh Zareinia, and Farrokh Janabi-Sharifi. A Brief Review on Robotic Grippers Classifications. *2019 IEEE Canadian Conference of Electrical and Computer Engineering, CCECE 2019*, pages 1–4, 2019.

B

Appendix B

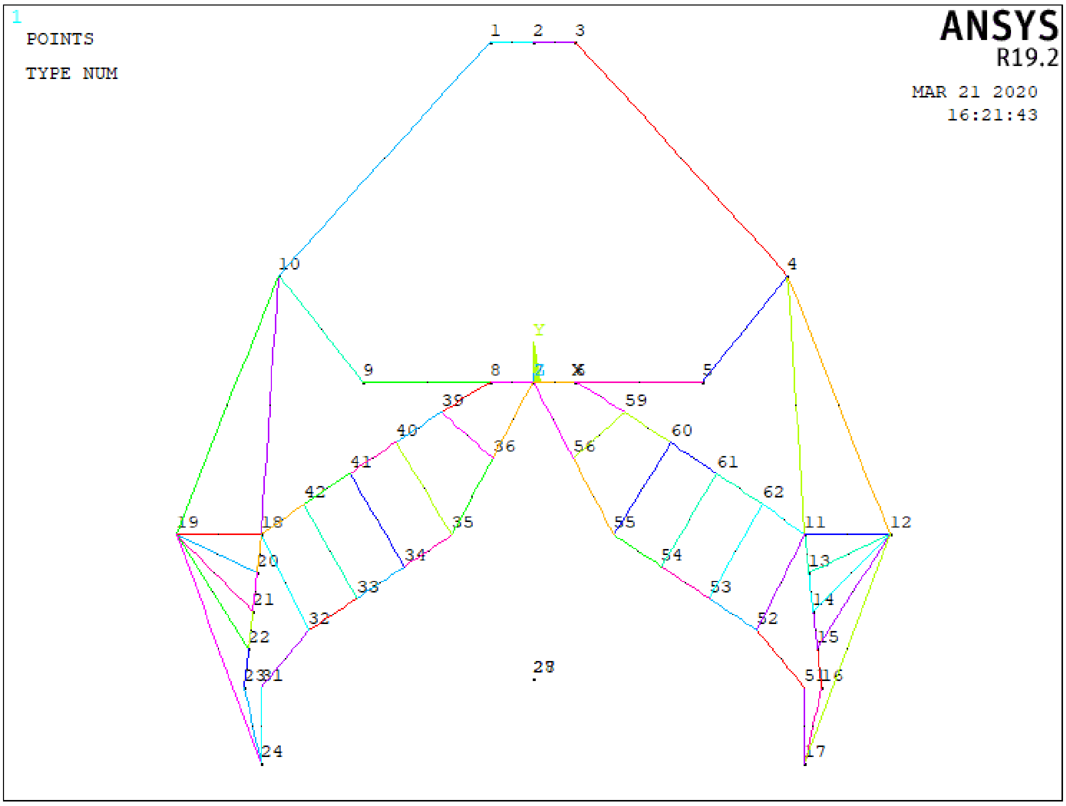

Figure B.1: Gripper concept 3.2 nodes

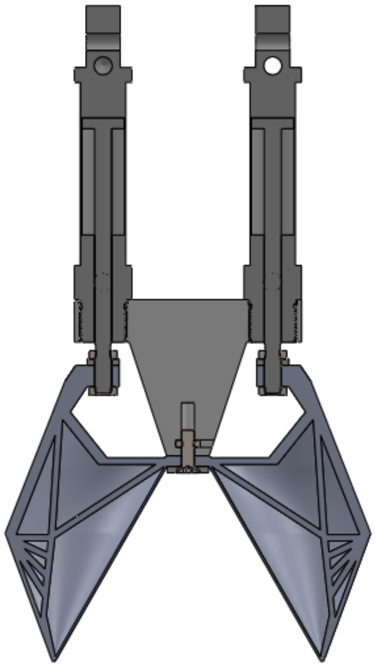

Figure B.2: schematic front view of working prototype 1 of gripper concept 3.

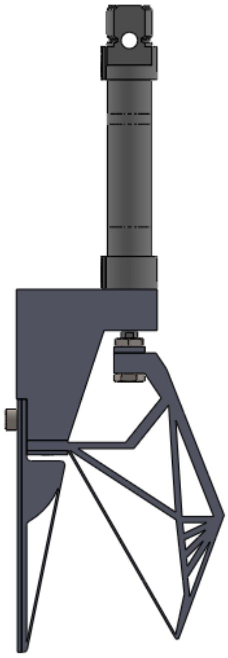

Figure B.4: Prototype 3 front view

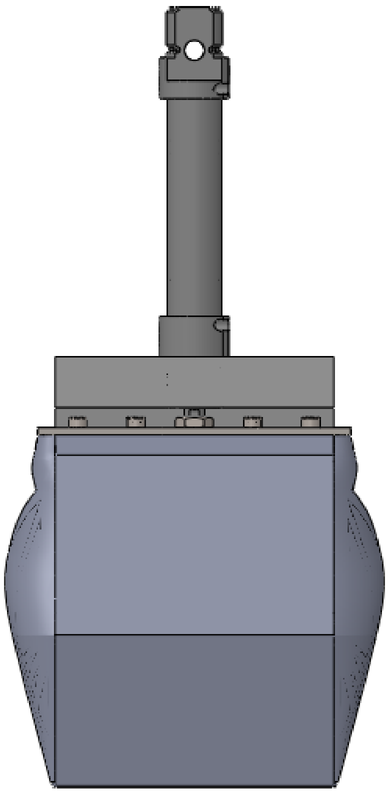

Figure B.3: schematic side view of prototype 1 of gripper concept 3

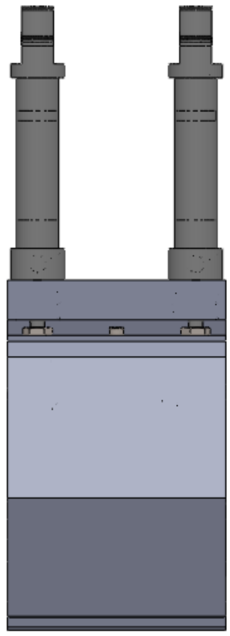

Figure B.5: Prototype 3 side view

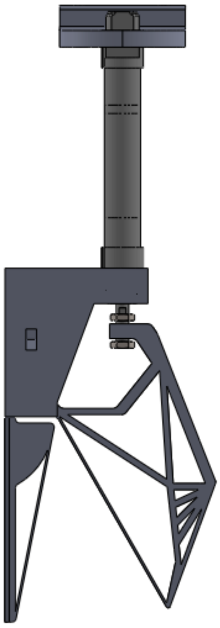

Figure B.6: Prototype 4 front view

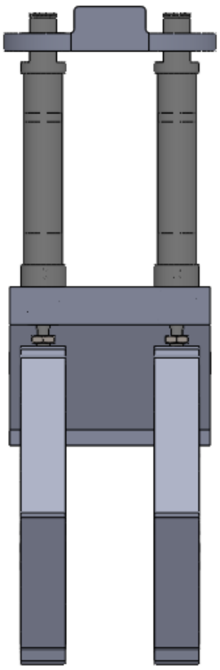

Figure B.7: Prototype 4 side view

Figure B.8: Gripper prototype 1 leveled before testing

Figure B.9: Gripper 3 tested in x direction on the compliant side of the gripper

Figure B.10: Gripper 3 tested in x direction on the thin finger side of the gripper

Figure B.11: Damage experiment gripper 2

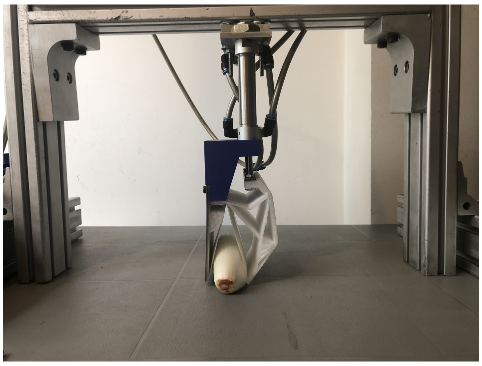

Figure B.12: Damage experiment gripper 3

Figure B.13: Damage experiment gripper 4

Figure B.14: Modified chicory with a drilled through aluminium tube to carry the gravitational load applied on the cable and preventing the cable from cutting through the chicory.

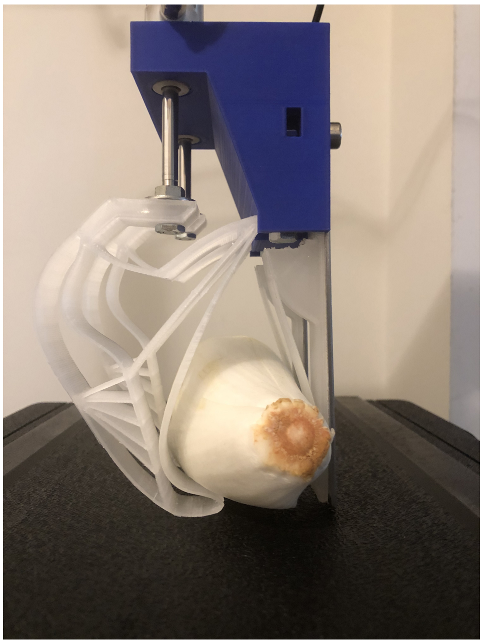

Figure B.15: Iteration 2 in damage experiment.

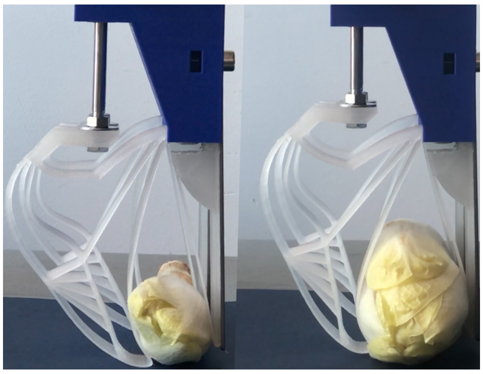

Figure B.16: Iteration 3 gripping small and large chicories without damage.

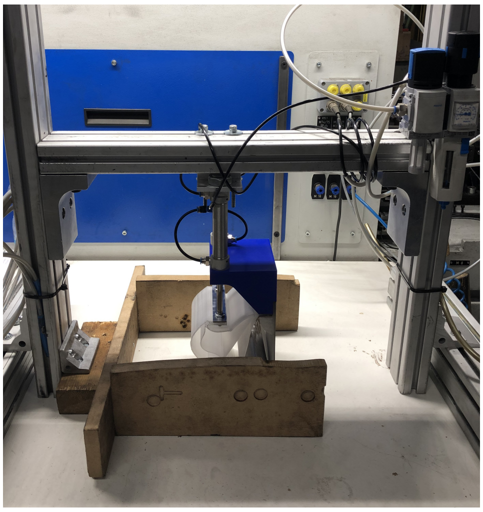

Figure B.17: Iteration 4 endurance experiment setup overview.

Figure B.18: Pick up endurance test with real chicory samples for a duration of 10000 gripping repetitions.

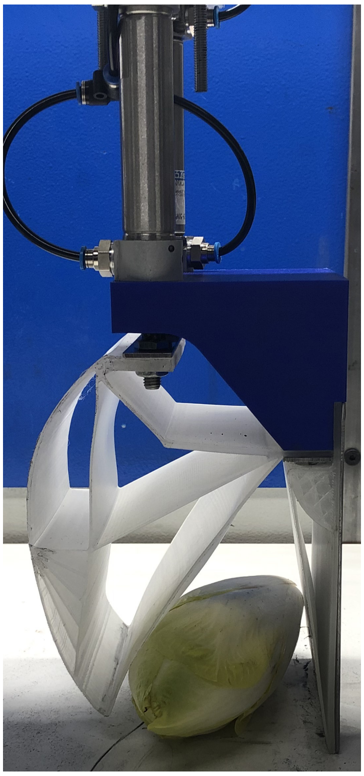

Figure B.19: Rotated (around z axis) chicory sample in gripper iteration 4. This rotation has been performed 100× for a small and large chicory sample.

Figure B.20: Time series of closing gripper (prototype iteration 4), closing time is 23 ms.

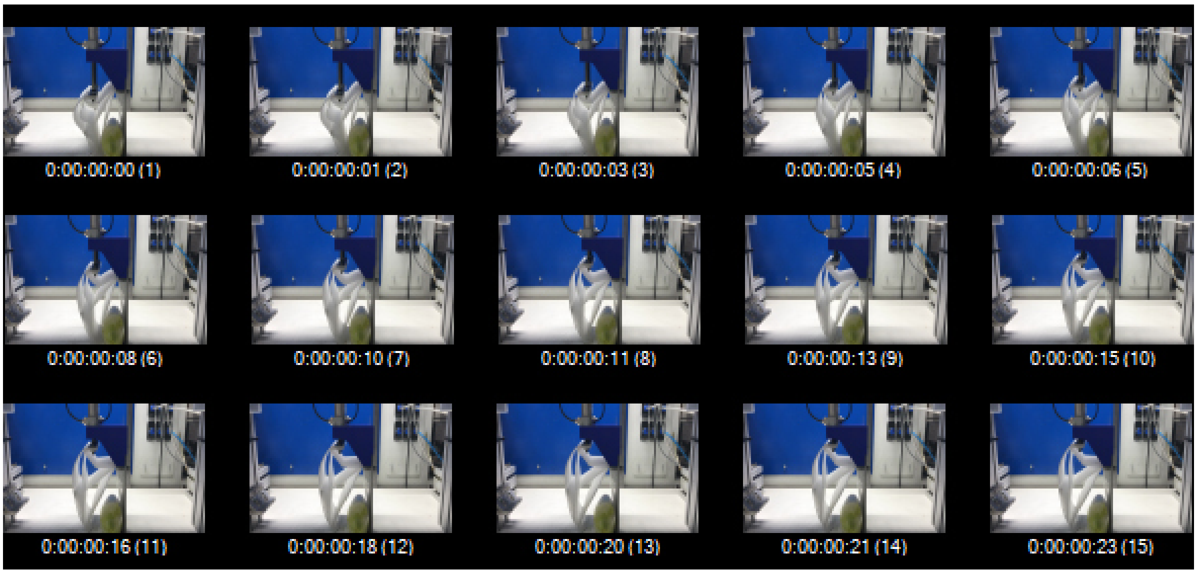

Figure B.21: Time series of opening gripper (prototype iteration 4), opening time is 23 ms